Optical Signal Processing Using Fiber-based Four-wave Mixing for Single and Mixed Format Optical Networks

Irneza binti Ismail

Department of Communication Engineering and Informatics

The University of Electro-Communications, Tokyo, Japan

A Thesis Submitted in Partial Fulfillment of the Requirements for the Degree of

DOCTOR OF PHILOSOPHY

March 2016

Optical Signal Processing Using Fiber-based Four-wave Mixing for Single and Mixed Format Optical Networks

Approved by the supervisory committee:

1. Professor Kishi Naoto, Supervisor

2. Professor Oki Eiji

3. Professor Ueno Yoshiyasu

4. Professor Nishioka Hajime

5. Associate Professor Matsuura Motoharu

単一もしくは混合フォーマット光ネットワークのための光ファイバの四光波混合を用いた光信号処理

イルネザ　ビンデイ　イスマイル

概要

この論文では、光 AND ゲート四光波混合（FWM：four-wave mixing）技術による単一のポンプ使用して各種信号の変換で単一および複数のチャネルを変換するための簡単な技術提案した 。ラマン断熱ソリトン圧縮機（RASC：raman adiabatic-soliton compressor)は連続波 (CW: continuous waves) に基づいた単一のポンプと圧縮 RZ (return-to-zero) パルスを使用しています。入力ポンプ信号として RASC から圧縮された RZ パルスについては、各動作におけるピコ秒幅のパルスが 変換することができます。入力信号は、RZ クロックポンプの変換された信号の形状及び改善消光比からの圧縮クロックの特性を継承することが、より大きな持続時間を有します。これにより、FWM の再生特性を実現することができます。変換された信号の情報は、各種の信号変換で達成された入力データ信号パワーペナルティも低くなりました。

Abstract

As data rates in broadband optical networks continue to grow, all optical signal processing technologies are expected to become important for future high bit-rate communication systems to address the growing demand for network flexibility, low cost and high bandwidth. Along the line of the capacity increased, many new modulation formats have been introduced. The most straightforward format is on-off-keying (OOK) modulation format. The state of art reveals that the differential phase-shift keying (DPSK) modulation format is the best candidate for high-speed long haul network segment, while OOK is suitable for short reach network segment. However, the next generation transmission systems will more likely employ mixed modulation formats. Thus, the shift towards these changes to be applied in many applications is necessary. Hence, it is worth investigating several signal processing, not only by using a single modulation format but also mixed modulation formats. In order to realize such systems, the scheme requirement must be transparent to modulation format and bit-rate. One of the promising candidates is based on the third-order nonlinear susceptibility $x^{(3)}$ in a nonlinear fiber, which is also called four-wave mixing (FWM). Fiber-based FWM, in a highly nonlinear fiber (HNLF) is a preferable choice due to its fast nonlinear response and high conversion efficiency. FWM technique can be also be used as an all-optical AND logic gates and signal regenerator.

In optical fiber communication systems, signal distortions due to chromatic dispersion in fiber dominantly limit transmission length and bit-rate. An improvement in the distorted signal is crucially needed, as the processed signal will become more degraded after some distance of transmission. Optical phase conjugation (OPC) and tunable dispersion compensation modulator

(TDCM) are two attractive schemes used to increase the signal robustness in transmission systems. It is also desirable if a practical function such as flexible picosecond width-tunability can be accomplished. The advantageous of flexible converted pulse width are for the creation of higher bit-rate signals and the ability to support wider bandwidth requirements. In this thesis, the experimental demonstration using compressed RZ clock from Raman adiabatic-soliton compressor (RASC) and continuous wave (CW) signal as a pump signals in all-optical fiber-based FWM AND-gate using single and mixed OOK-DPSK modulation formats in many applications can be realised. The applications including: all-optical nonreturn-to-zero(NRZ)-to-return-to-zero(RZ) wavelength-waveform conversions, all optical wavelength multicasting, all channel OTDM demultiplexing, and transmission performance between the midspan of OPC and TDCM.

We experimentally demonstrated an all-optical NRZ-DPSK-to-RZ-DPSK waveform-wavelength conversion with flexible picosecond width-tunability and signal regeneration with reshaping functionality. The scheme is based on a RASC and a fiber-based AND-gate. In the first demonstration, we demonstrate waveform-wavelength conversion of a 10-Gb/s DPSK signal without input signal degradation over wide input-output wavelength ranges. The measurement results of the converted RZ-DPSK signal are pedestal-free, and its converted pulse width can be adjusted by tuning the Raman pump power in RASC. Further investigation of the regenerative properties due to chromatic dispersion is conducted at several Raman pump power settings over 40-km standard single-mode fibers (SSMFs) without dispersion compensation. Also, low power penalty with an error-free operation is obtained for the RZ-DPSK regenerated converted signal.

Next, an all-optical 1-to-6 wavelength multicasting of a 10-Gb/s picosecond-tunable-width converted OOK data signal using a parametric pulse source from a RASC is experimentally demonstrated. Width-tunable wavelength multicasting within the C-band with approximately 40.6-nm of separation with various compressed RZ data signal inputs has been proposed and

demonstrated. The converted multicast pulse widths can be flexibly controlled down by tuning the Raman pump powers of the RASC. Nearly equal pulse widths at all multicast wavelengths are obtained. Furthermore, wide open eye patterns and low power penalties at the 10^{-9} BER level are found.

An all-optical demultiplexing of 40-Gb/s hybrid OTDM mixed format channels by using RASC-flexible control-window is also demonstrated. Error-free operations with less than 1.3-dB power penalties were obtained and this scheme is expected to be scalable toward higher bit-rates.

Further demonstration related to NRZ-to-RZ waveform-wavelength conversion for 4 x 10-Gb/s multichannel mixed OOK-DPSK data formats, deploying a single FWM and RASC has been done. The fiber-based switch in HNLF based on parametric process between mixed data signals and the compressed RZ clock from RASC. By flexibly tuning the Raman pump power from RASC in between 0.20 and 0.90 W, high quality converted signal can be achieved. Bit-error-rate measurements show negative power penalties for the obtained RZ signals with pedestal-free pulses.

Finally, we demonstrated the transmission performance between the midspan of TDCM and OPC schemes with specialty using multichannel-mixed OOK and DPSK format. The OPC scheme has the advantage over the penalties performance compared to TDCM scheme.

To my beloved husband, **Hazrie Hamdan**;

To my parents, **Ismail Harun** and **Zanariah Mohammed**;

To my cute three kids **Hariz, Hafiz and Hannah**;

And all my family;

Without whom none of my success would be possible

Thank you very much for all the support given with love and

understandings

Acknowledgements

Contents

CONTENTS

List of Figures

LIST OF FIGURES

List of Tables

ACRONYMS

Chapter 1

Introduction

In the current years, optical photonic communication systems is evolving exponentially, driven by a growth in the number of connections along with the demand for data traffic and higher bandwidth applications, mostly internet and video contents. In order to provide services relying on higher bandwidth requirements, high-speed optical signal processing technologies must be improved not only for transmission nodes but also in the transmission lines. Thus, the key technologies such as, ultra-short pulse generation, all-optical demultiplexing, multicasting, waveform-wavelength conversion, all-optical regeneration , and etc are required for future transmission systems employing both OTDM and WDM techniques. A general overview of fiber optical network architecture, optical multiplexing techniques, modulation formats, motivation and research aims, and lastly structure of the thesis are explained in this chapter.

1.1   Architecture of Fiber Optical Network

Fiber optical transmission plays an essential role in telecommunication services over global network transport. As shown in Fig. 1.1, the simplified model for communications networks includes three segments namely ultra-high capacity core networks, regional/metro networks and lastly, last-mile access networks. Table 1.1 shows the typical distances covered by transmission spans in photonic networks.

A core network that is interconnected by the access network offers various services to the customers such as direct telephone calls over the public-switched telephone network. Generally, the core network delivers routes to exchange information among

1. INTRODUCTION
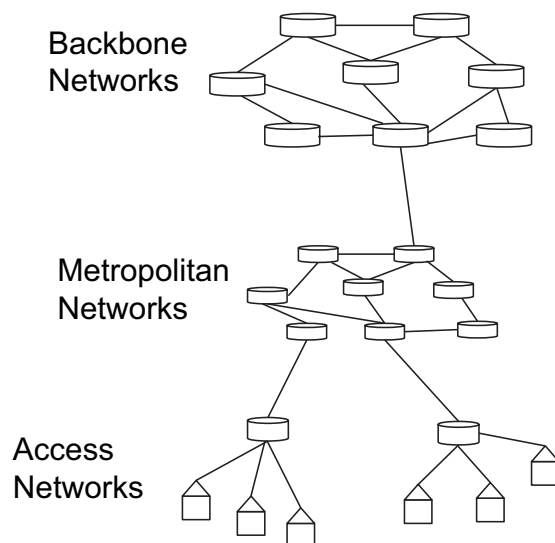
Figure 1.1: Optical networks hierarchy

Optical Transmission System	Distance (km)
Access	< 100
Metro	< 300
Regional	300 - 1000
Long-haul	1000 - 3000
Ultra long-haul	> 3000

Table 1.1: Classification of optical transmission systems.

various sub-networks. Routers and switches are the most used devices for the core networks, with switches being used more often. Meanwhile, network and data link layer technologies such as asynchronous transfer mode (ATM), IP, synchronous optical networking (SONET) and dense wavelength division multiplexing (DWDM) are the main technologies for the core facilities. For enterprises usage, a 10 Gb/s Ethernet technology is also can be used. Metropolitan is the introduction of MANs (Metropolitan access networks) that is based on gigabit Ethernet. Moreover, MANs are larger than LANs (local area-networks), but smaller than WANs (wide area-networks), which is designed to be used in city or town.

The access network is a last-mile network that is connected from the customer to the metropolitan network. In this networks, various kinds of end-user applications are possible, spanning from residential inter- net access to business and storage area networks.

Legacy last-mile networks are still largely based on copper networks, either co-axial or twisted pair. Optical fibers have a significant advantage over copper networks due to its much higher bandwidth-distance product, which enables high-speed connections over longer distances.

1.2   Optical Multiplexing Techniques

In telecommunication networks, multiplexing is an effective method to transmit a multiple information streams over a single fiber coming from different sources or data streams. Two basic forms of multiplexing are OTDM and WDM methods, as shown in Fig. 1.2. In order to increase the bit-rate, data streams from many lower-speed data streams are divided into units with same size and interleaved into the time slots by means of OTDM. If the bit-rate of the several signals is B, the total aggregate rate of multiplexed signals is NB, where N is the number of data streams signals. For instance, in order to achieve high-speed OTDM transmission systems, it is very important for optical sources to generate a high quality pulses with short pulse width at repetition rates from 10 to 40 GHz [1]. For example, typical values for 40 Gb/s transmission can be estimated to be less than 10 ps assuming a maximum width of 40 percents of the time slot, with less than 630 fs for 640 Gb/s OTDM [2]. At the receiver side, the essential component is an optical demultiplexer (DEMUX). Other than that, the purpose of DEMUX is to extract the lower speed tributaries to its base rate, using all-optical switches [3-5]. The key limitations in high bit-rate OTDM are pulse distortion caused by crosstalk in the DEMUX and fiber dispersion. Thus, it is desirable to have a signal pulse widths that are significantly shorter than a bit period on the multiplexed channel [6].

On the other hand, WDM data streams are carried simultaneously on the same transmission line by allocating different carrier wavelengths within the bandwidth of the single channel [7–9]. The multiplexer at the transmitter side is needed to join the signals together into a same fiber, and DEMUX at the receiver to split these channels apart [10]. Moreover, the wavelengths used in WDM systems are based on standardised grid by an International Telecommunications Union (ITU) frequency [11]. At the wavelength of 1550 nm, signal spacing of 0.80 nm equal to frequency spacing of 100 GHz, is a typical standard spacing for WDM systems. The invention of the Erbium doped fiber amplifier

(a) OTDM Mux

(b) WDM Mux
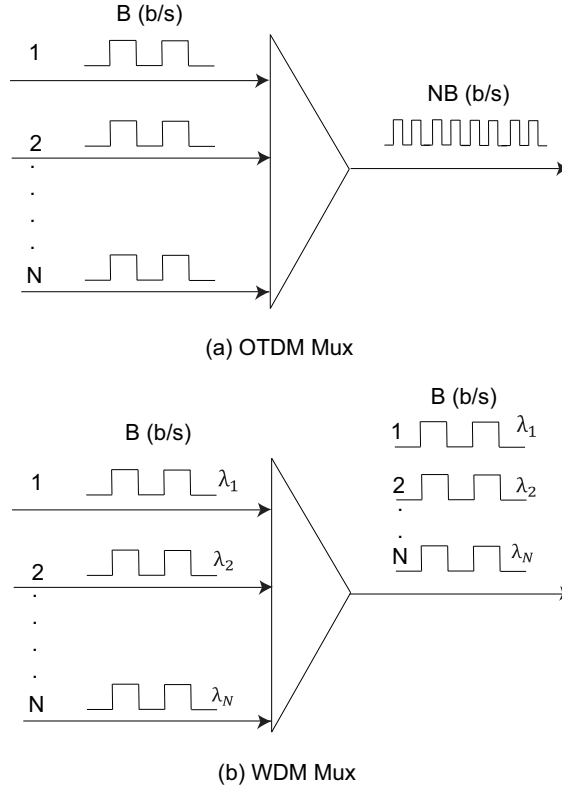
Figure 1.2: Different multiplexing techniques for increasing the transmission capacity of an optical fiber. (Optical time division multiplexing (b) wavelength division multiplexing. Both techniques take in N data streams, each of B (b/s), and multiplex them into a single fiber with total aggregate rate of NB (b/s).

(EDFA) in the late 1980s led to the deployment of WDM systems by amplifying signals at many wavelengths simultaneously. Both WDM and EDFAs effectively can reduce long-haul transmission cost and increase the information capacity of a fiber up over 1 Tb/s. Performance of the WDM systems may be limited by the nonlinear effects [12–14] and can be controlled by proper choice of channel spacing and power.

1.3 Binary Modulation Format

As shown in Fig. 1.3, different modulations formats exist in optical networks use intensity, phase, frequency or polarisation modulation to send data information or to increase the transmission tolerance. In this thesis, we focus on the basic binary modulation formats that have popularly been deployed in optical network transmission
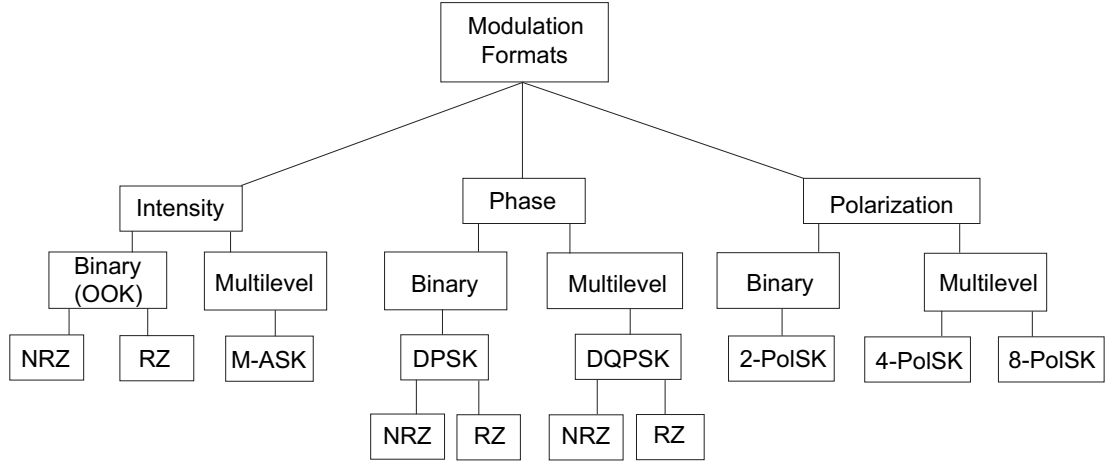
Figure 1.3: Commonly used modulation formats in optical communication systems.

systems. As a reference format, on-off keying (OOK) modulation format, either non-return-to-zero (NRZ) or return-to-zero (RZ), has been used as the format of choice in optical transmission systems. Another format such as DPSK is evaluated in comparison to OOK modulation format. Firstly, section 1.3.1 introduces the OOK modulation format briefly describing its characteristics and implementation devices. Secondly, section 1.3.2 describes DPSK format that is likely to replace OOK format in the future optical networks. In the future optical networks, various modulation formats may be selectively adopted depending on the different bit-rate and size of the optical network. Thus, the importance of mixed modulation formats such as OOK and DPSK signals is explained in section 1.3.3.

1.3.1   On-Off Keying (OOK)
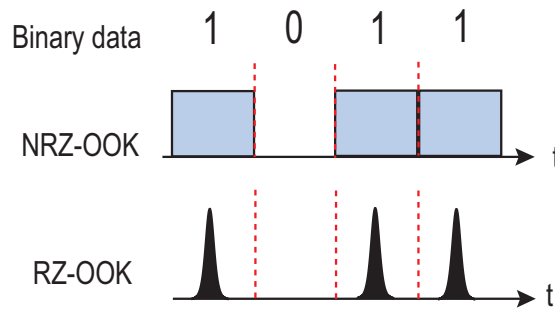
Figure 1.4: OOK modulation binary digital data.

1. INTRODUCTION

Since 1970's, OOK has been the format of choice for long-haul optical transmission systems. Different kinds of line coding can be applied to an OOK signal, and the most commonly used are NRZ and RZ. In the NRZ-OOK format as illustrated in Fig. 1.4, the pulse signal occupies the entire bit signal for 1 bit and no pulse for a 0 bit. However, RZ signal occupies exactly half of a bit period for a 1 bit and also no pulse for a 0 bit. Furthermore, the bandwidth of an NRZ format is smaller than a RZ format. The advantages of OOK format are its simplicity and low cost [15, 16]. Otherwise, a bad nonlinear tolerance characterisation can easily occur due to the existence of a strong optical carrier. Apart from that, the improvement can be done by using RZ-OOK signal. However, RZ signals needs higher peak transmit power to preserve similar energy per bit, hence the similar BER with NRZ modulation format.
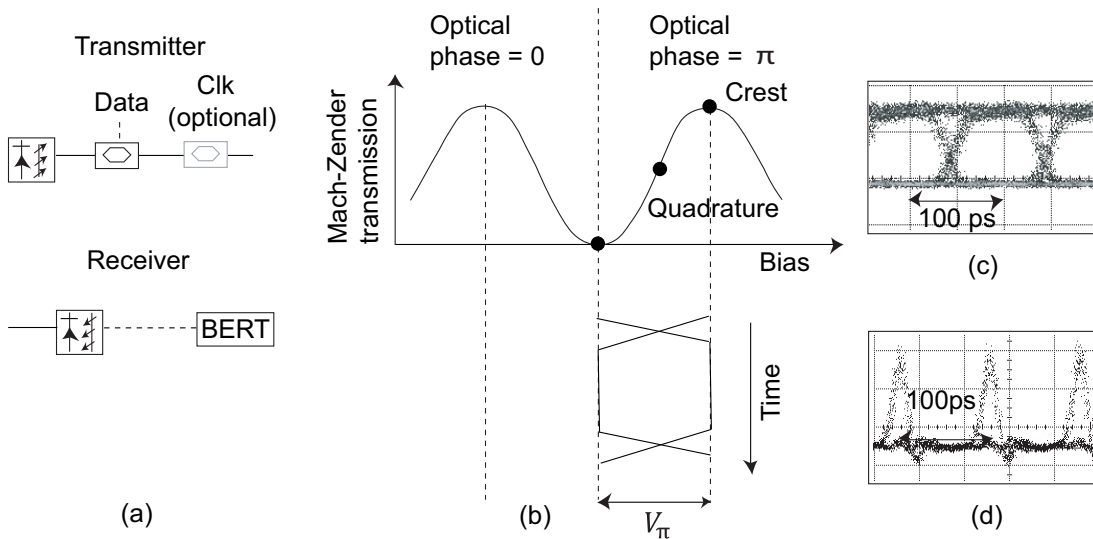
Figure 1.5: OOK modulation format, (a) modulation transmitter and receiver, (b) MZM operation and eye diagram of (c) demodulated NRZ-OOK and (d) RZ-OOK (50 ps/div.)

The structure of OOK signal transmitter of Mach-Zhender modulator (MZM) and receiver is shown in Figure 1.5 (a). At the transmitter, the modulation is obtained by switching a laser source between ON or OFF. Also, the modulation output can be achieved either by using MZM or electro-absorption types. However, MZM is preferred during long haul transmission in order to decrease the modulation residual chirp. The operation of a MZM for NRZ-OOK modulation is depicted in Figure 1.5 (b). For instance, MZM is biased in the quadrature point and is driven from minimum to max-

imum transmittance. The electrical drive signal is required, therefore peak-to-peak amplitude of V_π. MZM nonlinear transmission function can be suppressed through overshoots and ripples on the electrical drive. The back-to-back eye patterns of 10 Gb/s NRZ-OOK and demodulated RZ-OOK are depicted in Fig. 1.5 (c).
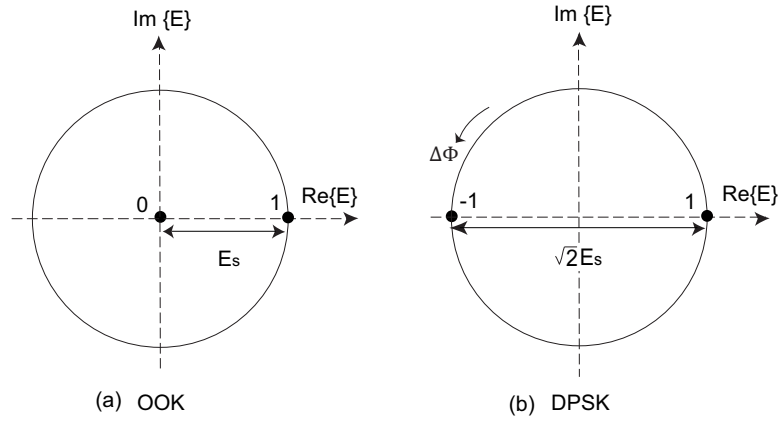
Figure 1.6: Signal constellation of binary (a)OOK and (b) DPSK.

1.3.2   Differential Phase-Shift Keying (DPSK)
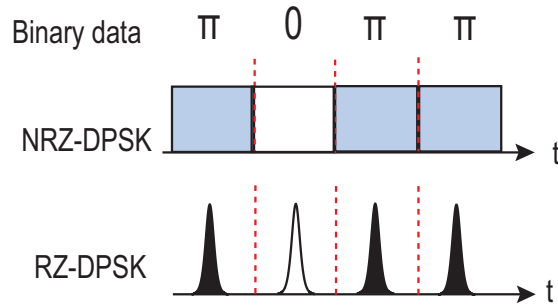
Figure 1.7: DPSK modulation binary digital data.

DPSK format carries the information in phases and the optical power appears in each bit slot [17]. The transmitted data of OOK format is either 1 or 0, but binary DPSK either NRZ or RZ encodes the data as 0 or π shift (i.e., 1 or -1) with constant amplitude as shown in Fig. 1.7. The main advantage of DPSK format in comparison with OOK signals is the lower optical signal noise ratio (OSNR) around 3 dB by using balanced detection [18, 19]. As shown in DPSK constellation diagram in Fig. 1.6 (b),

7

the separation between the two constellation points in DPSK is increased by $\sqrt{2}E_s$ when the same average signal power is used. The other advantage of DPSK format is more robust to some nonlinear effects, due to its optical power being evenly more distributed when compared with OOK format [17].
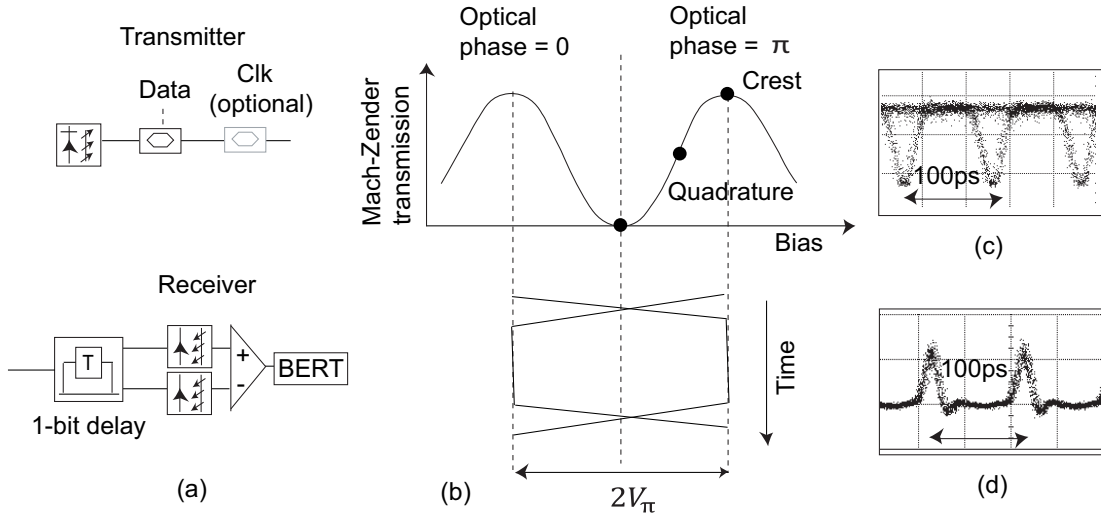
Figure 1.8: DPSK modulation format, (a) modulation transmitter and receiver of MZDI, (b) MZM operation and eye diagram of (c) demodulated NRZ-DPSK and (d) RZ-DPSK (50 ps/div.)

Transmitter of DPSK signal can be performed by using a phase modulator (PM) or by MZM. PM introduced chirp in between symbol transitions which can limit transmission tolerances due to nonlinear impairments and dispersion. On the other hand, MZM does not suffer from modulator induced chirp. Thus, MZM is more practical in comparison with PM. The required devices for DPSK transmitter are the same as OOK, based on MZM. As shown in Fig. 1.8 (a), the transmitter of MZM that created DPSK signal by biasing the electrical signal in the trough of the modulator curve. In order to obtain the "3-dB benefit" both MZDI output arms have to be detected simultaneously that is also known as balanced detection. As depicted in Fig. 1.8 (b), the electrical driving voltage has a peak-to-peak amplitude ideally $V_{pp} = 2V_\pi$. The amplitude is twice in comparison with NRZ-OOK modulation format. The principle layout of Mach-Zehnder delay-line interferometer (MZDI) receiver is shown if Fig. 1.8 (a). An MZDI consists of a delay T is equal to the bit period. A detector "amplitude imbalance, β is defined as [17]

$$\beta = \frac{S_A - S_B}{S_A + S_B} \tag{1.1}$$

where S_A and S_B are generally an opto-electronic factors for the destructive (A) and constructive (B) MZDI output arms. Thus, the balanced detection is achieved when $\beta = 0$ for $S_A = S_B$.

1.3.3 Mixed Modulation Formats

With the explosive growth in demand for higher capacity in optical networks, mixed modulation formats for signal transmission in WDM systems become essential. In future optical network applications, the modulation format may be upgraded from commonly used OOK to upgraded format DPSK or mixed together in backbone long-haul transmission lines. Thus, the influence of both formats in different applications must be considered and studied. In this thesis, some applications using mixed optical OOK and DPSK formats are demonstrated because they are mostly used.

Early-stage works based on potential applications using mixed modulation formats are further discussed in chapter 4. The work is focusing on waveform-wavelength conversion, optical demultplexing and transmission performance in between OPC and TDCM schemes.

1.4 Motivation and Research Aims

Optical networks segments, including backbone, metro, and access connected by nodes have different properties with diverse functionality. The higher service demand from the access segment towards upper level segments will lead to higher rate of functionality in the future. As the channel bit rate is moves from 2.5 Gb/s to higher bit-rates, the modulation formats, multiplexing systems, as well as traffic granularity are designed to meet the requirement of the sub-networks specifications. In the new era of network paradigm, different wavelength channels have different capacities (10/40/160 Gb/s) [20, 21]. However, the trade off has been found related to the suitability of modulation format, power penalty at the receiver site and complexity of the sub-networks when dealing with this network segment [22]. Besides, traffic demand across different networks may not require higher rates. Depending on traffic load, for example, the short reach of 40 Gb/s with OOK format is limited to short distances but, the scenario

likely can be improved with the use of 40-Gb/s DPSK format. Thus, intelligent line rates assignments with different modulation formats for overall network cost need to be explored. Various modulation formats are proposed for optical signal transmission in OTDM and WDM networks [16]. Generally, there is no specific modulation format that is better than others. In this thesis, we considered the popularly used OOK and DPSK modulation formats.

In various network applications, traditionally used modulation format such as OOK may be upgraded to advanced format or mixed together in the same transmission lines depending on their scales, applications, and costs. For instance, the necessity of such format combinations may be beneficial in the future, where switching or routing traffic from the WDM-based network segment with the assistance of add-drop multiplexer (OADM) are to transmit it further over fiber or to different OADM [22]. In addition, when optical signals are transmitted between different networks, the conversion between various optical modulation formats becomes a key functionality for network interconnection. Both OOK and DPSK modulation formats have its own advantages and disadvantages. For example, OOK format signal could be employed for a short reach path in a metro or regional segments due to its advantages such as having a simple configuration, while DPSK format can be used for long-haul backbones and access networks [23]. Besides that, signal processor ability to convert multiple channels with different modulation formats in the same operation scheme may be cost-effective and have less complex designs. Usually, a signal converter or processor is designed specifically to process a specific data format, and its application is limited. To adapt to different network applications, it is highly desirable to process various formats via a single converter in a flexible manner. On the other hand, the existing networks can be upgraded without the need to replace the equipment or change the in-line settings of the signal converter and transmission line. Thus, by employing mixed modulation formats in various network applications, the network cost can be reduced.

WDM systems have several problems that need to be monitored. The problems include linear and nonlinear effects of the transmission line, polarization mode dispersion (PMD), and crosstalk between adjacent channels. In general, impairments caused by chromatic dispersion, amplifier noise and fiber nonlinearities strongly limit the transmission reach of higher bit-rate signal than lower bit-rate signal [24]. To further reduce the signal-quality constraint, a long transmission path with higher bit-rate could be

transmitted using an upgraded modulation format, which is resistant to signal impairments and having high-bandwidth distance product [16, 20]. Moreover, as highlighted in ref. [25], the inter-channel crosstalk severely degrades the quality of the converted signals when single modulation formats such as OOK are passed simultaneously through the same processors. In order to overcome such limitations, the shift towards an alternative modulation formats is necessary. By introducing new system channels, the fiber total transmission capacity may possible to be increased, thus, the core networks bottleneck effect can be reduced. In addition, the influences of nonlinear effect can be minimize because the upgraded modulation formats provides a number of superior properties such as greater protection from interchannel crosstalk, better to channel filtering, less exposed of non-linear effects and chromatic dispersion effect. Apart from that, studies relating to mixed modulation formats have been relatively few and so far, there has not been any research focusing on all-optical signal processing with mixed modulation formats using the same optical signal converter. Thus, the consideration of this transition to facilitate the maintenance in optical networks is very important.

All-optical signal processing is a key technology for flexible optical network development. A suitable optical device should be able to operate at a data rate of 10 Gb/s or higher and over a wide wavelength range covering at least one band, for example C-band. In addition, varieties of all-optical signal conversion schemes based on nonlinearities and photonic devices have been proposed [26, 27]. However, none of these mentioned works focus on mixed modulations in various signal processing using the same operation devices. In order to realize mixed modulation format all-optical signal processing, the scheme must be considered to preserve the phase information. As highlighted in ref. [28], the XGM technique is more sensitive to OOK modulation format. Thus, it is not suitable to be used together with the upgraded format such as DPSK due to the intrinsic process. On the other hand, in the XPM method, a combination with interferometric device is necessary [29, 30] and intermediate conversion to an intensity modulation format such as ref. [31] needs to be added. Therefore, the complexity of this method can hardly be used to demonstrate signal processing with mixed modulation format. Furthermore, the self-sphase modulation (SPM) process is only appropriate for amplitude-modulated signals such as OOK instead of phase-modulated signals [26]. Other than that, to realize optical signal processing with single and mixed modulation formats that can preserve phase data signal, the best candidate is based on third-order

1. INTRODUCTION

nonlinear susceptibility χ^3 in a nonlinear fiber, which is known as four-wave mixing (FWM). For instance, the FWM process in fiber-based has the potential of accommodating mixed format signal processing, which has been shown for single modulation format of OOK or DPSK wavelength-waveform conversion, demultiplexing, and multicasting [32]. Meanwhile, HNLF has the advantages such as relatively high nonlinear coefficients, ultra-fast response, low insertion loss and uniform property along the fiber length [33]. Furthermore, FWM in optical fibers can enable all-optical signal processing functions, such as AND logic gates and signal regenerator. Thus, it would be of great interests to study fiber-based FWM AND-gate technique in mixed-transparently convert OTDM or WDM channels without using more that one pump signal.

Digital optical communications primarily employ between NRZ and RZ signals in linking and interfacing between OTDM and WDM networks. Considering different scales and requirements of different optical networks, the two types of formats may be selectively used. Among the available modulation formats, picosecond RZ pulse signal is still the most popular format for long haul systems, due to its simple configuration and large tolerance to impairment effects. Moreover, the picosecond range generates pulsewidth find application in the OTDM system. For an example, the pulsewidth for 160 Gbit/s OTDM transmission, can be estimated to be less than 2.5 ps, assuming a maximum width of 40 Gb/s of the time slot [34]. Moreover, the generation of picosecond RZ converted optical data should be in transform limited and have sech^2 form and small pedestal. Otherwise, the pulsewidth would increase during propagation in transmission lines and the data information will be lost due to the nonlinear interaction among pulses. At the same average optical power, a pulse with a larger pedestal would have smaller peak power, which is crucial for the high power pulse applications. Thus, a reliable and flexible high repetition source delivering short pulses in the broadband wavelength range and capable of being used with various applications appears to be the key device. Besides, we should also note that the picosecond converted pulses with flexibility in terms of pulsewidth variations allow considerably greater versatility and are proven to be beneficial in optimizing system performance. Apart from that, the adiabatic pulse compression technique utilizing Raman amplification has allowed pulse compression to picosecond durations, but exhibited problems with small pedestal. This useful approach not only is more benefit over continuous wave (CW) due to flexible spectral width, but also can provide energy as a pump in the HNLF process without

the use of extra erbium-doped fiber amplifier (EDFA). The main focus is based on the parametric process using one strong pump at a zero dispersion wavelength, with a single or mixed binary modulation format as the input probe pulse. Moreover, the used input pump signals in our research are CW and compressed RZ pulse clock with variations of input pulsewidth. This thesis is set out to determine a number of optical signal processing technologies including waveform-wavelength conversion with reshaping, all-optical demultiplexing, wavalength multicasting, and transmission performances which might significantly influence the design of long-haul transmission systems in the foreseeable future.

1.5 Thesis Structure

All-optical signal processing technologies are expected to become important for future high bit-rate communication systems to address the growing demand for network flexibility, low cost and high bandwidth. One of the promising candidates based on parametric process in a nonlinear fiber, is called FWM. Our scheme enables all-optical signal processing functions, such as an all-optical AND logic gates and regenerator. In addition, for high capacity optical transmission systems, high quality characteristics of the input and output pulses are also mandatory. A key requirement is using a compressed RZ clock pulse train from Raman amplifier-soliton compressor (RASC) and CW signal as a pump in FWM AND-gate process. As capacity increases, many new advanced modulation formats have been introduced. For these reasons, the shift towards traditional use of OOK format and the updated DPSK to be applied in many applications is necessary. This method serves as a basis for the base of all-optical signal processing techniques in our thesis including: all-optical NRZ-to-RZ data binary waveform-wavelength reshaping conversion single channel of DPSK format and mixed OOK-DPSK formats, all-optical RZ-OOK multicasting, all channel OTDM mixed format demultiplexing, and mixed format conversion between TDCM and OPC schemes. The thesis structure consists of five chapters as illustrated in Fig. 1.9.

Chapter 1 presents the general overview of fiber optical network architecture, optical multiplexing techniques, modulation formats, motivation and research aims of the thesis are explained.

Chapter 1
Introduction
(Scope and Aims)

Chapter 2
Technical
background

Chapter 3
Single modulation format
optical signal processing

3.1 Waveform-wavelength with
    reshaping conversion
3.2 All-optical wavelength multicasting

Chapter 4
Mixed modulation format
optical signal processing

4.1 All-optical signal demultiplexing
4.2 Waveform-wavelength conversion
4.3 Transmission performance between
    OPC and TDCM schemes

Chapter 5
Summary and
Outlook

Figure 1.9: Thesis structures.

Chapter 2 describes the theories operation of all-optical signal processing based on FWM AND-gates with CW and RZ pulsed pump in fiber HNLF. Furthermore, impairments that are relevant for long-haul fiber optic communication systems and important methods that are used in this thesis are also discussed. Lastly, the RZ compressed pulse concept using RASC and its usage is presented in the section of this chapter.

Chapter 3 presents a few demonstrations of an all-optical signal processing using single modulation format either OOK or DPSK. In the first section under this chapter, an NRZ-DPSK-to-RZ-DPSK waveform-wavelength conversion with flexible picosecond width-tunablity and signal regeneration with reshaping functionality. In the first demonstration, waveform-wavelength conversion of a 10-Gb/s DPSK signal without input signal degradation over wide input-output wavelength ranges is presented. In the second demonstration, it is also shown that the waveform-wavelength conversion with reshaping properties due to chromatic dispersion can be successfully converted at different Raman pump power settings over fiber links without dispersion compensation. In the second section, we experimentally demonstrate, for the first time, an all-optical

14

wavelength multicasting with width-tunable outputs. In our proposed diversity scheme, wide wavelength multicasting with nearly equal pulse widths is obtained.

Chapter 4 presents a few demonstrations of an all-optical signal processing by using mixed modulation format of OOK and DPSK either in WDM and OTDM schemes. In the first section, an all-optical demultiplexing of 40-Gb/s hybrid OTDM channels by using RASC-flexible control-window is demonstrated. In the second section, simultaneous four channels of mixed data formats waveform-wavelength conversion with tunable-width converted signals deploying the same devices as in Chapter 3. Four input NRZ mixed format probe channels at different wavelengths are interacted with compressed RZ clock pump to yield four converted RZ mixed data channels, where only one case of signal modulation format allocation is chosen. A full comparison for waveform-wavelength conversion in different format allocation is out of the research scope. Then, in the last section describes the experimental concept and results of the transmission performance between the midspan of TDCM and OPC with specialty using multichannel-mixed OOK and DPSK format.

Lastly, **Chapter 5** summarizes this thesis and a short outlook is given.

1. INTRODUCTION

References

[1] M. Saruwatari, "All-optical siganl processing for terabit/second optical transmission," *J. of Sel. Top. Quantum Electron.*, vol. 6, no. 6, pp. 1363-1374, Nov/Dec 2000.

[2] T. Morioka, "Ultrafast optical technologies for large-capacity TDM/WDM photonic networks," *Optical and Fiber Communications Research*, vol. 4, no. 1, pp. 14-40, 2007.

[3] B. -E. Olsson, and D. J. Blumenthal, "WDM to OTDM multiplexing using an ultrafast all-optical wavelength converter," *IEEE Photon. Technol. Lett.*, vol. 13, no. 9, pp. 1005-1007, 2004.

[4] G. K. P. Lei and Chester Shu, "Reconfigurable OTDM demultiplexing using time- and wavelength-interleaved pulses in an optical parametric amplifier," *IEEE Photon. Technol. Lett.*, vol. 23, no.16, pp. 1127-1129, Aug. 2011.

[5] P. Samadi, L. R. Chen, I. A. Kostko, P. Dumais, C. L. Callender, S. Jaacob, and B. Shia, "Reconfigurable OTDM demultiplexing using FWM in highly nonlinear fiber and a tunable planar lightwave circuit," *IEEE Photon. Technol. Lett.*, vol. 24, no.1, pp. 13-15, Jan. 2012.

[6] R. S. Tucker, G. Eisenstein, and S. K. Korotky, "Optical time-division multiplexing for high bit-rate transmission," *J. Lightwave Technol.*, vol. 6, no. 11, pp. 1737-1749, Nov. 1988.

[7] R. Ramaswami, and K. N. Sivarajan, *Optical networks: A practical perspective*, Morgan Kaufmann Publishers Inc. (1998).

REFERENCES

[8] G. E. Keiser, "A review of WDM technology and applications," *Elsevier Optical Fiber Technology*, vol. 5, no. 1, pp. 3-39, January 1999.

[9] H. Yoshimura, K. -I. Sato, and N. Takachio, "Future photonic transport networks based on WDM technologies," *IEEE Communications Magazine*, vol. 37, no. 2, pp. 74-81, Feb. 1999.

[10] F. Tong, "Multiwavelength receivers for WDM systems," *IEEE Communications Magazine*, vol. 36, no. 12, pp. 42-49, Dec. 1998.

[11] ITU-T Recommendation G.692, Optical interfaces for multichannel systems with optical amplifiers, March 1997.

[12] N. Shibata, K. Nosu, K. Iwashita, and Y. Azuma, "Transmission limitations due to fiber nonlinearities in optical FDM systems," *IEEE Journal on Selected Areas in Communications*, vol. 8, no. 6, pp. 1068-1077, August 1990.

[13] D. M. Spirit, A. D. Ellis, and P. E. Barnsley, "Optical time division multiplexing: systems, networks," *IEEE Communications Magazine*, vol. 32, no. 12, pp. 56-62, December 1994.

[14] S. Kawanishi, H. Takara, T. Morioka, O. Kamatani, K. Takiguchi, T. Kitoh, and M. Saruwatari, "Single channel 400 Gbit/s time-division-multiplexed transmission of 0.98 ps pulses over 40 km employing dispersion slope compensation," *IEEE Electronics Letter*, vol. 32, no. 10, pp. 916-918, May 1996.

[15] E. Lazzeri, A. T. Nguyen, N. Kataoka, N. Wada, A. Bogoni, and L. Poti, "All optical add and drop multiplexing node for hybrid topology networks," *J. Lightwave Technol.*, vol. 29, pp. 3676-3682, Dec 2011.

[16] P. Winzer and R. -J. Essiambre, "Advanced Optical Modulation Formats for high-capacity optical transport networks," *J. Lightwave Technol.*, vol. 24, no. 12, pp. 4711-4728, Dec 2006.

[17] A. H. Gnauck and P. J. Winzer, "Optical phase-shift-keyed transmission," *J. Lightwave Technol.*, vol. 23, no. 1, pp. 115–130, Jan 2005.

[18] P. A. Hummblet and M. Azizoglu, "On the bit error rate of lightwave systems with optical amplifiers," *J. Lightwave Technol.*, vol. 9, no. 11, pp. 1576–1582, Nov 1991.

[19] S. R. Chinn, D. M. Boroson, and J. C. Livas, "Sensitivity of optically preamplified DPSK receivers with Fabry-Perot filters," *J. Lightwave Technol.*, vol. 14, no. 3, pp. 370–376, Mar 1996.

[20] A. Nag, M. Tornatore, B. Mukherjee, "Optical network design with mixed line rates and multiple modulation formats," *J. Lightwave Technol.*, vol. 28, no. 4, pp. 466–475, Feb. 2010.

[21] N. Sambo, F. Cugini, G. Bottari, and P. Iovanna, "Toward high-rate and flexible optical networks," *IEEE Commun. Mag.*, vol. 50, no. 5, pp. 66–72, May 2012.

[22] E. Lazzeri, A. T. Nguyen, N. Kataoka, N. Wada, A. Bogoni, and L. Poti, "All optical add and drop multiplexing node for hybrid topology networks," *J. Lightwave Technol.*, vol. 29, no. 24, pp. 3676–3682, Dec. 2011.

[23] T. Mizuochi, K. Ishida, T. Kobayashi, J. Abe, K. Kinjo, K. Motoshima, and K. Kasahara, "A comparative study of DPSK and OOK WDM transmission over transoceanic distances and their performance degradations due to nonlinear phase noise," *J. Lightwave Technol.*, vol. 21, no. 9, pp. 1933–1943, Sept. 2003.

[24] G. P. Agrawal, *Fiber-optic communication systems*, Wiley Interscience, (2002).

[25] P. Devgan, R. Tang, V. S. Grigoryan, and P. Kumar, "Highly efficient multichannel wavelength conversion of DPSK signals," *J. Lightwave Technol.*, vol. 24, no. 10, pp.3677–3681, Oct. 2006.

[26] A. E. Willner, S. Khaleghi, M. R. Chitgarha, and O. F. Yilmaz, "All-optical signal processing," *J. Lightwave Technol.*, vol. 32, no. 4, pp.660–680, Feb. 2014.

[27] L. Yan, A. E. Willner, X. Wu, A. Yi, A. Bogoni, Z. -Y. Chen, and H. -Y. Jiang, "All-optical signal processing for ultrahigh speed optical systems and networks," *J. Lightwave Technol.*, vol. 30, no. 24, pp.3760–3770, Dec. 2012.

[28] E. Ciaramella, "Wavelength conversion and all-optical regeneration: achievements and open issues," *J. Lightwave Technol.*, vol. 30, no. 4, pp.572–582, Feb. 2012.

REFERENCES

[29] N. J. Doran and D.Wood,"Nonlinear-optical loop mirror," *Opt. Lett.*, vol. 13, no. 1, pp. 56-58, 1988.

[30] K. A. Rauschenbach, K. L. Hall, J. C. Livas, and G. Raybon, "All-optical pulsewidth and wavelength conversion at 10 Gb/s using a non- linear optical loop mirror," *IEEE Photon. Technol. Lett.*, vol. 6, no. 9, pp. 1130-1132, Sep. 1994.

[31] P. Vorreau, A. Marculescu, J. Wang, G. Bottger, B. Sartorius, C. Bornholdt, J. Slovak, M. Schlak, C. Schmidt, S. Tsadka, W. Freude, and J. Leuthold,"Cascadability and regenerative properties of SOA all-optical DPSK wavelength converters," *Photon. Technol. Lett.*, vol. 18, no. 18, pp. 1970-1972, Sept. 2006.

[32] H. Nakazawa and H. Weber *Ultrahigh-speed optical transmission technology*, Springer Science, (2007).

[33] S. Watanabe,"Optical signal processing using nonlinear fibers," *J. Opt. Fiber. Commun.*, vol. 3, no. 1, pp. 1-24, 2006.

[34] T. Morioka, "Ultrafast optical technologies for large-capacity TDM/WDM photonic networks," *Optical and Fiber Communications Research*, vol. 4, no. 1, pp. 14–40, 2007

Chapter 2

Technical Background

Previously, nonlinearities would limit the performance of fiber-optic communication systems limiting capacity and reach of fiber-optic transmission systems. However, since 1980s the situation has been changed and found to be mostly irrelevant for system design due to the limitation caused by fiber losses and group-velocity dispersion (GVD). FWM is one of the well-known nonlinear effects in optical fibers. FWM can be be used as an all-optical AND logic gates and signal regenerators. As data rates increased, the impact of impairments such as chromatic dispersion limits the feasible transmission distance. For the reason, more sophisticated methods are required to improve the transmission quality. Furthermore, as we move towards higher bit-rates, ultra-short optical pulses are required to be formed and multiplexed. Furthermore, the use of RZ format with tunable pulsewidth can be optimized to provide the best immunity against transmission impairments. With this interest, in this chapter, the nonlinear effect of FWM to be used for the demonstrations within this thesis are briefly introduced together its applications for all-optical signal processing. The impairments such as chromatic dispersion that is relevant for long-haul fiber optic communication systems and an important method that are used in this thesis are also discussed in the next section. Finally, the RZ compressed pulse using Raman adiabatic soliton compressor (RASC) and its benefits is presented in the last section.

2. TECHNICAL BACKGROUND

2.1 Pulse Propagation

In 1926, Erwin Schrodinger proposed the Schrodinger equation the space and time-dependence of a quantum mechanical system that present a central role in quantum mechanics. The nonlinear Schrodinger equation (NLSE) presents an evolution in quantum mechanics and models a single polarization optical field E(z,t) in an optical fiber [1] as,

$$\frac{dE}{dz} = - \underbrace{\frac{\alpha}{2}E}_{attenuation} - \underbrace{\frac{i}{2}\beta_2\frac{\delta^2 E}{\delta T^2}}_{dispersion} + \underbrace{\frac{1}{6}\beta_3\frac{\delta^3 E}{\delta T^3}}_{dispersionslope} + \underbrace{i\gamma|E|^2 E}_{Kerr} \tag{2.1}$$

where E, is the optical field complex envelope, z the propagation distance, $T = t - z/v_g$ is the time measured in a retarded frame and α attenuation coefficient in [Np/km]. Meanwhile, $i\gamma|E|^2 E$ is the nonlinear contribution to the NLSE. The derivation of the nonlinear come wave equation, which presents the propagation of light through an optical fiber and written as,

$$\nabla \times \nabla \times E(z,t) = -\frac{1}{c^2}\frac{\delta^2 E(z,t)}{\delta t^2} - \mu_0\frac{\delta^2 p(z,t)}{\delta t^2} \tag{2.2}$$

∇, E(z,t), and P(z,t) represent the differential vector operator, vector of electrical field and the dielectric of polarization vector, respectively.

The origin of fundamental level of nonlinear response is related to harmonic motion of bound electrons under the effect of an applied field. Thus, the total polarization P induced by electric dipoles is not linear in the electric field E, but satisfies the more general relation as [1],

$$P = \epsilon_0(\chi^1 E + (\chi^2 EE + (\chi^3 EEE + ...) \tag{2.3}$$

where ϵ_0 is the vacuum permittivity and (χ^j) is jth order susceptibility. Generally, in the transmission systems the susceptibilities that is higher than the 3rd order are very small and can be neglected. The linear susceptibility (χ^1) contributes a dominant part to P through effects like power loss and material dispersion. This effects are included through the refractive index n and the attenuation coefficient . The (χ^2) is responsible for such nonlinear effects for instance difference frequency generation (DFG) that can be employed in a periodically-poled lithium-niobate (PPLN) waveguide. The (χ^2) that

can be neglected if related to symmetric molecule structure such as silica glasses SiO_2 or semiconductor optical amplifier (SOA). As a result, the dominant nonlinear effects are mainly related to the third order susceptibility (χ^3).

Nonlinearities can be divided into two categories: first category is the effects arising from the refraction on nonlinear index such as self-phase modulation (SPM), cross-phase modulation (XPM), cross-gain modulation (XGM), FWM and stimulated scattering (Raman and Brillouin). Another category is the effects of stimulated scattering including Raman and Brillioun.

The refractive index for the nonlinear effects that originates from nonlinear refraction can be written as,

$$n(\omega, |A|^2) = n_0(\omega) + n_2 \frac{|A|^2}{A_{eff}} \tag{2.4}$$

where n_0, n_2 , $|A|^2$, and A_{eff} are linear, nonlinear refractive index, optical power inside the nonlinear medium, and effective mode area of medium, respectively. The intensity dependence of the refractive index leads to the intensity dependence of the phase and resulting in a large number of interesting nonlinear effects such as SPM and XPM. As a conclusion from Eq. (2.4), the impact of the Kerr effect is proportional to the optical power of $|A|^2$. Due to the fiber attenuation effects during fiber transmission, the signal power is exponentially reduced. Thus, the influence of Kerr effect in the first part will become the strongest. It is usually referred as a high power region. For a fiber with length L, the high power region is defined by effective length as [1]

$$L_{eff} = \frac{1 - \exp(-\alpha L)}{\alpha} \tag{2.5}$$

The Kerr impact during transmission system with length L is given by the nonlinear length L_{NL}, which is defined as

$$L_{NL} = \frac{1}{\gamma P_{in}} \tag{2.6}$$

where where P_{in} is the optical power launched into the fiber and γ the fiber nonlinear coefficient and the equation is given as

$$\gamma = \frac{2\pi n_2}{\lambda A_{eff}} \tag{2.7}$$

2.2 Theory of FWM
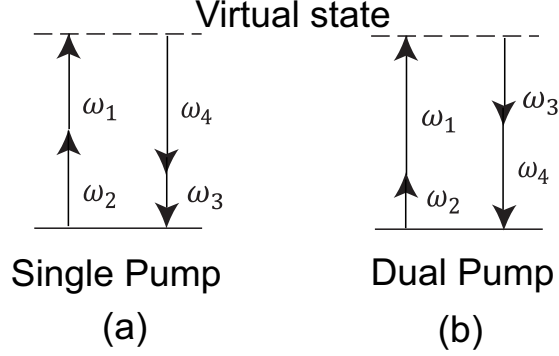
Figure 2.1: (a) Single pump and (b) dual pump FWM.

FWM is one of a well-known nonlinear effects in optical fibers which is also the first of the Kerr-nonlinear effect. FWM is a kind of optical parametric oscillation. The FWM process originates from third order nonlinear susceptibility ($\chi^{(3)}$). The nonlinear Schrodinger mathematical description can be used as the starting point to describe the interaction among the waves involved in the FWM process.

$$\frac{dE_p}{dz} + \frac{1}{2}\alpha E_p = i\gamma(|E_p|^2 + 2|E_s|^2 + 2|E_i|^2)E_p + 2i\gamma E_p^* E_s E_i \exp(\mathrm{i}\Delta\beta\mathrm{z}) \qquad (2.8)$$

$$\frac{dE_s}{dz} + \frac{1}{2}\alpha E_s = i\gamma(|E_s|^2 + 2|E_i|^2 + 2|E_p|^2)E_s + 2i\gamma E_i^* E_p^2 \exp(-\mathrm{i}\Delta\beta\mathrm{z}) \qquad (2.9)$$

$$\frac{dE_i}{dz} + \frac{1}{2}\alpha E_i = i\gamma(|E_i|^2 + 2|E_p|^2 + 2|E_s|^2)E_i + 2i\gamma E_s^* E_p^2 \exp(-\mathrm{i}\Delta\beta\mathrm{z}) \qquad (2.10)$$

where z is the longitudinal coordinate of the fiber, α is the attenuation coefficient of the fiber, and E_p, E_s and E_i are the electric field of the pump, input signal and idler waves. γ is the nonlinear coefficient and is given by Eq. (2.7). Meanwhile, $\Delta\beta$ is phase-matching factor and can be obtained later under this section.

FWM occurs when the light of two or more different wavelengths is inserted into a fiber, to form a new idler wave. For example, when three signal with frequencies ω_1, ω_2, and ω_3, the frequency of the new generated FWM idler are as follows [2]:

$$\omega_{1,2,3} = \omega_1 \pm \omega_2 \pm \omega_3 \tag{2.11}$$

In general, considering M original channels of a WDM system, possible number of possible FWM idlers is written by [3]:

$$N = 0.5M^2(M - 1) \tag{2.12}$$

Fig. 2.1 (a) and (b) are a depicted figures show degenerate FWM operation based on an energy level. When a two strong pump at the same frequency $\omega_1 = \omega_2 = \omega_p$ generates a low-frequency side band at ω_3 and a high-frequency sideband at ω_4, when we assume $\omega_4 > \omega_3$. These sideband in Raman scattering are called as the Stokes and anti-Stokes bands, respectively, which are often also called the probe and idler bands [4]. The idler frequency is converted symmetrically to the probe signal frequency with respect to the pump signal. The idler frequency equation may be written as:

$$\omega_p - \omega_3 = \omega_4 - \omega_p \tag{2.13}$$

$$\omega_3 = 2\omega_p - \omega_4 \tag{2.14}$$

$$\omega_i = 2\omega_p - \omega_s = \omega_p - \Delta\omega \tag{2.15}$$

Notes: Assumed that ω_s, ω_i, and ω_p are the frequencies of probe signal, idler, and pump waves. $\Delta\omega$ is the wavelength spacing between pump and input signal as shown in Fig. 2.2 (a).

Similarly, the idler signal electrical field is proportional to:

$$E_i(t) \propto (E_p)^2 E_s^*(t) \tag{2.16}$$

Meanwhile, the general case of two independent pump as shown in the fig. 2.2 (b) where two pumps at different frequencies ω_{p1} and ω_{p2} are sent into the nonlinear device, the generation of multiple mixed idler signals such as:

$$\omega_{i1} = 2\omega_{p1} - \omega_s = \omega_{p1} + \Delta\omega \tag{2.17}$$
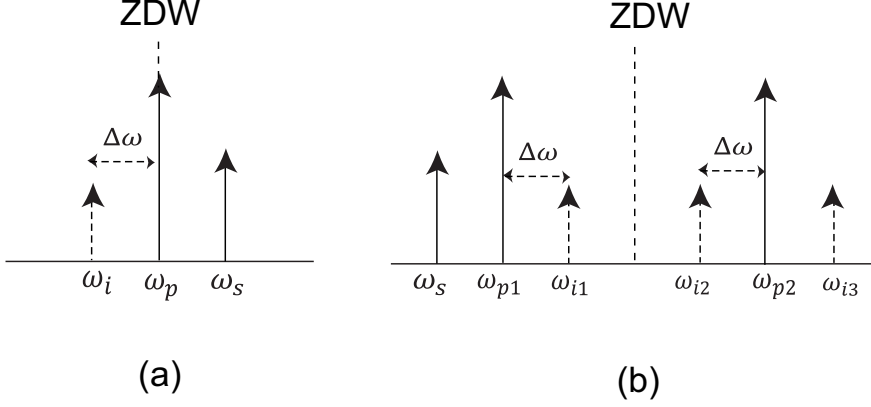
Figure 2.2: (a) Single pump and (b) dual pump degenerate FWM frequency signal allocation.

$$\omega_{i2} = \omega_{p1} + \omega_{p2} - \omega_s = \omega_{p2} - \Delta\omega \tag{2.18}$$

$$\omega_{i3} = \omega_s + \omega_{p2} - \omega_{p1} = \omega_{p2} + \Delta\omega \tag{2.19}$$

In addition, electrical amplitudes proportional to:

$$E_{i1}(t) \propto (E_{p1})^2 E_s^*(t) \tag{2.20}$$

$$E_{i2}(t) \propto E_{p1}E_{p2}E_s^*(t) \tag{2.21}$$

$$E_{i3}(t) \propto E_s(t)E_{p2}E_{p1}^*(t) \tag{2.22}$$

Simultaneous interaction in between two pump FWM resulted in both phase conjugate and also non-phase conjugate during wavelength conversions.

Four-wave-mixing (FWM) is dependent on phase matching when the pump allocation is allocated around zero dispersion wavelength (ZDW) [5, 6]. FWM efficiency, η can be expressed as [7, 8],

$$\eta = \frac{\alpha^2}{\alpha^2 + \Delta\beta}\{1 + \frac{4\exp(-\alpha L)\sin^2(\Delta\beta L/2)}{[1 - \exp(-\alpha L)]^2}\} \tag{2.23}$$

where $\Delta\beta$ is referred to as the phase-matching factor or propagation constant,

$$\Delta\beta = -\frac{2\pi c \cdot \lambda_0^3}{\lambda_p^3 \lambda_s^2} \frac{dD_c}{d\lambda}(\lambda_p - \lambda_0)(\lambda_p - \lambda_s)^2 \tag{2.24}$$

where λ_0, λ_p, and λ_s are ZDW, pump and probe signal wavelength, respectively. D_c is fiber dispersion. According from Eq. (2.24), the FWM efficiency depends on the fiber dispersion and channel separation. The maximum value of $\eta = 1$ when the phase matching is satisfied, for an example $\Delta\beta = 0$. In the case of pump wavelength is at ZDW, the phase mismatch that occurred caused by the fiber dispersion will be vanished [9]. FWM efficiency is dependent to the phase-matching condition, that is related to conservation of momentum. The relationship is due to the group velocities of the interacting waves when different channels propagate at different velocities, making FWM efficiency low. However, at the ZDW, different channels propagate at approximately the same velocity. Furthermore, the FWM efficiency will become high when the probe wavelength is located near to the wavelength of λ_0. Hence, the FWM efficiency decreases for channels that are located farther away and by the increase of fiber dispersion. Eventough smaller channel spacing can increase FWM efficiency, due to interchannel crosstalk the system performance can severely be degraded. However, dispersion-shifted fibers (DSFs) with a dispersion value of about 4 ps/(km-nm) is large enough to suppress FWM [10].

2.2.1   Basic Concept of FWM AND-Gate
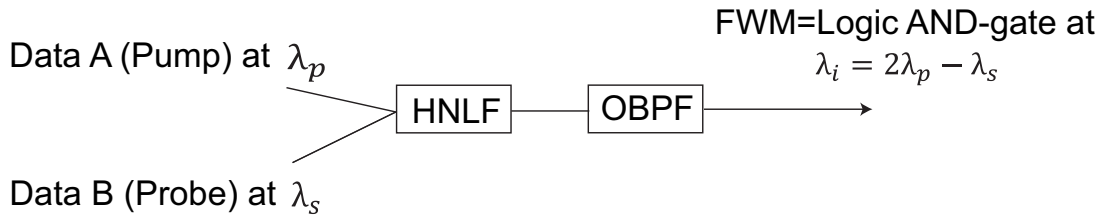
Figure 2.3: Schematic diagram of all-optical AND-gate.

The principle operation of an all-optical signal processing in various nonlinear media is mostly used logic gates. All-optical logic functions such as AND, NOT, OR, and XOR have been demonstrated using nonlinear effects including semiconductor optical amplifier (SOA), cross gain modulation (XGM), cross-phase modulation (XPM), and four-wave mixing (FWM) [11–13].
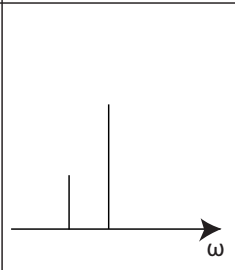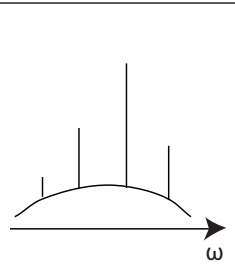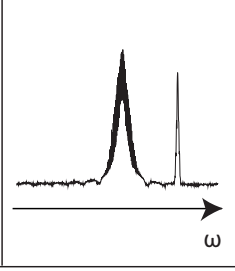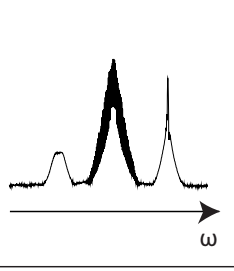
Data A (Pump signal)	Data B (Probe signal)	A AND B operation
0	0	1
0	1	0
1	0	0
1	1	1

Table 2.1: AND-gate logic operation

The basic operation of a FWM-based AND gate is shown in Fig. 2.3. An optical AND-gate operation is based on two serial data A and data B. Data A at frequency ω_1 and data B at ω_2 are pump and probe signals, respectively. When both signals are injected into HNLF, the idler signal with the frequency of $\omega_i = 2\omega_p - \omega_s$ is generated, that is equal to the AND logic gate operation. In the AND logic gate as shown in table 2.1, if both inserted signals are equivalent to "1" the FWM output signal is equal to "1", otherwise will be "0". The optical filter are required to filter out the generated idler wavelengths after AND-gate.

Figure 2.4: Comparison of FWM with CW and with picosecond RZ pulse.

All experimental considerations presented in this thesis are based on continuous wave (CW) and RZ pulse train input pump signals. As shown in Fig. 2.4, the main FWM applications under CW signal pump arrangement are wavelength conversion and

optical phase conjugation (OPC). The term pulsed FWM AND-gate is used, if inserted probe and pump signals are both short RZ optical pulses in the range of picoseconds width. For a number of applications, such as demultiplexing, add-drop multiplexing, regenerative waveform-wavelength conversion, and sampling, it is desirable to generate shorter width of the converted signal. Thus, as shown in Fig. 2.4 the use of a pulse train RZ in fiber-based AND-gate is therefore indispensable for picosecond converted pulse generation. Detail explanation for applications is explained detail under section 2.2.2.

2.2.2   Applications of Fiber-based AND-Gate

In fiber-based AND-gate, FWM can be used in different applications. HNLF has been developed as an optical fiber that is suitable to be used as nonlinear medium in a variety of optical signal processing technologies [14]. The main applications of HNLF FWM AND-gate are wavelength-waveform conversion, signal regeneration, optical phase-conjugation, sampling gate and demultiplexer.

2.2.2.1   Wavelength Conversion and Signal Regeneration

More than 20 years ago the concepts of wavelength conversion and signal regeneration have been studied by researchers. Wavelength conversion and signal regeneration represents a key functionality for improving signal routing and signal quality for optical networks. Particularly, wavelength conversion at key network nodes allow interoperability, reconfigurability and wavelength reuse [15–18]. One of the reasons is the high demand for efficient transportation of data information in WDM optical networks [9]. The wavelength converter is a simple device that functioning as a signal converter that convert data on an inserted wavelength to a new possibly different wavelength among N wavelength in a system [20]. Potential characterization of an all-optical wavelength converters are (a) ability to operate with different modulation format, (b) independence to polarization, (c) wide wavelength conversion to both longer and shorter wavelengths, (d) high operational speed, and (e) simple configuration [20, 21]. Few techniques using different nonlinear media have been proposed [22–26] to make these functions more effective and robust.

FWM in fiber-based hold great interest with the advantages of high speed conversion, ultrafast response and wide wavelength tuning range [27]. The concept of
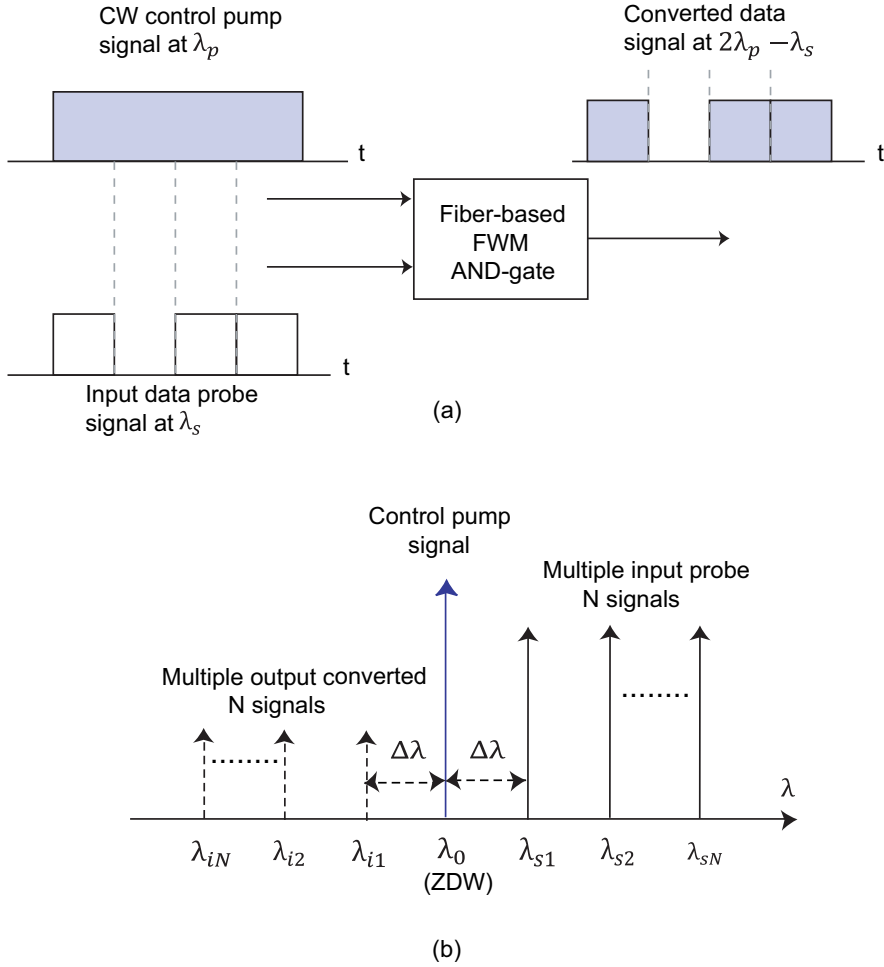
Figure 2.5: All-optical AND gate operated as wavelength converter.

wavelength conversion based on single pump FWM technique is shown in Fig. 2.5. The following requirements must be met in order to achieve these functionality:

(a) wavelength of the pump signal must be allocated within zero-dispersion wavelength (ZDW). As shown in Fig 2.5 (a), a data signal at the frequency of λ_s and for example continuous wave (CW) as a control pump at the λ_p, resulting a conversion of data signal to another wavelength λ_i equal to $2\lambda_p$ - λ_s. At the output of fiber-based AND-gate FWM, the wavelength converted data signal have a shape and temporal position same as the input data signal. In addition, as shown in Fig. 2.5 (b) the multichannel wavelength conversion is possible when several input wavelengths are simultaneously converted. The proposed wavelength converter using single pump for multiple input

30

signal able to maintain the similar performances for the converted channels at the detuning wavelength of $2\lambda_p - (\lambda_{sN} + N \cdot \Delta\lambda)$ in the FWM spectrum. λ_{s1} is the wavelength for the first input channel, $\Delta\lambda$ is the channel spacing between multiple channels and $N = 0, 1, 2, 3...$ The FWM conversion bandwidth will become narrower if $\Delta\lambda$ become larger.

(b) minimized the chromatic dispersion variation in the longitudinal direction of the fiber. A wide wavelength conversion bandwidth can be achieved when the consideration to coherence of the fiber length is considered. The short fiber length can also satisfy the requirement in (c) that results in consistent dispersion along the fiber [28, 29].

(c) polarization states between the pump and input data signal must coincide. In addition, the state of polarization consists of vertical and horizontal that propagate along fiber will have difference group velocities ($\triangle\beta$), as [30],

$$\triangle\beta = \frac{\omega \triangle n}{c} \qquad (2.25)$$

where ω, $\triangle\beta$, and c are angular optical frequency, birefringence of the fiber and velocity of light, respectively. The fiber birefringence effect can be called as differential group delay (DGD). Element of certain DGD is defined as,

$$\triangle\tau = L \cdot \triangle\beta \qquad (2.26)$$

L is the length of the birefringence element. Thus, reducing length of birefringence element can control the problem of polarization effect. HNLF-dispersion shifted fiber (DSF) length $\simeq$500 m with PMD value of 0.05 ps/rt-km that is used in our works is sufficiently small enough to fulfill above mentioned requirements. In our work, the polarization states of pump and inserted signal is adjusted by using two polarization controllers (PCs) to optimize the highest conversion efficiency.

Optical signal regeneration is the technique for remove the signals that have been impaired caused by noise when signal propagate in a path through a network and as well as in the switching nodes. Due to the degradation of the amplitude because of random fluctuations in the power levels of logical marks "1" and logical spaces "0". Thus, signal regeneration implementation need to be installed to clean up and enhanced robustness while maintaining the flexibility in the network [31]. Signal regeneration consist of three levels as shown in Fig. 2.6: 1R(re-amplification), 2R(re-amplification and reshaping),
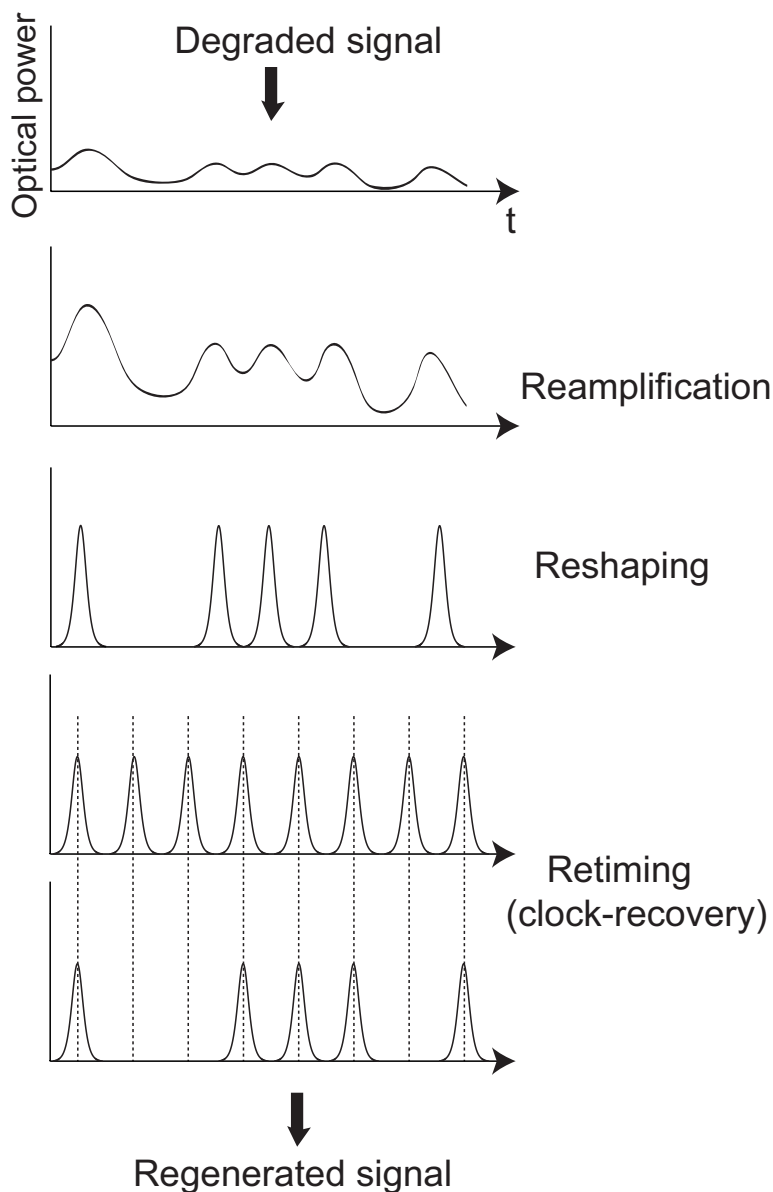
Figure 2.6: 3R all-optical signal regeneration.

and 3R (re-amplification, reshaping, and retiming) that can be done in the optical domain by nonlinear optical devices. In both cases, the crucial stage is reshaping that could provide enhancement of extinction ratio and intensity noise reduction. A commonly used regeneration configuration in the case of amplitude signal is shown in Fig. 2.5. An input data signal at wavelength λ_A and a pump signal at wavelength λ_B are applied to the input(s) of a gating device. For 1R regeneration, In the case of 2R

regeneration, the clock recovery or timing clock is absent. As for 3R regeneration, an optical clock is required to perform a clock decision function and provide only retiming. The regenerated pulses follow by the shape of the clock pulses [32, 33]. Thus, clock function is an important part of the reshaping. In our work in section 3.1.4.3, the use of RZ clock pump FWM approach to realize reshaping effect at different pulsewidth for a waveform-wavelength conversion for degraded signal. The signal regeneration properties of FWM converted power is expressed as [33]:

$$P_i = \eta \gamma^2 P_p^2 P_s \exp(-\alpha \mathrm{L})\{\frac{[1 - \exp(-\alpha \mathrm{L})]^2}{\alpha^2}\} \qquad (2.27)$$

where η is the FWM efficiency, γ is the nonlinear coefficient of the fiber, and α is the attenuation coefficient of the fiber. P_i, P_p and P_s are the powers of the idler, pump and the probe signals of FWM, respectively.
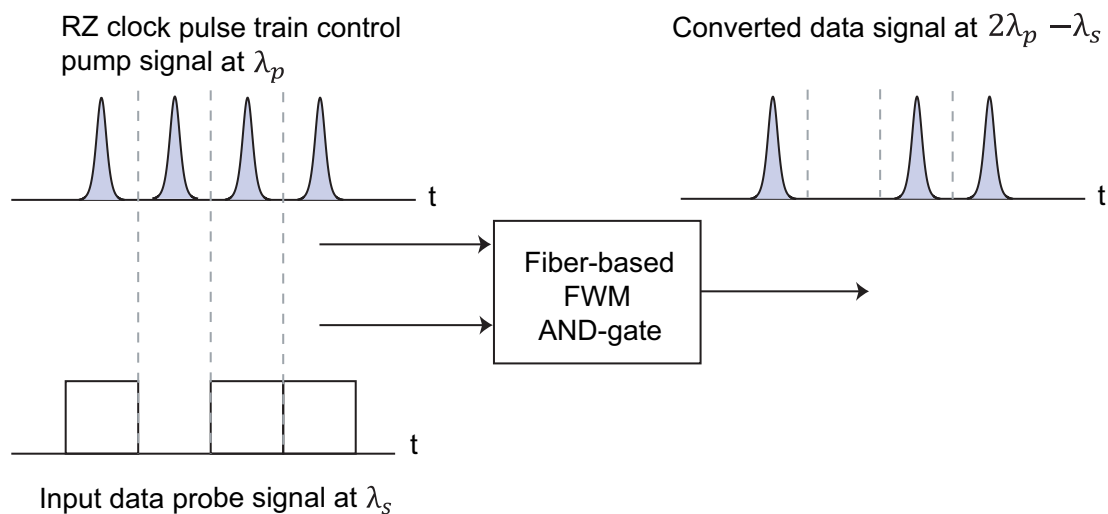
Figure 2.7: All-optical FWM AND-gate operated as reshaping waveform converter.

The same wavelength conversion configuration also can be used as a signal regeneration with reshaping by replacing the CW with a periodic RZ clock pulse as shown in Fig. 2.7. On the other hand, NRZ-to-RZ waveform-wavelength conversion with signal reshaping can be realized if NRZ modulation input data probe signal at the wavelength is inserted together with the input RZ clock pump. The experiment is presented in section 3.1, where the signal regeneration through 2R properties of the fiber-based FWM AND-gate device using degraded input NRZ signal.

2. TECHNICAL BACKGROUND

2.2.2.2   Other Applications

An OTDM demultiplexing and optical sampling based on a fiber-based FWM AND-gate can also be implemented by using an RZ clock pulse as a control pump signal as shown in Fig. 2.8. An optical sampling technique can be performed employing an RZ clock pulse to extract optical samples from the data input stream.

RZ clock pulse train control
pump signal at λ_p

Demultiplexing data signal at $2\lambda_p - \lambda_s$

Fiber-based
FWM
AND-gate

OTDM data probe signal at λ_s
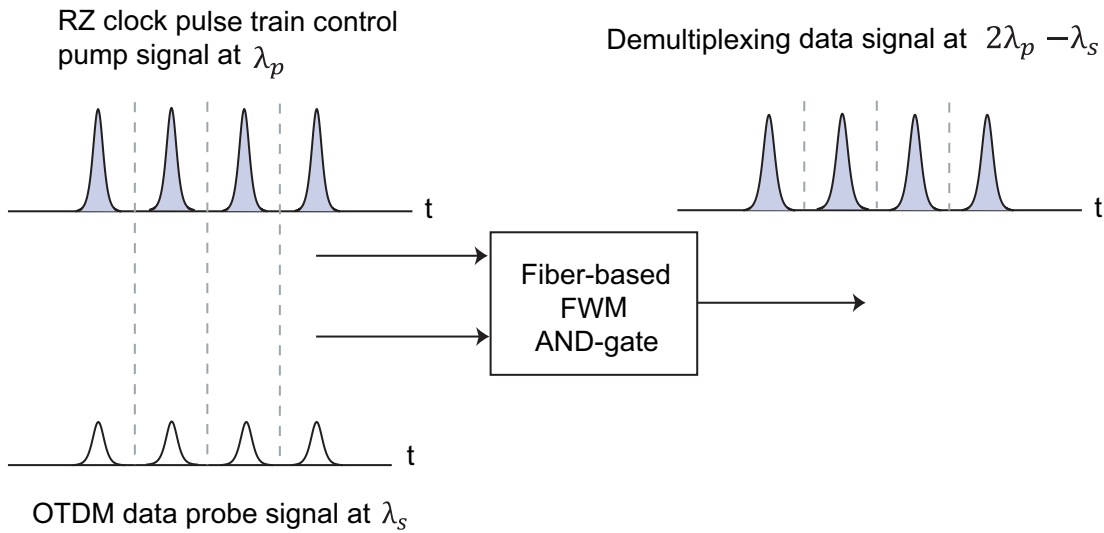
Figure 2.8: All-optical AND gate operated as demultiplexer and sampling gate.

In order to achieve a high temporal resolution sampling, the width of the gating window must be as small as possible [34]. On the other hand, in demultiplexing technique, the demultiplexer FWM AND-gate function can be used to extract one channel at the bit-interleaving OTDM data stream for further electrical signal processing at the receiver [35]. As shown in Fig. 2.8, the gating window should have a reasonable width to avoid timing misalignment among adjacent channels [36]. The target demultiplexed channel can be selected by aligning the position of the RZ control pulses with respect to the input OTDM data signal. At the high-speed OTDM systems up to 160 Gb/s, the synchronization between control pump pulse and data stream can be realized through clock recovery [37–39]. However, the clock recovery studies is beyond the scope of our research work.

2.3 RZ Pulse Train Pulse Clock using RASC

An invaluable element for ultrafast optical communication systems is a sub-picoseconds RZ optical pulse train generator at the data clock speed or bit rate [40, 41]. With the increase of bit rate, higher repetition rate of RZ pulse train is needed. The most common method to generate RZ pulse train is using a mode-locked laser (MLL). However, MLLs are expensive and not affordable for some laboratories and real system applications. Through FWM AND-gate, the parametric gain in HNLF was able to generate converted RZ pulse at the output with narrow widths.

2.3.1 Basic Concept of Raman Amplification
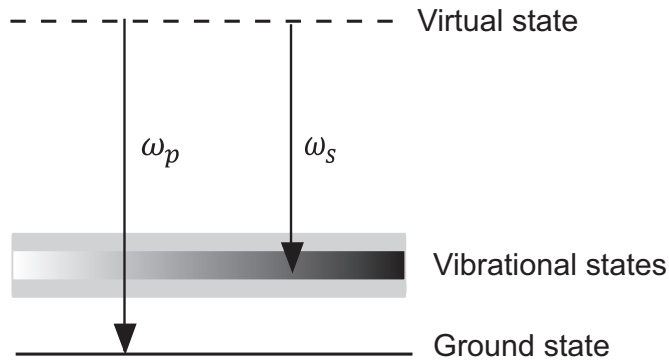
Figure 2.9: Energy level scheme associated with SRS.

Optical amplifiers offer some benefits over regenerators. Regenerators usually used specifically to the bit rate and modulations formats but amplifiers are insensitive to the bit rate or formats. Therefore, an amplifiers are easily upgraded compared to regenerators. Two competing technologies emerged: the first was erbium- doped fiber amplifiers (EDFA) and the second Raman amplification. The concept of RA is based on SRS that was introduced early in the 1970s [42]. The Raman amplifier (RZ) rely on the SRS effect of transmission fiber, that transfers the energy of higher-frequency pump signals to lower-frequency signals [43]. Three important points of SRS affects are (1) can be occurred in any fiber; (2) when the pump photon is excited to a virtual level, gain of Raman can be occurred at any signal wavelength by proper choice of the pump wavelength; and (3) the gain process of Raman is very fast. As shown in Fig. 2.9, when the frequency of the scattered photon is longer than the incident photon, meaning

that the energy has been lost in the process. Thus, the scattered wavelength photons can produce stimulated emission of another photon at the same wavelength, hence amplification [44]. The characteristics of transmission fiber impact Raman gain and must be taken into account in amplifier design. Commonly used fibers included SMF, DSF, DCF and etc. Using two to three pump lasers with small different wavelengths in the 1480-nm region comprises a broadband amplifier that covers C to L-band. Different pump powers are required to achieve the same gain. RA provides more flexibility than EDFA. Both gain and gain shape can be adjusted by pump powers. RAs offered the following advantages: (1) existence of Raman Raman gain in every fiber for terminal ends cost-effective improvement, (2) the availability of gain over entire region from approximately 300 to 2000 nm, (3) the gain spectrum can be fitted by adjusting the pump wavelengths and, (4) a relatively broad-band amplifier with a bandwidth 5 THz, and the gain is practically flat over a wide wavelength range.
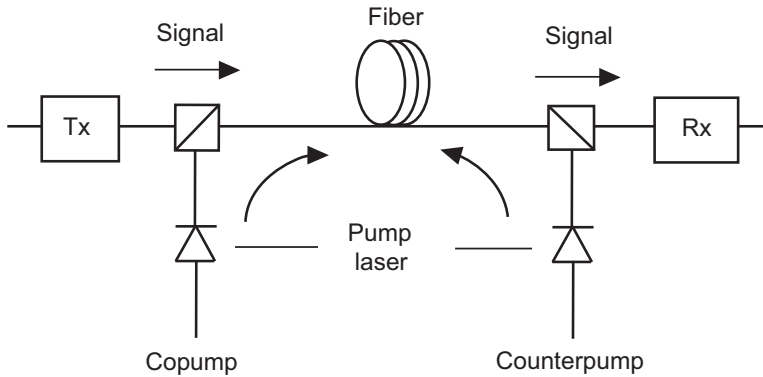
Figure 2.10: Schematic of an optical communication system employing Raman amplification [43].

As shown in Fig. 2.10, the RA generally contains a gain fiber, a WDM coupler for combining the pump and the signal at the transmitter and receiver ends. The signal propagation are from the transmitter (Tx) to the receiver (Rx). The RA can be designed either as a distributed or discrete (lumped) amplifier. The RA can be pumped using three different configurations: forward pumping (copump), backward pumping (counterpump), and both direction as bidirectional pumping. In distributed RA, it comprises with a long transmission fiber (usually greater than 40-km) and with the pump attached to the end of a span. The other option is lumped amplifier in which all the pump power is confined to a relatively short fiber typically around 5-km that

is inserted into the transmission line to provide gain [45]. Fig. 2.11 shows the typical Raman gain spectra for several typical fibers. Eventhough these fibers have different designs, the Raman gain spectra are mostly the same. The differences comes from the doped core of germanium and the magnitude approximately proportionally inverse to the fiber effective area [45].
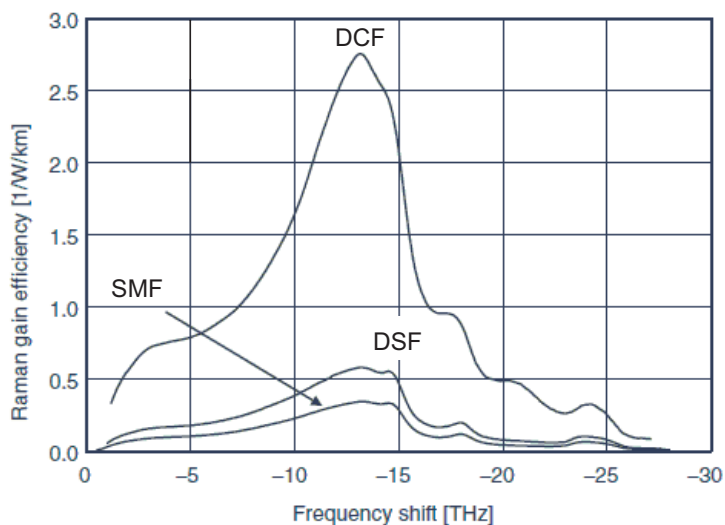
Figure 2.11: Typical Raman gain efficiency spectra for SMF, DSF, and DCF [43].

2.3.2 Compressed RZ Pulse Train using RASC

As mentioned in section 2.2.1, pump signal used in our thesis can be either CW or RZ pulsed train. In our thesis, RASC is used to generate a high quality compressed RZ pulse train for the pump. The RASC consists of a constant dispersion fiber, such as a dispersion-shifted fiber (DSF) and does not require any special fibers [46–48]. The system operation is based on adiabatic soliton compression. Soliton refer to as undistorted pulse when pulse is propagates through a nonlinear medium without any distortion of shape and spectrum. Fundamental soliton induced by combination of SPM and GVD effect in anomalous dispersion region where $D > 0$ and $\beta_2 < 0$. In the presence of SPM in the $\beta_2 < 0$ region, the spectral broadening due to GVD determines two situations qualitatively different. During this time the red frequency components travel slower than blue components and moves toward the pulse center. Meanwhile, the blue frequency shifted pulse that is trailing edge, travels more faster, and also moves

2. TECHNICAL BACKGROUND

toward the center of the pulse. SPM induced positive chirp and dispersion induced negative chirp. Both effects can partially or even cancel each other results in chirp-free and compression of the pulse. Fundamental soliton equation is consider when only Kerr-nonlinearity and second order dispersion in the nonlinear Schrodinger (NLS) equation is written as [1],

$$i\frac{\delta u}{\delta z} - \frac{\beta_2}{2}\frac{\delta^2 A}{\delta T^2} + \gamma|A|^2 A = 0 \tag{2.28}$$

Variable z represents an optical pulse passing in z-direction through an optical fiber exhibiting group velocity dispersion (GVD) and self-phase modulation (SPM). β_2 is the GVD parameter while γ is third order nonlinearity of the medium. Introducing three dimensionless variables, $U = (A/\sqrt{P_0})$, $\xi = (z/L_D)$, $\tau = (T/T_0)$ the equation can be cast in the form,

$$i\frac{\delta u}{\delta \xi} = \beta_2\frac{1}{2}\frac{\delta^2 U}{\delta \tau^2} - N^2|U|^2 U \tag{2.29}$$

where P_0 is the peak power, T_0 is the duration of incident pulse. In addition ξ and τ are the normalized distance and time variable parameter. Assume that pulses propagate in the region of anomalous GVD ($\beta_2 < 0$) where the dispersion length L_D and the nonlinear length L_{NL} are defined as $L_D = (T_0^2\ /\ |\ \beta_2\ |)$, and $L_{NL} = (1/\gamma P_0)$. Parameter N is introduced as,

$$N^2 = \frac{L_D}{L_{NL}} = \frac{\gamma P_0 T_0^2}{|\ \beta_2\ |} \tag{2.30}$$

The NLS equation in canonical form equation is given by,

$$u(\xi,\tau) = \text{sech}(\tau)\exp(\frac{i\xi}{2}) \tag{2.31}$$

In the context of optical fibers, equation (2.31) indicates that if a hyperbolic secant pulse with duration T_0 and the peak power P_0 is inserted into an ideal lossless optical fiber, the pulse with propagate without any changes along the long propagation link. From Eq. (2.30), the peak power for fundamental soliton during N=1 , when $T_{FWHM} = 1.76T_0$ is written by,

$$P_0 = (\frac{|\ \beta_2\ |}{\gamma T_0^2}) \approx (3.11\frac{|\ \beta_2\ |}{\gamma T_{FWHM}^2}) \tag{2.32}$$

or

$$P_0 = \frac{0.776\lambda^3 D A_{eff}}{\pi^2 c n_2 T_{FWHM}^2} \tag{2.33}$$

where the T_{FWHM} is full width at half maximum (FWHM) in the time domain of the optical pulse. Based on the arrangement from the equation in (2.34), the relationship between the pulse width T_{FWHM}, the peak power of the fundamental soliton pulse P_0 can be obtained as,

$$T_{FWHM} \propto \sqrt{\frac{1}{P_0}} \tag{2.34}$$

From relation (2.34), an increase in the soliton peak power P_0 would result in the reduction of pulse width T_{FWHM}. Since input RZ data is a fundamental soliton ($N = 1$) of the sech^2 pulse; RZ pulse signal is adiabatically amplified in the DSF as the Raman pump power (P_r) value in RASC is increased. The application of distributed Raman optical gain through the DSF is intended to increase the soliton power and to reduce the pulse duration simultaneously. Thus, it is possible to have flexibility in the picosecond input-output converted RZ data signal from the RASC. Using the combination of strong input pump data produced by the RASC at a zero dispersion wavelength as a pump signal with probe input data signals into HNLF AND-gate, the FWM can be achieved.
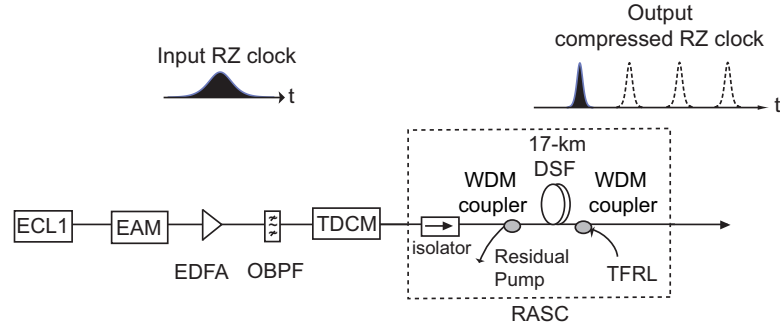
Figure 2.12: Schematic diagram of RASC.

The configuration diagram of RASC is shown in Fig. 2.12. A 10-Gb/s input RZ clock at a 1553-nm wavelength was generated with an external cavity laser diode (ECL) and an electroabsorption modulator (EAM). An erbium-doped fiber amplifier (EDFA) and an optical bandpass filter (OBPF) were used to compensate the insertion loss of

the EAM and also to set the conditions for fundamental soliton power in the RASC. A tunable dispersion-compensating module (TDCM) was used to suppress the frequency chirping induced by the EAM. Based on adiabatic soliton compression operation, the RASC consisted of a 17-km DSF and a tunable fiber Raman laser (TFRL). The DSF had anomalous dispersion of 3.8 ps/nm/km, dispersion slope of 0.059 $ps/nm^2/km$ at 1553 nm. The Raman pump wavelength was set at 1452 nm to promote high-quality compression performance. In this thesis, the application of the compressed RZ pulse will be discussed in chapter 3–6.

2.4 Performance Impairments

The transmission capacity of data signals is limited by various parameters distortion such as linear and nonlinear effects. Two main parameters that effect the performance of a single-mode fibers are chromatic and polarization mode dispersion. These distortions can cause optical signal to be broaden as they travel along a fiber. In order to increase optical transmission performances, it is more important to decrease the effects of transmission impairments in fibers. The effects can be reduced either through development and restructure of the fiber itself or by compensating for deleterious effects [49].

2.4.1 Impairment Effects

Below is the lists of signal impairment effects that influence optical transmission links and may degrade the network performance:

• **Dispersion**, is the name given to any effect that causes different spectral components of the light impulse (different wavelengths) propagate in the optical fiber at different speeds that arriving to receiver at different times [2]. Thus, the distortion of the transmitted information will leads to interference between adjacent pulses that called as an intersymbol interference (ISI). The dispersion consists of three main types: the modal dispersion, chromatic dispersion and polarization mode dispersion (PMD). Modal dispersion occurs only in multimode fibers in which each modes travels at a different speed. In other hand, chromatic dispersion also called group velocity dispersion (GVD) originates due to the frequency dependence of the group speed.

• **PMD**, arises when the two polarization states of the fundamental mode may oscillate

in different group velocities due to asymmetries in the fiber. Therefore, the result of PMD is an additional ISI.

• **Nonlinear effects**, occurs at high-power level due to the factor of attenuation and the refractive index that dependent on the optical power in a fiber. The two categories of nonlinear effects are *nonlinear inelastic scattering process* and *nonlinear variations of the refractive index.*

• **Reflections** from splices and connectors that influence stabilization of laser sources and can be eliminated using optical isolators.

When any of these impairment effects take place in the system, the reduction of the power penalty occurs in decibels. Our main goal in this section is to understand the phenomenon of chromatic dispersion and the limitation related by it.

2.4.2 Chromatic Dispersion
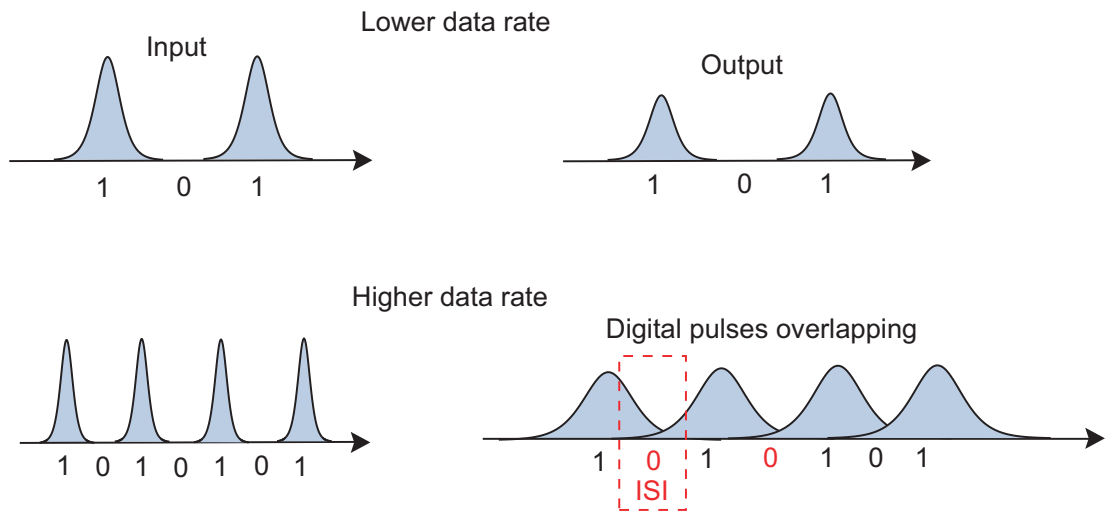
Figure 2.13: The dependence of pulses overlap on transmission rate.

With optical amplification greatly mitigating the effects of attenuation, the effects of fiber dispersion become more important. A narrow pulse transmitted on a fiber has tendency to spread out as it travels along the fiber. As shown in Fig. 2.13, when a pulse merges to the extent that it overlaps neighboring pulses, the resultant ISI sharply increases the BER. This fiber dispersion phenomenon imposes a limit on the bit rate that can be supported on a dispersive fiber of a given length. Distortion occur from group velocity dispersion (GVD) as the frequency components of the signal propagate

2. TECHNICAL BACKGROUND

with different velocities. Generally, the frequency-dependent propagation constant $\beta(\omega)$ can be expended in a Taylor series around a central frequency ω_0 as,

$$\beta(\omega) = \beta_0 + \beta_1(\omega - \omega_0) + \frac{1}{2}\beta_2(\omega - \omega_0)^2 + \frac{1}{6}\beta_3(\omega - \omega_0)^3...... \tag{2.35}$$

β_0 in (1/km) is a constant phase shift. β_1 in (ps/km) represents to the speed at which the envelope of the pulse propagates. The second order term β_2 devotes as the acceleration of the spectral components in the pulse, that known as group velocity dispersion (GVD) (ps^2/km). The β_3 is third order derivative in (ps^3/km) and also called as group velocity dispersion (GVD).

Commonly in fiber optic communication, D and S are used for dispersion and dispersion slope, respectively. Both define as a change in GVD and GVD slope with respect to a reference wavelength λ, respectively. Both expressions that are related to β_2 and β_3 as,

$$D = \frac{\delta\beta_2}{\delta\lambda} = -\frac{2\pi c}{\lambda^2}\beta_2 \quad S = \frac{\delta D}{\delta\lambda} = \frac{4\pi c}{\lambda^3}(\beta_2 + \frac{\pi c}{\lambda}\beta_3) \tag{2.36}$$

where D, and S are expressed in (ps/nm/km) and (ps^2/nm/km), respectively. Chromatic dispersion term is usually used to represent the fiber dispersion.

The relative time delay $\Delta\tau_g$ for a fiber length for a fiber length of L and the spectral width of the pulse $\Delta\lambda$ is,

$$\Delta\tau_g = DL\Delta\lambda \tag{2.37}$$

where relative time delay $\Delta\tau_g$, $\Delta\lambda$ and fiber length L are measured in picoseconds, nanometers and kilometers, respectively. In some optical communication systems, the wavelength spread $\Delta\lambda$ is determined by the range of wavelengths emitted by the optical laser source. Dispersion limited distance is given by,

$$L = \frac{1}{DB\Delta\lambda} = \frac{1}{DB(cB)} \propto \frac{1}{B^2} \tag{2.38}$$

The dispersion limited reach varies inversely as the square of data rate [1]. At the higher bit-rate it is necessary to use narrower light pulses.

There are two basic chromatic dispersive effects in a fiber: waveguide dispersion and material dispersion. The material dispersion is caused by the dependence of the

refractive index of the material, n used to make optical fiber that is also frequency dependent. Thus, different frequency signals travels at different velocities in the same fiber. This phenomenon is shown in Fig. 2.14 (a). Apart from material dispersion, waveguide dispersion is caused by boundary condition in between core and cladding surface which are influenced by profile parameters of the graded index fiber [50]. A possible explanation is shown in the Fig. 2.14 (b).
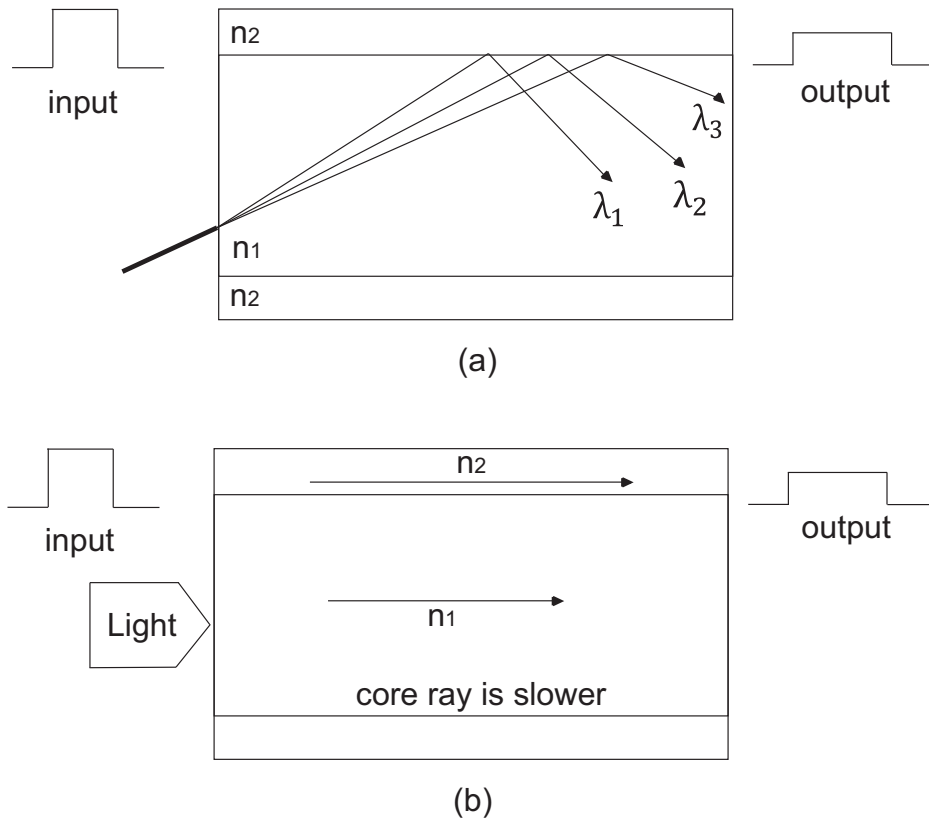
Figure 2.14: (a) Material dispersion and (b) waveguide dispersion.

Components of the dispersion parameter can be divided into material D_M and waveguide components D_W,

$$D = D_M + D_W \qquad (2.39)$$

$$D_M = -\frac{2\pi}{\lambda^2}\frac{dn_g}{d\omega} = \frac{1}{c}\frac{dn_g}{d\lambda} \qquad (2.40)$$

$$D_W = -\frac{2\pi\Delta}{\lambda^2}\{\frac{n_g^2}{+}\frac{dn_g}{d\omega}\frac{dV(b)}{dV}\} \tag{2.41}$$

where n_g is the group index of refraction of the cladding material, Δ is the index step, V is the normalized frequency and b is the normalized propagation constant.

Fig. 2.15, shows the dispersion as a wavelength in between three types of fiber (SSMF, NZDSF, DSF) [28]. In SSMF, the material dispersion is negative at short wavelengths and positive at the longer wavelengths. As shown in Fig. 2.15, the zero dispersion wavelength is approximately at 1300 nm. In the C-band the dispersion of SSMF is varies in between 15–18 (ps/nm/km) and typical slope is 0.06 (ps/nm^2/km). Since the dispersion is accumulated with distance along fiber, the dispersion compensation method has to be employed.
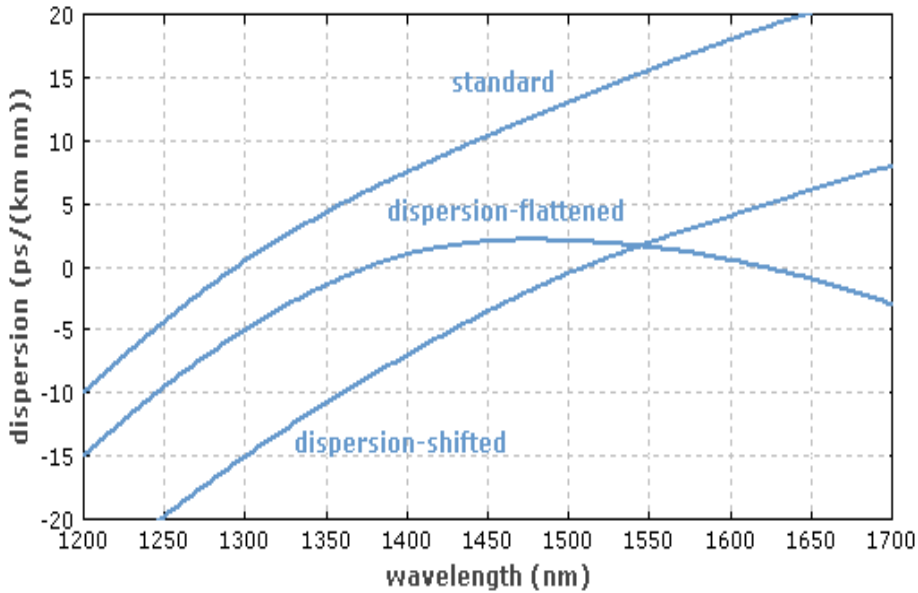
Figure 2.15: Chromatic dispersion as a function of wavelength for various types of fiber.

2.4.3 Dispersion Compensation

Chromatic dispersion and loss are becoming an essential factor that affected the transmission reach of an optical communication performance. For example, the maximum transmission length are about 1000-km for a 2.5 Gb/s and drop to 4-km for 40 Gb/s over SSMF (D = 16 ps/km/nm) [51, 52]. Therefore, dispersion compensation is necessary
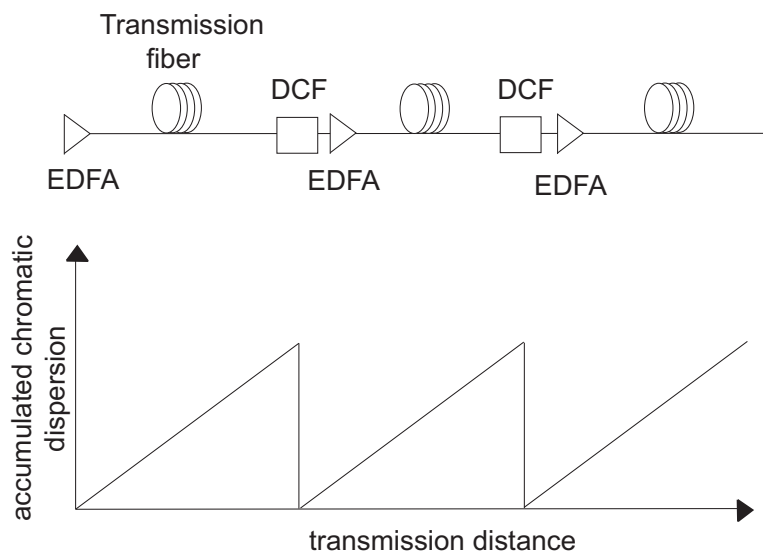
Figure 2.16: Dispersion map using DCF in transmission link.

to improve transmission performance. Various methods allow for compensation of the chromatic dispersion. For instance, the use of dispersion compensating fibers (DCF) [53, 54], and chirped fiber bragg gratings (FBG) [55, 56]. In conventional method, DCF modules are placed after each span of transmission link for dispersion compensation. DCF is a kind of special fiber which has negative dispersion characteristics in comparison with SSMF. Therefore, DCF can compensate for the accumulated positive dispersion and also has negative dispersion slope in the operation wavelength range [57, 58]. As shown in Fig. 2.16, DCF can either be inserted at the end or the beginning of an installed fiber link between two EDFAs. Unfortunately, DCFs have the disadvantage of high loss and high PMD [58].

Another compensation approach is using FBG. When pulse that is dispersed by the transmission fiber is recompressed using multichannel FBG reflector [59]. The level of compensation is based on FBG written pattern. One of the advantage of FBG compared to DCF system is low insertion loss for large distance compensation. However, the accumulated dispersion in both methods may change because of dynamic reconfiguration in the networks, laser and modulator chirp or change in environment, and etc [60]. Alternatively, tunable dispersion compensation module (TDCM) is a fully integrated tunable compensator that provides accurate dynamic control of chromatic dispersion for any channel in high-speed communication networks. The benefits of TDCM included

replacement of many conventional DCF modules usage and large tuning range. TDCM have been fabricated using a number of technologies such as microelectromechanical systems [61], FBG [62], wavelength-grating router [63], and virtually imaged phased array (VIPA) [64]. However, some of these technologies limited to negative dispersion and small tuning range up to ±800ps/nm [65].
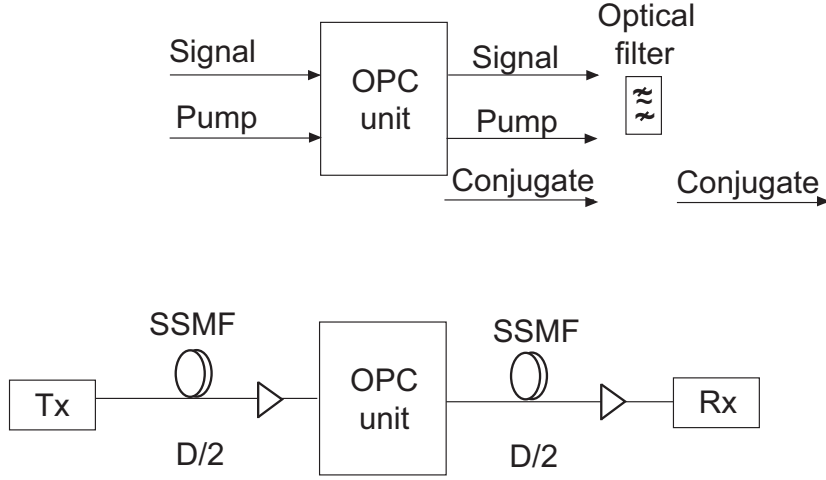
Figure 2.17: OPC-based dispersion compensation.

Optical phase conjugation (OPC) or also called mid-span spectral inversion (MSSI) is an another method to both FBG and DCF sytems with the advantage can operate various modulation format and bit-rate [66]. Most of OPCs systems convert a signals to its conjugated signal idler via FWM in optical fiber or nonlinear medium. The advantages of fiber-based OPC are its simple implementation and preferred in such application where the nonlinear signals distortions is a serious limitation [67, 68]. From Eq. (2.1), the propagation of a signal pulses related to nonlinear, dispersive and lossy medium can be presented in terms of complex amplitude of the signal A, as,

$$\frac{dA}{dz} = -\frac{\alpha}{2}A - \frac{i}{2}\beta_2\frac{\delta^2 A}{\delta T^2} + \frac{1}{6}\beta_3\frac{\delta^3 A}{\delta T^3} + i\gamma|A|^2 A \qquad (2.42)$$

where β_2 and β_3 represent group velocity in ps^2/nm and dispersion slope in ps^3/nm, respectively.

The complex conjugate (*) can be written as,

$$\frac{dA^*}{dz} = -\frac{\alpha}{2}A^* + \frac{i}{2}\beta_2\frac{\delta^2 A^*}{\delta T^2} + \frac{1}{6}\beta_3\frac{\delta^3 A^*}{\delta T^3} - i\gamma|A^*|^2 A^* \qquad (2.43)$$

From Eq. (2.43), both sign of β_2 and Kerr effect γ are inverted. Thus, GVD in a transmission link with the same fiber before and after can be compensated. However, Kerr effect dependent on the optical power of the signal and is compensated depends on transmission link design. Meanwhile, attenuation α and dispersion slope β_3 remain unchanged. The effect of β_3 cannot be compensated by using OPC, but accumulates along the systems [69].

Additionally, all effects compensation such as odd dispersion, SPM and SRS can be done by combining OPC scheme and suitable chosen dispersion map [70 – 72]. Fig. 2.17, shows the mechanism of OPC. By placing an OPC in the middle of a transmission link, the generated phase conjugated signal by the OPC carries the same information as the original data but the signal spectrum is inverted. The data signal at wavelength λ_{signal} is coupled together with a pump signal at frequency λ_{pump} and fed into OPC medium such as HNLF. At the output after OPC, a conjugate signal is converted at a new wavelength $\lambda_{conjugate}$ as,

$$\lambda_{conjugate} = 2\lambda_{pump} - \lambda_{signal} \qquad (2.44)$$

The conjugate signal is separated from both pump and original signals by an optical filter. Another point that need to be considered is related to polarization dependence of the FWM process. Practically, the OPC output signal must be insensitive to the polarization of the input signal. Realization can be done if the pump wavelengths are located symmetrically in relation to the ZDW and output OPC signal is generated at the same frequency of the input signal [73].

References

[1] G. P. Agrawal, *Nonlinear fiber optics*, 4th Edition Academic Press, San Diego, USA, (2007), Chapter 10.

[2] R. Ramaswami, K. N. Sivarajan, and G. H. Sasaki, *Optical networks: A practical perspective*, 3rd edition Elsevier, Burlington, USA, (2010).

[3] F. Forghieri, R.W. Tkach, and A. R. Chraplyvy, *Fiber nonlinearities and their impact on transmission systems*, in I. P. Kaminow and T. L. Koch (Eds.), Optical Fiber Telecommunications, Vol. IIIA, Academic Press, San Diego, CA, 1997.

[4] M. F. S. Ferreira, *Nonlinear effects in optical fibers*, John Wiley and Sons, Hoboken, New Jersey, 2011.

[5] N. Shibata, R. P. Braun, and R. G. Waarts, "Phase-mismatch dependence of efficiency of wave generation through four-wave mixing in a single-mode optical fiber," *IEEE J. Quantum Electron.*, vol. QE-23, pp. 1205–1210, 1987.

[6] A. E. Willner, S. Khalleghi, M. R. Chitgarha, and O. F. Yilmaz, "All-optical signal processing," *J. Lightwave Technol.*, vol. 32, no. 4, pp. 660-680, Feb. 2014.

[7] S. Song, C. T. Allen, K. R. Demarest, and R. Hui, "Intensity-dependent phase-matching effect on four-wave mixing in optical fibers," *J. Lightwave Technol.*, vol. 17, no. 11, pp. 2285-2290, Nov. 1999.

[8] S. J. Jung, J. Y. Lee, and D. Y. Kim, "Novel phase-matching condition for a four-wave mixing experiment in an optical fiber," *Opt. Express*, vol. 14, no. 1, pp. 35-43, Jan. 2006.

REFERENCES

[9] K. Kikuchi and C, Lorattanasane, "Design of highly efficient four-wave mixing devices using optical fibers," *IEEE Photon. Technol. Lett.*, vol.6, no. 8, pp. 992-994, Aug. 1994.

[10] G. Agrawal, *Fiber-optic communications systems, 4th Edition*, John Wiley and Sons, Hoboken, New Jersey, 2010.

[11] A. Bogoni, L. Poti, R. Proietti, G. Meloni, F. Ponzizni, and P. Ghelfi, "All-optical signal processing," *IEEE Electron Lett.*, vol. 41, no. 7, pp. 435-436, March 2005.

[12] J. -Y. Kim, J. -M. Kang, T. -Y. Kim, and S. -K. Han, "All-optical multiple logic gates with XOR, NOR, OR, and NAND functions using parallel SOA-MZI structures: Theory and experiment," *J. Lightwave Technol.*, vol. 24, no. 12, pp. 3392-3399, 2006.

[13] A. Bogoni, X. Wu, I. Fazal, and A. E. Willner, " Gbits photonic logic gates," *J. Lightwave Technol.*, vol. 27, pp. 4221–4227, 2009.

[14] J. H. Lee , "All-optical signal processing using specialty fibers,"*presented at the conference of Optical Fiber Communication Conference and Exposition (OFC)*, OTuD7, San Diego, USA, Feb. 2008.

[15] S. J. Yoo, "Wavelength conversion technologies for WDM network applications," *J. Lightwave Technol.*, vol. 14, no. 6, pp. 955-958, June 1996.

[16] G-W. Lu, K. S. Abedin, and T. Miyazaki, "Experimental demonstrations of all-optical phase-multiplexing using FWM-based phase interleaving in silica and bismuth-oxide HNLFs," *J. Lightwave Technol.*, vol. 27, no. 4, pp. 409-416, Feb. 2009.

[17] B. Mukherjee, "WDM optical communication networks," *J. Lightwave Technol.*, vol. 18, no. 10, pp. 1810-1824, Oct. 2000.

[18] E. Lazzeri, A. T. Nguyen, N. Kataoka, N. Wada, A. Bogoni, and L. Poti, "All optical add and drop mutiplexing node for hybrid topology networks," *J. Lightwave Technol.*, vol. 29, no. 24, pp. 3676-3682, Dec. 2011.

[19] K. E. Stubkjaer, A. Kloch, P. B. Hansen, H. N. Poulsen, D. Wolfson, K. S. Jepsen, A. T. Clausen, E. Limal, and A. Buxens, "Wavelength converter technology," *IEICE Trans. Commun.*, vol. E-82-B, no. 2, pp. 390-400, Feb. 1999.

[20] B. Ramamurthy and B. Mukherjee, "Wavelength conversion in WDM networking," *J. Lightwave Technol.*, vol.16, no. 7, pp. 1061-1073, Sept. 1998.

[21] E. Ciarramella, "Wavelength conversion and all-optical regeneration: achievements and open issues," *J. Lightwave Technol.*, vol. 30 , no. 4, pp. 572-580, Feb. 2012.

[22] T. Durhuus, C. Joergensen, B. Mikkelsen, R. J. S. Pendersen, and K. E. Stubkjaer, "All-optical wavelength conversion by SOA's in a Mach-Zehnder configuration," *IEEE Photon. Lett.*, vol. 6, no. 1, pp. 53-55, Jan. 1994.

[23] K. Inoue and H. Toba, "Wavelength conversion experiment using fiber four-wave mixing," *IEEE Photon. Lett.*, vol. 4, no. 1, pp. 69-72, Jan. 1992.

[24] H. Wen, H. Jiang, X. Zheng, H. Zhang, and Y. Guo, "Performance enhancement of multiwavelength conversion of RZ-DPSK based on four-wave mixing in semiconductor optical amplifier," *IEEE Photon. Lett.*, vol. 19, no. 18, pp. 1377-1379, Sept. 2007.

[25] G-W. Lu, K. S. Abedin, and T. Miyazaki, "Experimental demonstrations of all-optical phase-multiplexing using FWM-based phase interleaving un silica and bismuth-oxide HNLFs," *J. Lightwave Technol.*, vol. 27, no. 4, pp. 409-416, Feb. 2009.

[26] J. Yu, X. Zheng, C. Peucheret, A. T. Clausen, H. N. Poulsen, and P. Jeppesen, "All-optical wavelength conversion of short pulses and NRZ signals based on nonlinear optical loop mirror," *J. Lightwave Technol.*, vol. 18, no. 7, pp. 1007-1017, Jul. 2000.

[27] K. Inoue, "Four-wave mixing in an optical fiber in the zero-dispersion wavelength region," *J. Lightwave Technol.*, vol. 10, no. 11, pp. 1553-1561, Nov. 1992.

[28] R. H. Stolen and J. E. Bjorkholm, "Parametric amplification and frequency conversion in optical fibers," *J. of Quant. Electron.*, vol. QE-18, no. 7, pp. 1062-1071, Jul. 1982.

REFERENCES

[29] O. Aso, M. Tadakuma, and S. Namiki, "Four-wave mixing in optical fibers and its applications," *Furukawa Review*, no. 19, pp. 63-68, 2000.

[30] I. Kaminow and T. Li,*Optical Fiber Telecommunications IVB: Systems and Impairments*, Academic Press, 2002.

[31] J. Berthold, A. A. M. Saleh, L. Blair, and J. M. Simmons,"Optical networking: past, present, and future," *J. Lightwave Technol.*, vol. 26, no. 9, pp. 1104-1118, 2008.

[32] S. Radic, C. J. McKinstrie, R. M. Jopson , J. C. Centanni, and A. R. Chraplyvy,"All-optical regeneration in one- and two-pump parametric amplifiers using highly nonlinear optical fiber," *IEEE Photon. Lett.*, vol. 15, no. 7, pp. 947-959, 2003.

[33] A. Bogris and D. Syvridis, "Regenerative properties of a pump-modulated four-wave mixing scheme in dispersion-shifted fibers," *J. Lightwave Technol.*, vol. 21, no. 9, pp. 1892-1902, Sept. 2003.

[34] J. Li, J. Hansryd, P.-O. Hedekvist, P. A. Andrekson, and S. N. Knudsen, "300 Gbit/s eye-diagram measurement by optical sampling using fiber based parametric amplification," *presented at the conference of Optical Fiber Communication Conf. and Exhibition*, vol. 4, 2001.

[35] C. Schubert, J. Berger, S. Diez, H. J. Ehrke, R. Ludwig, U. Feiste, C. Schmidt, H. G. Weber, G. Toptchiyski, S. Randel, and K. Petermann, "Comparison of interferometric all-optical switches for demultiplexing applications in high-speed OTDM systems," *J. Lightwave Technol.*, vol. 29, no. 4, pp. 618-624, Apr. 2002.

[36] H. G. Weber, R. Ludwig, S. Ferber, C. S-Langhorst, M. Kroh, V. Marembert, C. Boerner, and Colja Schubert, "Ultrahigh-speed OTDM-transmission technology," *J. Lightwave Technol.*, vol. 24, no. 12, pp. 4616-4627, Dec. 2006.

[37] D. T. K. Tong, K.-L. Deng, B. Mikkelsen, G. Raybon, K. F. Dreyer, and J. E. Johnson, "160 Gbit/s clock recovery using electroabsorption modulator-based phase-locked loop," *Electron. Lett.*, vol. 36, no. 23, pp. 1951-1952, November 2000.

[38] C. Boerner, C. Schubert, C. Schmidt, E. Hilliger, V. Marembert, J. Berger, S. Fer- ber, E. Dietrich, R. Ludwig, B. Schmauss, and H. G. Weber, "160 Gbit/s clock recovery with electro-optical PLL using a bidirectionally operated electroabsorption modulator as phase comparator," *Electron. Lett.*, vol. 39, no. 14, pp. 1071-1073, July 2003.

[39] T. Yamamoto, L. K. Oxenlwe, C. Schmidt, C. Schubert, E. Hilliger, U. Feiste, J. Berger, R. Ludwig, and H. G. Weber, "Clock recovery from 160Gb/s data signals using a phase-locked loop with an interferometric optical switch based on a semiconductor optical amplifier," *Electron. Lett.*, vol. 37, no. 8, pp. 509-510, April 2001.

[40] C. Yu, L.-S. Yan, T. Luo, Y. Wang, Z. Pan, and A. E. Willner, "Width-tunable optical RZ pulse train generation based on four-wave mixing in highly nonlinear fiber," *Electron. Lett.*, vol. 17, no. 3, pp. 636-638, March 2005.

[41] J. Yang, J. Hu, C. Yu, Y. K. Yeo and Y. Wang, "Multi-channel 80-GHz pulse train Generation Based on four-wave mixing in highly nonlinear fiber," *presented at the 14th OptoElectronics and Communications Conference (OECC)*, vol. TuA5, pp. 1559–1560, 2009.

[42] M. N. Islam, "Raman amplifiers for telecommunications," *IEEE J. Sel. Topics Quantum Electron*, vol. 8, no. 3, pp. 548-559, May/June 2002.

[43] C. K. Chan. Celvin, *Optical performance monitoring: Advanced techniques for next-generation photonic network*s, Academic Press, 2010.

[44] T. E. Stern, G. Ellinas, and K. Bala, *Multiwavelength Optical Networks: Architectures, Design, and Control*, Chapter 4, Cambridge University Press, 2009.

[45] C. Headley and G. P. Agrawal, *Raman Amplification in Fiber Optical Communication Systems*, Academic Press, 2005.

[46] S. V. Chernikov, D. J. Richardson, E. M. Dianov, and D. N. Payne, "Picosecond soliton pulse compression based on dispersion decreasing fiber," *Electron. Lett.*, vol. 28, no. 19, pp. 1842–1844, Sept. 1992.

REFERENCES

[47] S. V. Chernikov, J. R. Taylor, and R. Kashyap,"Experimental demonstration of step-like dispersion profiling in optical fibre for soliton pulse generation and compression," *Electron. Lett.*, vol. 30, no. 8. pp. 433–435, Mar. 1994.

[48] T. Inoue, H. Tobioka, K. Igarashi, and S. Namiki,"Optical pulse compression based on stationary rescaled pulse propagation in a comblike profiled fiber," *J. Lightwave Technol.*, vol. 24, no. 7, pp. 2510–2522 July 2006.

[49] T. E. Stern, G. Ellinas, and K. Bala, *Multiwavelength Optical Networks*, Second Edition Updated, Cambridge University Press, New York, 2009.

[50] G. Keiser, *Optical Fiber Communications*, Third Edition, McGraw-Hill, 2000.

[51] G. P. Agrawal, *Fiber-optic communication systems*, Fourth Edition, John Wiley and sons, 1997.

[52] D. D. Marcenac, D. Nesset, A. E. Kelly, and D. Gavrilovoc, "40 Gbit/s transmission over 103 km of NZDSF using polarization independent mid-span spectral inversion by four-wave mixing in a semicondutor optical amplifier," *Electron. Lett.*, vol. 34, no. 1, pp. 100-102, 1998.

[53] A. M. Vengsarkar and W. A. Reed, "Dispersion-compensating single-mode fibers: Efficient designs for first- and second-order compensation," *Optics Letters*, vol. 12, no. 11, pp. 924-926, 1993.

[54] L. Grner-Nielsen, M. Wandel, P. Kristensen, C. Jorgensen, L. V. Jorgensen, B. Edvold, B. Plsdttir, and D. Jakobsen, "Dispersion-compensating fibers," *J. Lightwave Technol.*, vol. 23, no. 11, pp. 3566–3579, 2005.

[55] F. Quellete, "Dispersion cancellation using linearly chirped bragg grating filters in optical waveguides," *Optics Letters*, vol. 12, no. 10, pp. 847-849, 1987.

[56] Y. W. Song, D. Starodubov, Z. Pan, Y. Xie, A. E. Willner, and J. Feinberg, "Tunable WDM dispersion compensation with fixed bandwidth and fixed passband center wavelength using a uniform FBG," *IEEE Photon. Lett.*, vol. 14, no. 8, pp. 1193-1195, Aug. 2003.

[57] L. Xia, X. Li, X. Chen, and S. Xie, "A novel dispersion compensation fiber grating with a large chirp parameter and period sampled distribution," *Opt. Commun.*, vol. 227, no. 4–6, pp. 311-315, Nov. 2003.

[58] R. Jones, J. Doylend, P. Ebrahimi, S. Ayotte, O. Raday, and O. Cohen, "Silicon photonic tunable optical dispersion compensator," *Opt. Express*, vol.15, no.24, pp. 15836-15841, Nov. 2007.

[59] L. Dong, M. Cole, A. D. Ellis, R. I. Laming, and T. Widdows, "40-Gbits 1.55nm RZ transmission over 109 km of non-dispersion shifted fibre with long continiously chirped fibre grating," *Eletron Lett.*, vol. 33, no. 18, pp. 1563-1565, 1997.

[60] X. Chen, X. Xu, M. Zhou, D. Jiang, X. Li, J. Feng, and S. Xie, "Tunable dispersion compensation in a 10-Gb/s optical transmission system by employing a novel tunable dispersion compensator," *IEEE Photon. Lett.*, vol. 16, no. 1, pp. 188-190, Jan. 2004.

[61] T. Sano, T. Iwashima, M. Katayama, T. Kanie, M. Harumoto, M. Shigehara, H. Suganuma, and M. Nishimura, "Novel multichannel tunable chromatic dispersion compensator based on MEMS and disffraction grating," *IEEE Photon. Lett.*, vol. 15, no. 8, pp. 1109–1100, Aug. 2003.

[62] Y. W. Song, D. Starodubov, Z. Pan, Y. Xie, A. E. Willner, and J. Feinberg, "Tunable WDM dispersionn compensation with fixed bandwidth and fixed passband center wavelength using a uniform FBG," *IEEE Photon. Lett.*, vol. 14, no. 8, pp. 1193–1195, Aug. 2003.

[63] C. R. Doerr, D. M. Marom, M. A. Cappuzo, E. Y. Chen, "40-Gb/s colorless tunable dispersion compensator with 1000-ps/nm tuning range employing a planar lightwave circuit and a deformable mirror," *presented at the OFC Conf.*, Anaheim, CA 2005, Postdeadline paper PDP5.

[64] L. D. Garret, A. H. Gnauck, M. H. Eiiselt, R. W. Tkach, C. Yang, C. Mao, and S. Cao, "Demonstration of virtually-imaged phased-array device for tunable dispersion compensation in 16 x 10 Gb/s WDM transmission over 480 km standard fiber," *presented at the OFC Conf.*, 2000, vol. 4, pp. 187–189.

REFERENCES

[65] G-H. Lee, S. Xiao, and A. M. Weiner, "Optical dispersion compensator with .4000-ps/nm tuning range using a virtually imaged phased array (VIPA) and spatial light modulator (SLM)," *IEEE Photon. Lett.*, vol. 18, no. 17, pp. 1819–1821, Sept. 2006.

[66] S. L. Jansen, G.-D. Khoe, and H. de Waardt, "Mixed data rate and format transmission (40-Gbit/s non-return-to-zero, 40-Gbit/s duobinary, and 10-Gbit/s non-return-to-zero) by mid-link spectral inversion" *Optics Lett.*, vol. 29, no. 20, pp. 2348–2350, Oct. 2004.

[67] J. Herrera, F. Ramos, and J. Marti, "Nonlinear distortion generated by DSF-based optical-phase conjugators in analog optical systems," *J. Lightwave Technol.*, vol. 20, no. 9, pp. 1688-1693, Sept. 2002.

[68] I. Zacharopoulos, "Influence of phase mismatch in dispersion-shifted fiber at 10 Gb/s," *IEEE Photon. Technol. Lett.*, vol.11, no. 4, pp. 430-432, Apr. 1999.

[69] M. Amemiya, "Pulse broadening due to higher order dsipersion and its transmission limit," *J. Lightwave Technol.*, vol. 20, no. 4, pp. 591–597, Apr. 2002.

[70] S. Watanabe and M. Shirasaki, "Exact compensation for both chromatic dispersion and Kerr effect in a transmission fiber using optical phase conjugation," *J. Lightwave Technol.*, vol. 14, no. 3, pp. 243–248, Mar. 1996.

[71] M. Tsang and D. Psaltis, "Dispersion and nonlinearity compensation by spectral phase conjugation," *Opt. Lett.*, vol. 28, no. 17, pp. 1558–1560, Sept. 2003.

[72] J. Pina, B. Abueva, and C. G. Goedde "Periodically conjugated solitons in dispersion-managed optical fiber," *Opt. Commun.*, vol. 176, pp. 397–400, Apr. 2000.

[73] R. M. Jopson and R. E. Tench, "Polarisation-independent phase conjugation of lightwave signals," *Eletron Lett.*, vol. 29, no. 25, pp. 2216–2217, 1993.

Chapter 3

Single Modulation Format All-Optical Signal Processings

This chapter presents two demonstrations of an all-optical signal processing using single modulation format either OOK or DPSK. In the first section under this chapter, an NRZ-DPSK-to-RZ-DPSK waveform-wavelength conversion with flexible picosecond width-tunablity and signal reshaping functionality. In the first demonstration, waveform-wavelength conversion of a 10-Gb/s DPSK signal without input signal degradation over input-output wide wavelength ranges is presented. In the second demonstration, it is also shown that the waveform-wavelength conversion with reshaping properties due to chromatic dispersion can be successfully converted at different Raman pump power settings over fiber links without dispersion compensation. In the second section, for the first time, an all-optical wavelength multicasting with width-tunable outputs is experimentally demonstrated. Width-tunable wavelength multicasting within the C-band wavelength ranges with various compressed RZ data signal inputs have been proposed and demonstrated. Nearly equal pulse widths at all multicast wavelengths with wide open eye patterns and low power penalties at the 10^{-9} BER level are obtained.

3.1   Introduction

Bit-rate and various format adaptations have become an essential requirement to achieve future high speed operation in different network topologies [1, 2]. Non-return-to-zero

3. SINGLE MODULATION FORMAT ALL-OPTICAL SIGNAL PROCESSINGS

(NRZ) and return-to-zero (RZ) signals are well-known formats that are widely employed at the nodes of wavelength division multiplexing (WDM) and ultrafast optical time division multiplexing (OTDM) networks [3-5]. In order to achieve interconnections and flexible network management between both networks, all-optical waveform conversion as well as wavelength conversion are required. In practical situations, all-optical signals have to travel over an unknown transmission length in different photonic nodes as they travel to destination nodes. Thus, the signal quality may degrade before any new signal processing has occurred. Therefore, an improvement in the distorted signal is crucially needed, as the processed signal will become more degraded after signal transmission. All-optical signal regeneration technique could be used to clean up the degraded signals that could be either 2R (reamplifying and reshaping) or 3R (reamplifying, reshaping, and retiming). In both cases the signal reshaping capabilities is required in order to increase the signal extinction ratio and intensity noise reduction. To overcome this issue, waveform-wavelength conversion with signal reshaping capability is highly desirable to mitigate such degradation in order to guarantee signal quality until the end of a node [6]. Additionally, the characteristics of the converted signal also play a critical role in optimizing system performance. For example, a signal will react differently owing to fiber dispersion and nonlinearities because the span between nodes is not the same. Hence, a practical function that flexibly shortens and manipulates width-tunable converted signals [7, 8], and this function can support wider bandwidth requirements and the creation of higher-bit-rate signals [9]. In order to obtain high data integrity over the entire network, simultaneous signal reshaping and width-tunability are desirable approaches instead of basic waveform-wavelength conversion. The desirable attributes of such a multifunction signal converter include a high efficiency, full transparency to bit rate and format, and the capability of performing over a wide wavelength range operation with negligible penalty. Fiber-based four-wave mixing (FWM) in a highly nonlinear fiber (HNLF) has received considerable interest and is a preferable choice for the realization these functionalities due to its fast nonlinear response and high conversion efficiency, regardless of the modulation format [10].

Nowadays, interest in advanced modulation formats such as differential phase-shift keying (DPSK) has become the preferred format owing to its robustness when subjected to signal distortion and its constant-intensity profile [11, 12]. Moreover, RZ-DPSK signals have also attracted attention, especially for long-haul transmission systems and

the formation of higher-bit-rate OTDM networks [13, 14]. To date, several schemes for all-optical NRZ-DPSK-to-RZ-DPSK waveform conversion have been proposed and demonstrated [15-18]. However, flexible width-tunable operation over a picosecond range for the converted signal was not performed in these studies. Adiabatic soliton compression techniques have attracted much attention for the generation of high-quality short-duration pulse trains over a picosecond range with a minimal pedestal while offering power amplification [19]. Thus, this useful approach can be extended by using the high-quality tunable ultrashort duration clock pump introduced in our experiment, which has benefited over continuous wave (CW) owing to its flexible spectral width. Recently, we have demonstrated waveform-wavelength conversion at a bit rate of 10 Gb/s by using only the on-off keying (OOK) format [20]. Nevertheless, sufficient conversion over a wide operating wavelength range and reshaping waveform-wavelength conversion for DPSK signal were not demonstrated in this experimental work. In addition, NRZ-DPSK-to-RZ-DPSK with flexible width-tunable converted signals over a picosecond range represents an added functionality, which have not been studied so far. The investigation will be discussed in this thesis under subsection 3.2.3.2.

Optical networks such as core, metro, and access networks are categorized by their size. Each network configuration can be differentiated based on the parameters such as transmission distance, capacity, and services provided. The demand for high-speed optical signals requires flexibility and transparency to process data channels in a cost-effective manner [21]. One attractive feature based on WDM is multicasting, which transmits data with simultaneous wavelength conversions and provides WDM network functionality [22–24]. Furthermore, a RZ modulation format is more robust to nonlinear impairments and crosstalk compared with a NRZ encoding [25], [26]. We consider the multicasting scheme (shown in Figure 3.1) with interconnections among nodes that uses the concept of a light tree or light path in a wavelength-routed network, which is connected from one source node to several destination nodes [27]. Node B acts as an intermediate node that links terminal node A to multicasting-destination nodes C, D, and E. At Node B, the switch functions to provide optical signal amplification, wavelength conversion, and signal reshaping. In any installed transmission network, for example, the signal pulse width will react differently under fiber-dispersion condition, nonlinearities, and receiver characteristics because transmission spans L_{BC}, L_{BD}, and L_{BE} are not the same. Individually and separately processing the channel and

3. SINGLE MODULATION FORMAT ALL-OPTICAL SIGNAL PROCESSINGS

adding a new function afterward to circumvent this problem are not feasible because of network complexity and cost. Recent studies in Refs.[28] and [29] have revealed that the transmission performance of different RZ pulse durations showed the existence of an optimum pulse duration for each transmission span with a particular cumulative dispersion. In addition, demonstrations of such necessity have been reported in Refs.[7] and [30] and proven to be beneficial in optimizing system performance. Therefore, the requirement to implement a practical function that flexibly shortens and manipulates width-tunable converted signals over the changes in the transmission distance is necessary. This flexibility can also support wider bandwidth requirements. Different approaches to the on-off-keying (OOK) modulation format have been proposed to achieve wavelength multicasting [31–36]. However, no study has presented a practical width-tunable management by deploying such requirement functionality. Thus, the ultimate goal is to simultaneously provide flexibility and tunability in the terminal equipment to optimize the transmission performance of WDM multicast channels via pulse-width management in a wide-wavelength operation range.
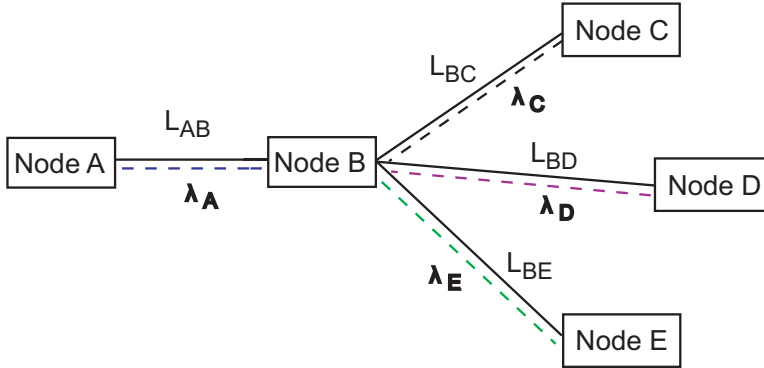
Figure 3.1: Multicasting scheme with interconnections among nodes.

One method to fulfill all requirements is to provide widely tunability to the data pulse width launched into an RZ multicast system. Numerous techniques such as supercontinuum, mode-locked lasers, and electro-absorption modulator have been used to generate ultra short optical pulses with high repetition rate [37–39]. Nevertheless, the key limitation associated with these methods is that the achievable duration of the generated pulses is limited. As an alternative method, pulse compression of an RZ data signal by adjusting the distributed Raman amplifier (DRA) gain while offering power

amplification in a flexible manner as demonstrated in Ref. [19] is required. Although width-tunable signals have been individually accomplished in this subject before, to the best of our knowledge, sufficient multicast conversion over a wide-wavelength operation has not yet been considered. Replication a single data channel into several different wavelengths of the WDM multicast channels can easily be implemented through FWM in a nonlinear medium. FWM in a highly nonlinear fiber HNLF is the best choice among other media owing to its advantageous properties such as fast nonlinear response and high conversion efficiency [40]. By adjusting the Raman pump power inside a RASC, simultaneous results in multicast conversion with width-tunable output can possibly be obtained. Further, because a compressed RZ data signal is used as a pump signal in the FWM process, the multicast idler signals will follow the shape of the compressed RZ data with pedestal-free and narrower width output.

3.2 Waveform-Wavelength Conversion of a Single DPSK Format

In this section, for the first time to the best of our knowledge, we extended our preliminary result in ref. [41] of all-optical NRZ-DPSK-to-RZ-DPSK reshaping waveform-wavelength conversion with a picosecond width-tunable converted signal over a wide range of operation. Our simple technique employed the combination of a fiber-based HNLF switch and a Raman-adiabatic soliton compressor (RASC). As a multifunction waveform-wavelength converter, this scheme offered the following advantages: (1) the RASC acted as both a pulse width controller and an amplifier, (2) the adjustable wider range could be operated for picosecond width tunable converted data controlled down to 2.87 ps, and (3) conversion operation could be achieved over the C band with a low power penalty. Overall, our approach highlighted the importance of width tunability over a picosecond range for the converted RZ-DPSK signal that proved to be beneficial in OTDM and WDM systems.

This section is organized as follows: subsection 3.2.1 explains the concept of this work. Next, subsection 3.2.2 and 3.2.3 described the experimental setup, results and discussion for DPSK format NRZ-to-RZ waveform-wavelength conversion.
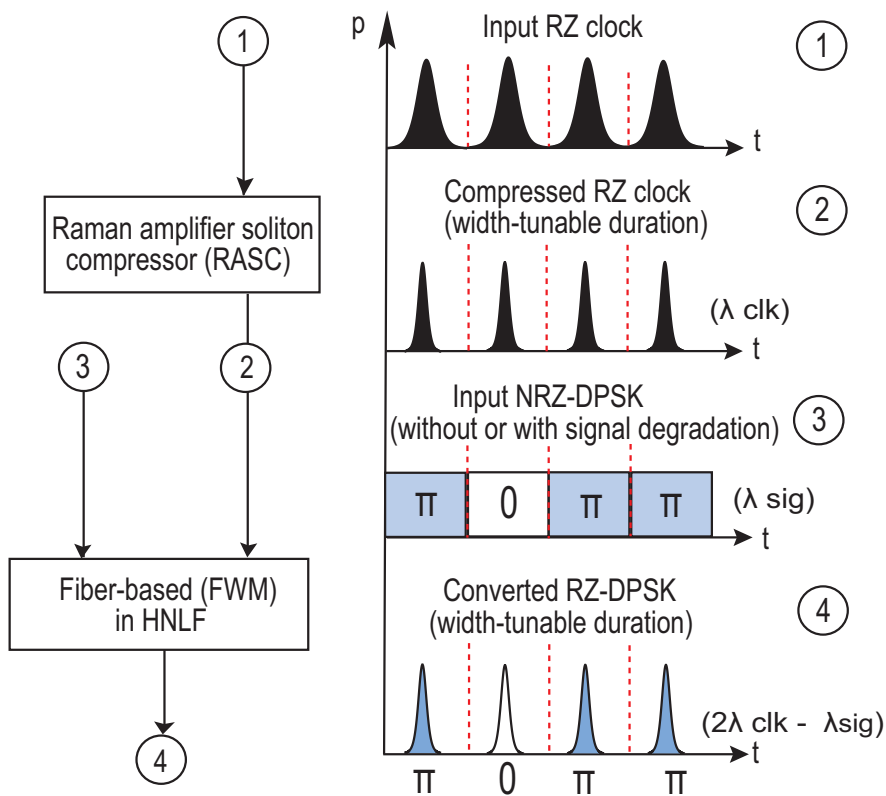
Figure 3.2: Operational principle for the all-optical NRZ-DPSK-to-RZ-DPSK converter with the function of waveform-wavelength conversion, picosecond width-tunability and signal reshaping.

3.2.1 Concept

The principle operation of an all-optical NRZ-DPSK-to-RZ-DPSK waveform-wavelength converter without of with input degraded signal for reshaping functionality and flexible width-tunable operations in picosecond range is shown in Fig. 3.2. The proposed scheme consists of two main stages. In the first stage, the RASC is used. This technique is based on adiabatic soliton compressor which can be realized using constant dispersion fiber, such as DSF and does not require any special fibers [43–45]. The application of distributed Raman optical gain through the fiber is intended to increase the soliton power and to reduce the pulse duration simultaneously [46]. In the second stage, a fiber-based switch in HNLF performs as an AND logic function based on a parametric process between input NRZ-DPSK signal (without or with input signal degradation) and the compressed RZ clock pulse. The compressed RZ clock train acts as the pump signal, while the input NRZ-DPSK data signal as the probe data signals. The operation is realized by aligning the position of the compressed RZ clock to the center point of input NRZ-DPSK signal using the phase shifter which was possible to eliminate the signal impairment caused by chromatic dispersion. It is commonly recognized that, for higher speed optical networks, a synchronous optical signal can be extracted using an all-optical clock recovery and timing extractions scheme. Several clock recovery and timing extraction techniques have been developed in Refs. [47–49] and can be applied to the proposed scheme. At 160 Gb/s and beyond, the optical clock recovery of an electro-optical phase-lock-loop (PLL) using a bidirectionally operated EAM as a phase comparator, as proposed in Ref. [50], is also a potential solution.

The combination of a RZ clock pump from RASC at the wavelength of (λ_{clk}) with another input NRZ-DPSK signal (λ_{sig}) into HNLF, the parametric gain can be achieved. The converted RZ-DPSK has a wavelength of ($\lambda_{FWM} = 2\lambda_{clk} - \lambda_{sig}$). During parametric FWM process, the compressed RZ clock pulse reshapes the FWM signal and results in a narrower pulse width because power of the FWM signal (P_{FWM}) is proportional to the square power of the compressed RZ clock (P_{clk}) [51, 52]. Thus, tuning the Raman pump power (P_r) value of the RASC able to convert RZ-DPSK with width-tunable signal in picosecond range.

3. SINGLE MODULATION FORMAT ALL-OPTICAL SIGNAL PROCESSINGS
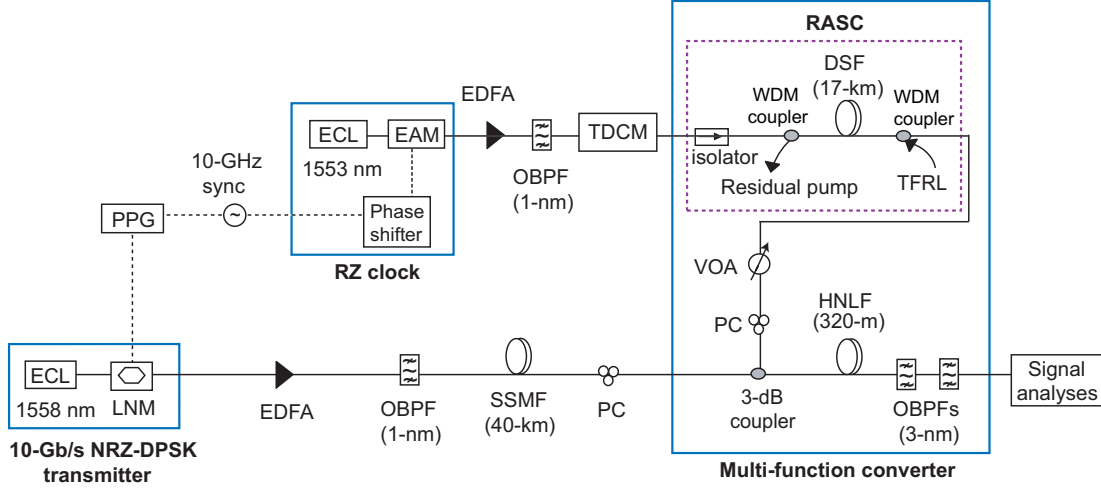
Figure 3.3: Experimental setup for an all-optical NRZ-DPSK-to-RZ-DPSK waveform-wavelength conversion with picosecond width-tunable output and reshaping functionality.

3.2.2 Experimental Setup

The experimental setup is illustrated in Fig. 3.3. A 10-Gb/s input RZ clock at a 1553-nm wavelength was generated with an ECL and an EAM. An EDFA and an OBPF were used to compensate the insertion loss of the EAM and also to set the conditions for fundamental soliton power in the RASC. A TDCM was used to suppress the frequency chirping induced by the EAM. Based on adiabatic soliton compression operation, the RASC consisted of a 17-km DSF and a TFRL. The DSF had anomalous dispersion of 3.8 ps/nm/km, dispersion slope of 0.059 ps/nm^2/km at 1553 nm. The Raman pump wavelength was set at 1452 nm to promote high-quality compression performance. A VOA was employed to control power after the signal had passed through the RASC and before the signal was sent to the HNLF. The compressed RZ clock pulse was set as a pump signal. The phase shifter was used to control the time delay of the compressed RZ clock with respect to its overlap with the input NRZ-DPSK signal. Conversely, the input NRZ-DPSK data signal was modulated using a 10-Gb/s LNM intensity modulator by a 10 Gb/s data with a PRBS of 2^{31}-1 from a PPG. The signal was synchronized with the RZ clock using direct synchronization instead of clock recovery. The data signal was amplified by an EDFA with an OBPF before it passed through a 3-dB coupler. The studies of the system's signal reshaping with simultaneous waveform-wavelength conversion was further investigated by transmitting the NRZ-DPSK data signal over

40 km SSMF without any dispersion compensation. PCs were used to maximize the interaction between the two input signals. Both input signals were passed through a HNLF to generate the FWM product. The HNLF with 320 m length had a zero dispersion wavelength at 1553 nm, dispersion slope of 0.023 ps/nm^2/km, and nonlinear coefficient of 28 W^{-1}·km^{-1}. Two OBPFs were used after the HNLF to isolate the FWM product and to remove ASE produced by the EDFA. The bandwidth of the OBPFs was 3 nm. The quality of the converted pulses was measured using an autocorrelator and BERT with a preamplified receiver.

3.2.3 Experimental Result and Discussion

3.2.3.1 Results of Waveform-Wavelength Conversion in the C-Band
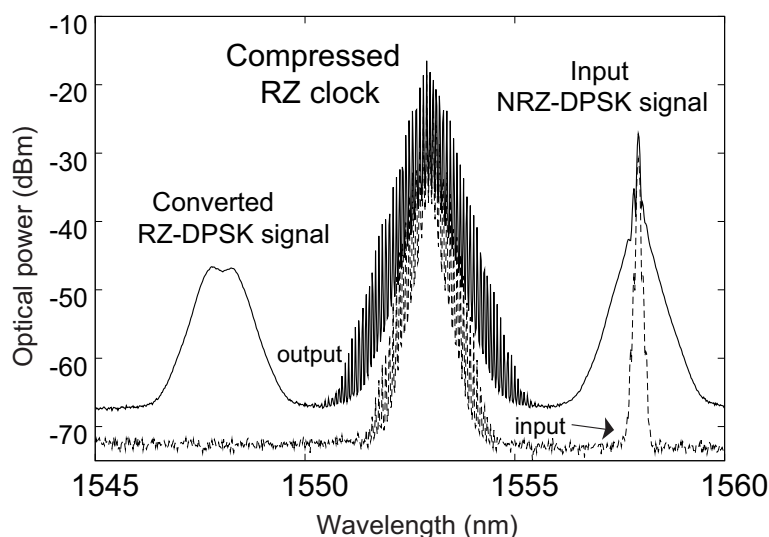
Figure 3.4: Signal spectra at the input (dashed line) and output (solid line) after passing through the HNLF at P_r value of 0.90 W.

Waveform-wavelength converters operating based on only a single channel could prove cumbersome when used in WDM networks, but the potentiality to operate multiple channels using a single converter could lead to network designs of reduced complexity. As WDM signals propagate through a large fiber span link between two EDFAs, the signal performance experiences additional degradation due to fiber dispersion, PMD, fiber nonlinearities, or combinations thereof. Tunable dispersion compensators can be used to mitigate the dispersion tolerance and PMD can be avoided through careful fiber

3. SINGLE MODULATION FORMAT ALL-OPTICAL SIGNAL PROCESSINGS

selection. However, individually and separately processing the channel and adding a new function or hardware item to retrospectively circumvent this problem are unfeasible approaches, because of the network complexity and associated cost. Recent studies presented in Refs. [28, 29] have revealed that the transmission performance results of differently converted RZ pulse durations indicate the existence of an optimum pulse duration for each transmission span with a particular cumulative dispersion. The next goal is to simultaneously provide both flexibility and tunability in a converter, so as to optimize WDM channel transmission performance via pulse-width management in a wide-wavelength conversion operation range.
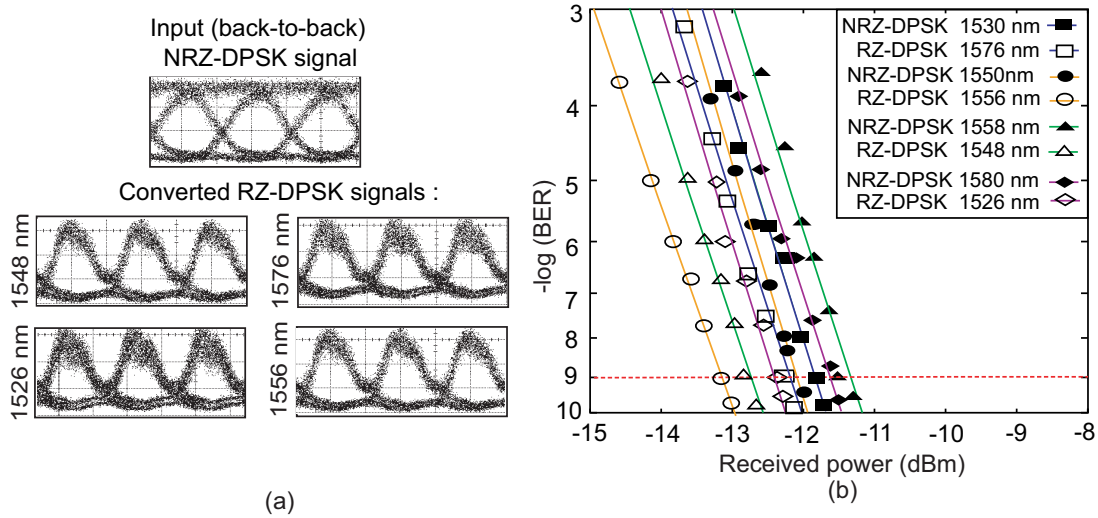
Figure 3.5: (a) Demodulated eye patterns and (b) BER curves for input (back-to-back) NRZ-DPSK signals and the converted RZ-DPSK signals after FWM (50 ps/div.)

An important feature for the waveform-wavelength converter is the operation in wide-wavelength conversion ranges. Firstly, we showed that the proposed converter scheme could effectively operate with 10-Gb/s NRZ-DPSK input signals and this scheme converted this signal to a 10-Gb/s RZ-DPSK signal with a width-tunable signal. Figure 3.4 shows the signal spectra measured at the input (dashed line) and output (solid line) of the HNLF with total input-output separation of 10 nm. The compressed RZ clock was chosen at the representative P_r value of 0.90 W and the wavelength was set at 1553 nm. The converted RZ-DPSK signal at 1548 nm was generated as the input NRZ-DPSK signals was located at 1558 nm. After the FWM process was applied over the AND logic function in the fiber-based switch, the converted RZ-DPSK signal

preserved the same information as the input NRZ-DPSK signal. Consequently, the spectral width of the converted RZ-DPSK data signal was broadened significantly and the pulse width was narrowed simultaneously through FWM process in HNLF.

Secondly, in order to observe the performance of the proposed scheme, several waveform-wavelength conversions were performed with separate input NRZ-DPSK signals were set at the wavelength of 1530, 1550, 1558, and 1580 nm, which corresponded to converted RZ-DPSK signal separations of 46, 6, 10, and 54 nm, respectively. The demodulated eye pattern are presented in Fig. 3.5 (a). As observed in Fig. 3.5 (a), the converted demodulated eye pattern at wavelengths of 1526 and 1576 nm was shown a slightly larger signal distortion than the other converted wavelengths. This finding resulted because FWM conversion efficiency was higher near the zero-dispersion wavelength. The BER measurements were taken to evaluate the system performance for input (back-to-back) NRZ-DPSK and the converted RZ-DPSK signals at different wavelength separations as shown in Fig. 3.5 (b). The improvements in receiver sensitivity of the converted RZ-DPSK signals were observed, with negative penalties varying from -1.3 to -0.8 dB over the wavelength ranges. Besides, the receiver sensitivity of the RZ-DPSK was better in comparison with NRZ-DPSK signal [53].

3.2.3.2 Results on Flexible Picosecond Width-Tunable Waveform-Wavelength Conversion

Both the pulse width of the compressed RZ clock after RASC and the converted RZ-DPSK signal after FWM are depicted as a function of P_r value in Fig. 3.6. The pulse width of the RZ clock pulse could be compressed as its peak power was increased with the increment of P_r value because the soliton condition was preserved during soliton propagation inside the RASC. The P_r values were tuned from 0.20 to 0.90 W. However, when P_r was tuned to a value exceeding 0.90 W, the pulse waveform was distorted and the pedestal component appeared in the pulse wing. This phenomenon resulted due to the deviations from the soliton condition. Additionally, the pulse widths of the converted RZ-DPSK signals after the FWM process were smaller than the pulse width of the compressed RZ clock. The converted RZ-DPSK signal (with the resulting pulse width decreasing from 13.0 to 2.87 ps) was obtained at P_r tuning range of 0.20 to 0.90 W. For an example, Fig. 3.7 (a) presents the autocorrelation traces of the compressed RZ clock and the converted RZ-DPSK signal at P_r value of 0.90 W. The converted signal
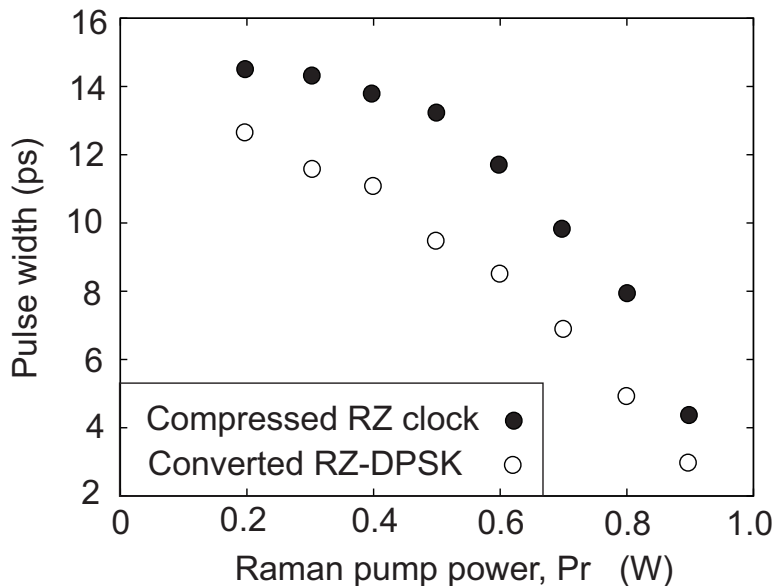
Figure 3.6: Raman pump power (P_r) dependency of the compressed RZ clock pulse width at the RASC's output and the converted RZ-DPSK signals after the FWM operation.

was considerably compressed to 2.87 ps as the compressed RZ clock pulse width was 4.20 ps at P_r value of 0.90 W. The converted pulse shape had no pedestal pulse at a total compression factor exceeding 6 was achieved which was sufficiently small to serve as the 160 Gb/s OTDM data signals' source. In other hand, the spectrum of the converted RZ-DPSK at P_r value of 0.90 W is shown in Fig. 3.7 (b). The spectrum bandwidth of the converted signals was 1.0 nm and the measured time-bandwidth product was 0.36. This findings resulted from optimum compression after FWM operation, which generated a minimum pedestal because the FWM signal power was varied quadratically with respect to the output of the compressed RZ clock power [52]. The result clearly demonstrated that a NRZ-DPSK signal has successfully been converted to a high-quality RZ-DPSK signal with a pedestal-free picosecond width-tunable output signal.

3.2.3.3 Reshaping Waveform-Wavelength Conversion with Tolerance to Chromatic Dispersion

Increasing the capacity of optical communications systems may require either an increased bit-rate, WDM usage, or, essentially, both. Thus, a long-haul communication network can be designed using a WDM with a higher bit-rate per channel. At higher
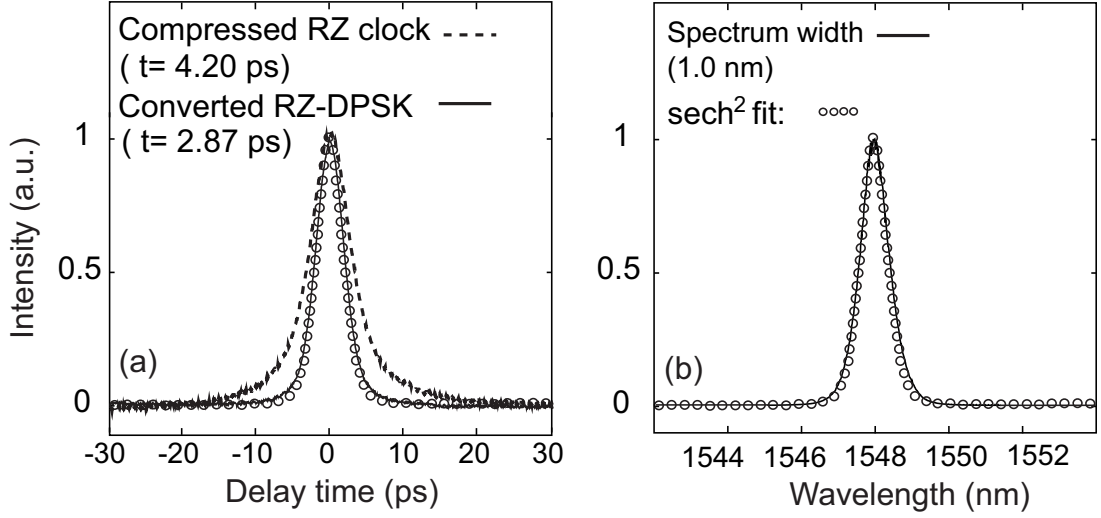
Figure 3.7: Characteristics of the converted RZ-DPSK data pulse at a P_r value of 0.90 W for (a) autocorrelation traces and (b) optical spectrum.
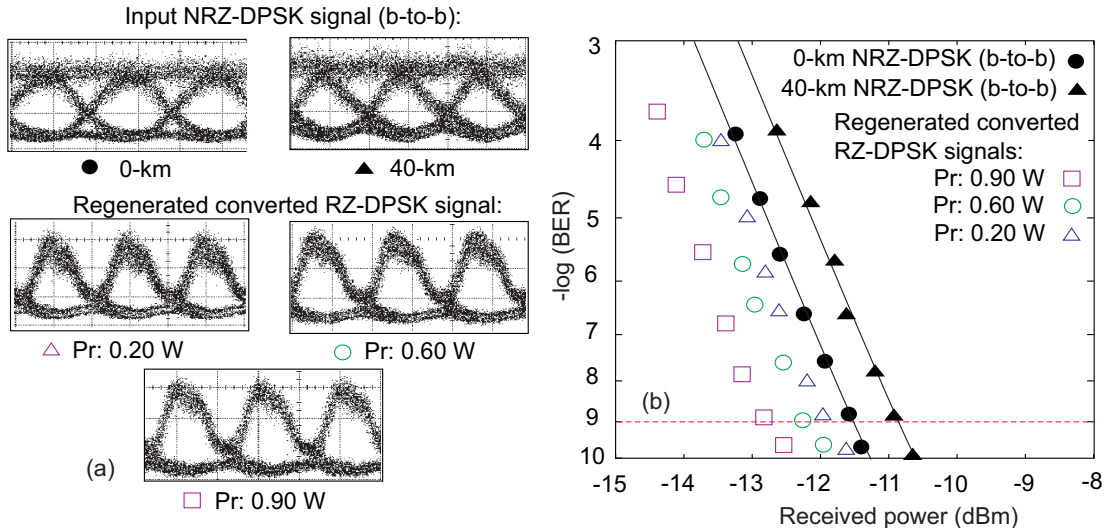
Figure 3.8: (a) Demodulated eye patterns and (b) BER characteristics for the original NRZ-DPSK signal, signal degradation after propagation through 40-km SSMF and its reshaping converted RZ-DPSK signals at all P_r values.

transmission bit-rates, signal broadening effects lead to inter-symbol interference caused by fiber dispersion. This becomes sufficiently severe to cause neighboring pulses to overlap. The requirement for dispersion compensation becomes important, owing to the low tolerance for impairment in the transmission link. At a higher bit-rate, the effect of

nonlinearity becomes more significant, and the RZ signal has been proven to be superior at higher bit-rates. The effect of dispersion can be eradicated by appropriate selection of the parameters related to the pulse shape, which, in effect, allows the original form to be recovered.

The maximum SSMF transmission length for the input degraded signals could be estimated based on Eq. (2.38) in section 2.4.2. For an example, for SSMF with dispersion value of 17 ps/nm/km at bit-rate of 2.5 Gb/s and $\Delta\lambda = 0.03$ nm, the distortion free signal length was around 784 km. However, when increasing the bit rate by a factor of 4, the effect of chromatic dispersion increased by a factor of 16 at bit-rate of 10 Gb/s. Thus, the dispersion-limited distance was approximately 60 km. Due to unavailability of long SSMF, an impaired input NRZ-DPSK signal was introduced by transmitting the signal over 40 km SSMF. This length corresponded to 680-ps/nm dispersion accumulation. Other conditions were the same as discussed in the previous section. Figure 3.8 (a) presents the demodulated eye patterns of original NRZ-DPSK signal and signal degradation after propagation through 40-km SSMF and its converted RZ-DPSK signals with reshaping at all P_r values. Although the obtained demodulated eye patterns were clear and open, clearer demodulated eye patterns in the case of P_r value at 0.90 W was observed than in other cases. Figure 3.8 (b) compares the BER measurement for the original NRZ-DPSK signal and signal degradation after propagation through 40-km SSMF with its corresponding reshaping converted RZ-DPSK signals. The receiver sensitivity of the original NRZ-DPSK signal and the transmission over 40 km was -10.9 and -11.5 dBm, respectively, corresponding to a power penalty of 0.60 dB. The small power penalty of less than 1 dB below 60 km transmission was also predicted in Ref. [54]. The best quality output would be achieved when the compressed RZ clock signal overlapped with the center of the input NRZ-DPSK data signal by optimizing the time delay of the phase shifter. If misalignment occurred, the converted signal quality would be degraded. The penalty improvement was enhanced when P_r value was set at the value of 0.90 W. Furthermore, analysis showed that the converted RZ-DPSK penalty was -1.95 dB in which the signal with the smallest pulse width at P_r value of 0.90 W yielded the best result owing to its higher extinction ratio compared to wider pulse width. Since the converted RZ-DPSK pulse width is narrower than that of the NRZ-DPSK, the RZ-DPSK has higher peak power than the NRZ-DPSK for the same received average power. Thus, the RZ-DPSK eye opening is wider and

results in superior receiver sensitivity for a given average power. The photocurrent at the optical receiver is proportional to the incident optical power, thus, the BER 10^{-9} value is further improved. Further, the width-tunable compressed RZ clock reshapes the converted signal and results in a narrower width after the FWM process. Similar results have also been obtained using a previous scheme [18]. In addition, as shown in Fig. 3.8 (b), converted signal at the smaller pulse width during Raman pump power of 0.90 W has better power penalty in comparison with longer pulse width due to higher peak powers for the same average powers that enhanced the FWM conversion efficiency. The receiver sensitivity gain is increased with the decreased of the pulse width, which should be attributed to the increased extinction ratio. Furthermore, as the short pulse input bandwidth is higher than that of the receiver front-end, the response of the impulse receiver is obtained. Thus, the receiver drives the largest possible voltage swing and gives the sharpest rising and falling edges, for a given optical energy.

For higher input data-rate signals, a pulse will be distorted and dispersed more in time because dispersion will become higher as the square of the increase in data-rate. Thus, the phase matching between pumps and input data signals become harder even for much smaller signal width of input RZ clock pump. However, such limitation can be solved by adding a highly accurate dispersion management such as tunable dispersion management together with existing devices to monitor the accumulated dispersion for the future work implementation.

3.3 All-Optical Wavelength Multicasting

In this section, based on our obtained preliminary results [19],[42], we present the extension of our studies to provide details of a simple implementation of an all-optical multicasting conversion method with tunability in both wavelength and picosecond pulse-width range. The multicasting scheme is realized using a fiber-based single-parametric-gate HNLF and a RASC pulse compressor. The simultaneous replication of six channel-multicast signals with width-tunable output is successfully carried out by tuning the Raman pump power as a control device up to 0.55 W. The current study contributes to our knowledge by providing the following meritorious factors: (1) the RASC acts as both a tunable pulse width compressor for multicast signals and an amplifier, (2) the adjustable wider range can be implemented for pedestal-free

picosecond width-tunable 6 × 10 Gb/s multicast-converted data controlled down to 2.67 ps (sevenfold) and can exhibit approximately the same high quality performance, and (3) 20.3-nm multicast up-conversion (input-output) can be achieved with a low power penalty. Producing more than six channel-multicast copies may be possible by adding more probe signals in the HNLF.

This section is organized as follows. Subsection 3.3.1 and 3.3.2 describes the concept and experimental setup, results and discussion for all-optical multicasting that introduced in this chapter. Lastly, the conclusion is given in subsection 3.3.3.

3.3.1 Concept and Experimental Setup

The operational principle of the proposed scheme is shown in Fig. 3.9. It is based on a parametric process in a HNLF FWM AND-gate between RZ-OOK width-adjustable compressed data and six CW probes. In the first stage, a RASC is used. The RASC consists of a constant dispersion fiber, such as a DSF and does not require any special fibers [43, 45]. The system operation is based on adiabatic soliton compression, which has a high-power output and a width-tunable pulse in the picosecond range by tuning the Raman pump power (P_r). The RASC acts as a pulse width controller and as an amplifier. Input RZ data is a fundamental soliton (N = 1) of the sech^2 pulse; it is adiabatically amplified in the DSF as the P_r value is increased. Based on the arrangement from the equation in ref. [46], the relationship between the pulse width τ_{FWHM}, the peak power of the fundamental soliton pulse $P_{N=1}$, and the chromatic dispersion D can be obtained as

$$\tau_{FWHM} \propto \sqrt{\frac{D}{P_{N=1}}} \tag{3.1}$$

From relation (1), an increase in the soliton peak power $P_{N=1}$ would result in the reduction of pulse width τ_{FWHM}. Thus, it is possible to have flexibility in the picosecond width-tunable output converted RZ data signal from the RASC. Using the combination of strong input pump data produced by the RASC at a wavelength λ_{pump} with several probe input CW signals λ_{sig} into HNLF, the FWM can be achieved. The duplicate multicast data signals will be generated at wavelengths $\lambda_{multicast} = 2\lambda_{pump} - \lambda_{sig}$. According to [51, 52] the multicasting signal power is proportional to the square of the input RZ data signal power, which acts as the pump of the FWM.
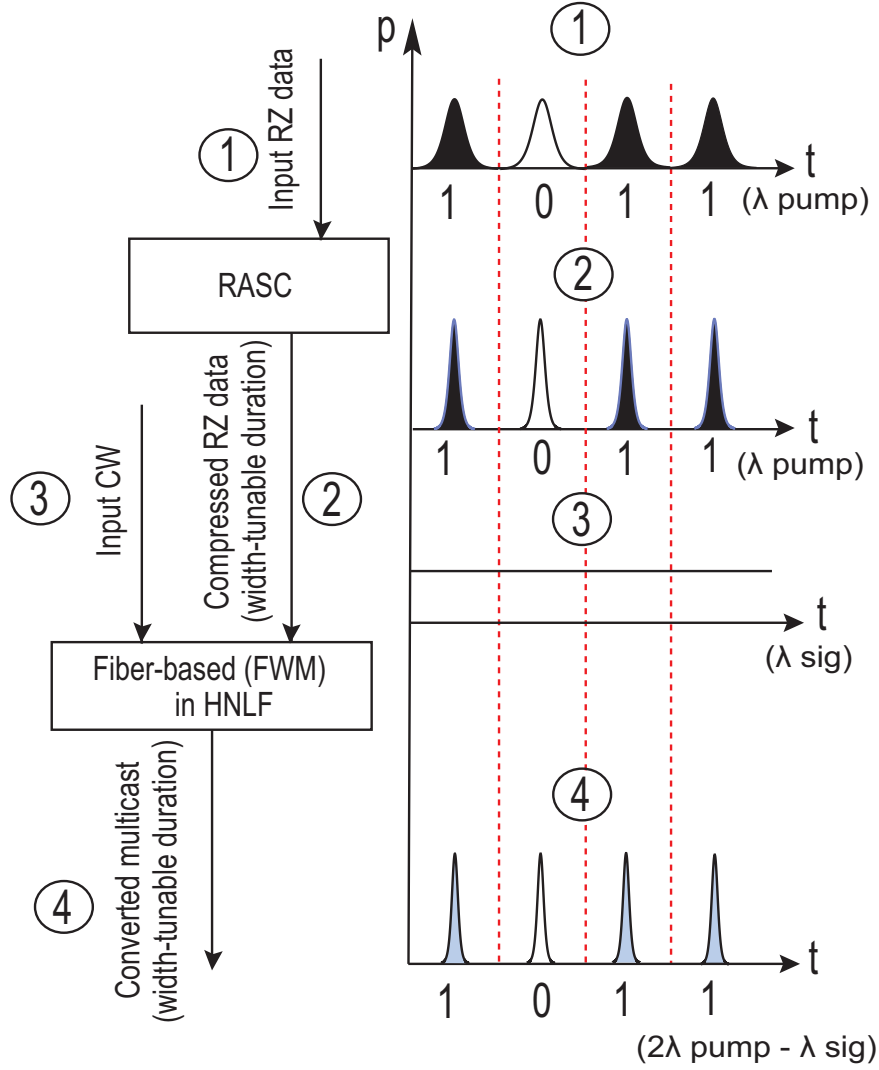
Figure 3.9: Operational principle of 1-to-6 wavelength multicasting with picosecond-width-tunable output signals.

From the viewpoint of network node as shown in Fig. 3.1, the multicast conversion based on a parametric process in a HNLF between RZ-OOK width-tunable compressed data and six CW probes is performed at node B. An RZ-OOK signal from node A will be flexibly compressed by RASC that is located at node B. The transmission characteristics of the signal before node B was not performed in our studies because we mainly concentrate on demonstrating the RASC functionality for the multicast
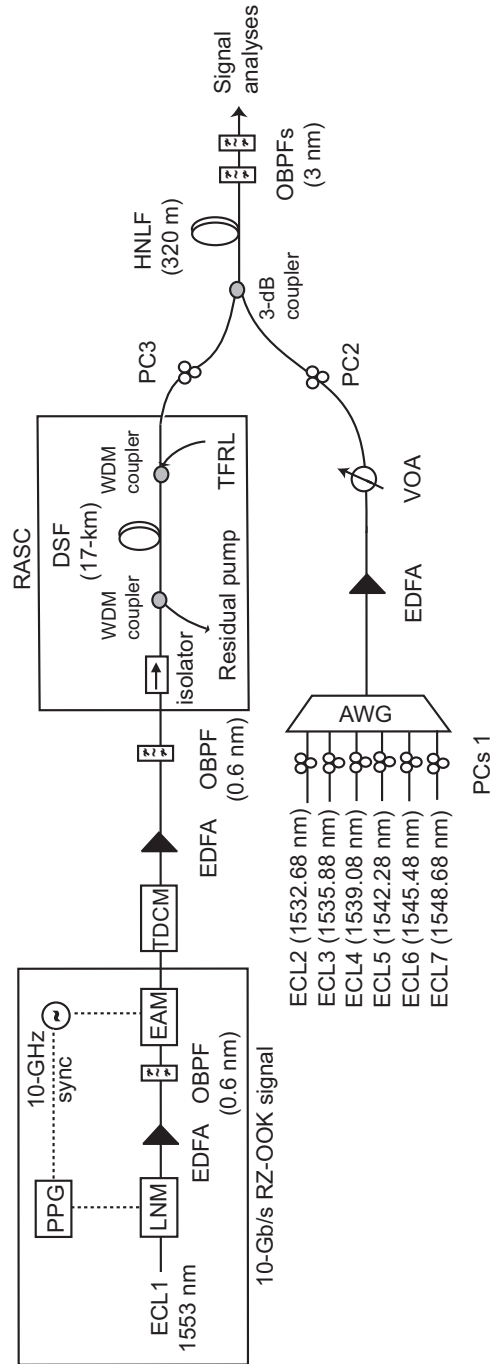
Figure 3.10: Experimental setup of 1-to-6 wavelength multicasting with picosecond-width-tunable output.

conversion application. The experimental arrangement for the multicasting conversion is shown in Fig. 3.10. A 10-Gb/s NRZ data signal with 1553-nm wavelength was generated using an ECL and a LNM modulator driven by electrical data from a PPG. The data signal was amplified and filtered by an EDFA with an OBPF. The data was converted into an RZ format by an EAM driven by a 10-GHz synthesizer. A TDCM was used to suppress the frequency chirping induced by the EAM. An EDFA and an OBPF were used both to compensate for signal loss due to the EAM and to set the conditions for fundamental soliton power in the RASC. Based on the adiabatic soliton compression operation, the RASC that located at node B consisted of a 17-km DSF and a TFRL. The DSF had anomalous dispersion of 3.8 (ps/nm)/km, an a dispersion slope of 0.059 (ps/nm^2)/km at 1553 nm. The Raman pump wavelength was set to 1452 nm to promote high-quality compression performance. The pulse width of the RZ data signal was compressed as its peak power increased with the increment of the Raman pump power because the soliton condition was maintained in the DSF during amplification. The compressed RZ data acted as a pump signal. Six probes of CWs with a wavelength spacing of 400 GHz at a wavelength from 1548.68 to 1532.68 nm were generated and multiplexed with an AWG. Polarization controllers 1 (PCs 1) on each CW channel functionality are to maintain polarization orthogonality between that particular CW channel and the compressed RZ data signal. The power of each probe was set to the same value and amplified using an EDFA. Both the compressed input of the RZ data and the CWs were passed through a HNLF to generate the multicast products. The HNLF of 320 m in length had a zero dispersion wavelength of 1553 nm, a dispersion slope of 0.023 (ps/nm^2)/km, and a nonlinear coefficient of 28 W$^{-1} \cdot$ km^{-1}. In a real system, an important parameter that needs to be concerned is polarization sensitivity. However, in order to obtain a high conversion efficiency for all the multicast channels, the polarization states of the input signal pump and CW probes of PC 2 and PC 3 need to be adjusted. If not, the conversion efficiency of the multicast channels will be low and may not be practical for a real system. Two OBPFs were used after the HNLF to isolate the FWM product and to remove ASE from the EDFA. The bandwidth of the OBPFs was 3 nm. The quality of the converted pulses was measured using an autocorrelator and a bit error rate tester (BERT) with a preamplified receiver.
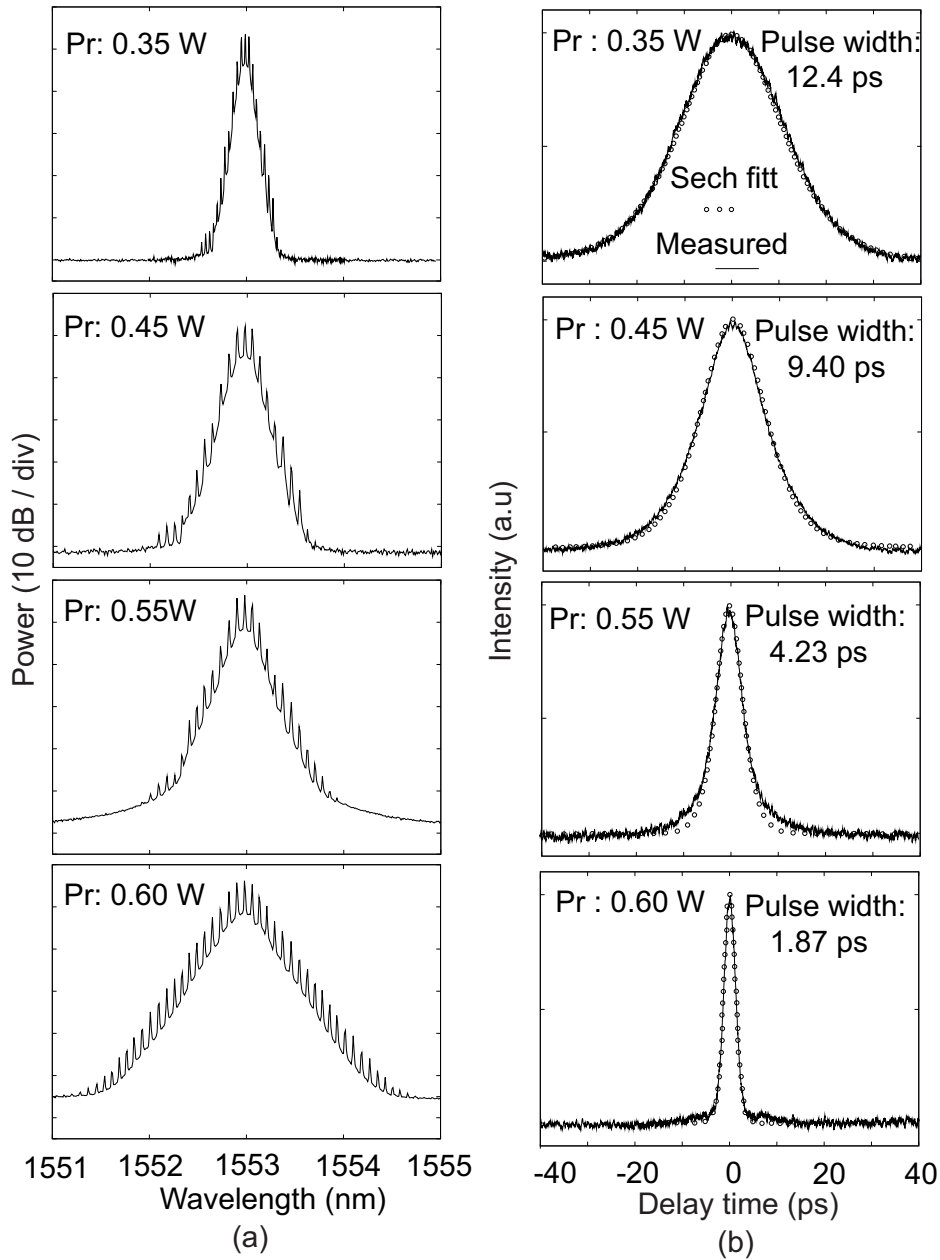
Figure 3.11: (a) Spectrum and (b) autocorrelation traces of the data signal at P_r values of 0.35, 0.45, 0.55, and 0.60 W.

3.3.2 Results and Discussion

The characteristics of the output data signal from the RASC were investigated using two 3-nm OBPFs for channel selection. The output optical spectra and the corresponding
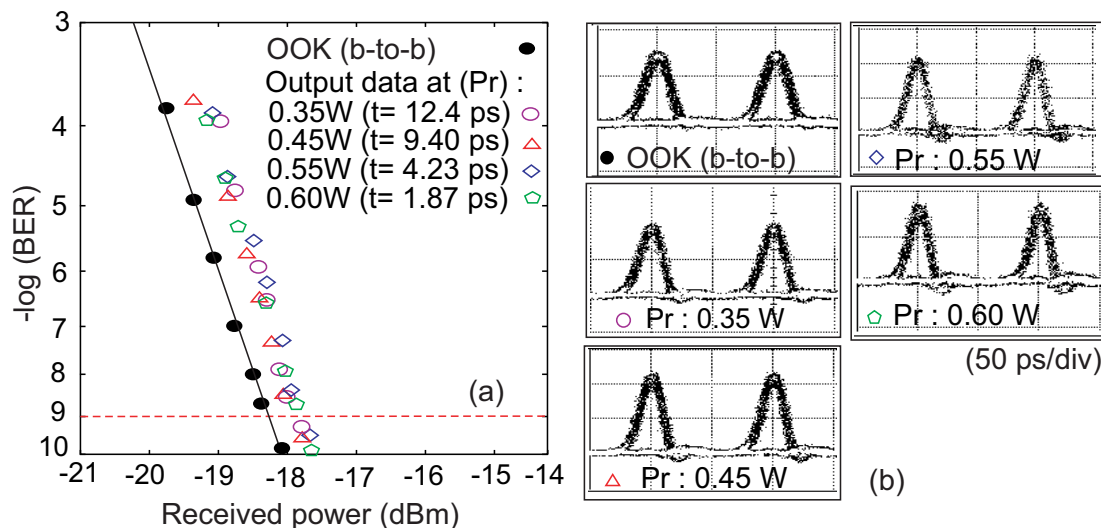
Figure 3.12: (a) BER characteristics of the RZ-OOK signal before and after pulse compression at different tuning Raman pump powers. (b) Output eye patterns of the converted pulses for different P_r values.

autocorrelation traces are shown in Fig. 3.11 (a) and (b), respectively. In Fig. 3.11 (b), the solid line shows the measured waveform and the circles show the sech^2 fitting waveform. As shown in the figure, the pulse width was compressed with an increment of the Raman pump power (P_r values), and the spectral width was broadened relative to the pulse compression. The input RZ data signal with a duration of 18 ps was significantly compressed to 12.4, 9.40, 4.23, and 1.87 ps as P_r was tuned to 0.35, 0.45, 0.55, and 0.60 W, respectively. The compressed pulses were well fitted by sech^2 functions in terms of both spectra and waveform. The measured spectral bandwidth was 1.40 nm and the time-bandwidth product was 0.33, estimated at a P_r of 0.60 W, which shows that the pulse had a transform-limited sech profile. On the other hand, adiabatic soliton pulse compression in RASC provides a highly compressed pulse with very small pedestals. At a P_r value of 0.60 W, the calculated peak-to-pedestal ratio was 14 dB; this power value can potentially be used for flexible up to higher bit-rate data signals for optical time domain multiplexing (OTDM) or WDM networks [1], [53]. The BER curves of the converted RZ data at different P_r values are plotted in Figure 3.12 (a). We achieved error-free operation for all compressed RZ data with a small power penalty of less than 0.5 dB compared to the back-to-back input signal. In addition, approximately a 0.1 dB variation of sensitivity among the converted pulses at various

3. SINGLE MODULATION FORMAT ALL-OPTICAL SIGNAL PROCESSINGS

P_r values was obtained. Figure 3.12 (b) shows the eye patterns of the compressed RZ data eye patterns for P_r values of 0.35, 0.45, 0.55, and 0.60 W, respectively. Even though the bandwidth of the employed electrical sampling oscilloscope was limited to 30 GHz, clear eye openings were observed. These openings indicated that the signals generated by the DRA achieved good performance and that they might be used as input data in multicasting applications.
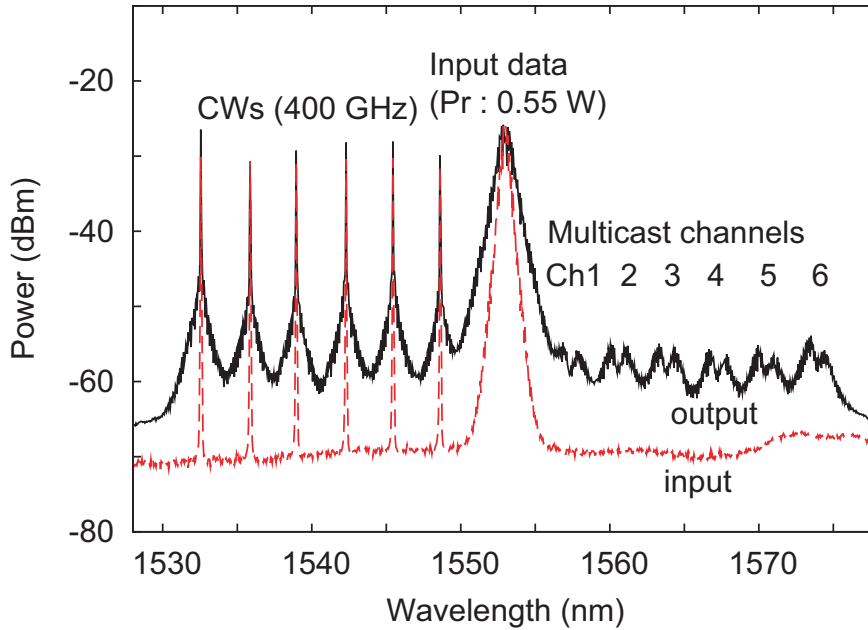
Figure 3.13: FWM spectra of the input (dashed line) and output (solid line) at a P_r value of 0.0 and 0.55 W, respectively.

Figure 3.13 shows the FWM spectra of 1-to-6 multicast channel conversion using the input data signal at a P_r of 0.55 W. The dashed and solid lines represent the input and output of the HNLF, respectively. When RZ pulsed data propagates with CWs signal in nonlinear gain medium for parametric process, the signal was amplified and converted to a new six-wavelength idler signals. From parametric amplification process in HNLF, the signal and the converted pulses follow the pulse shape of the RZ pulsed-pump as the amplification dependence on input pump power [36, 57]. The pulse width of the input data signals and wavelength converted pulses were narrower than of the RZ data pump due to compression effect received from parametric amplification gain during FWM operation [58]. Thus, the converted spectral outputs of the 6×10 Gb/s WDM RZ data
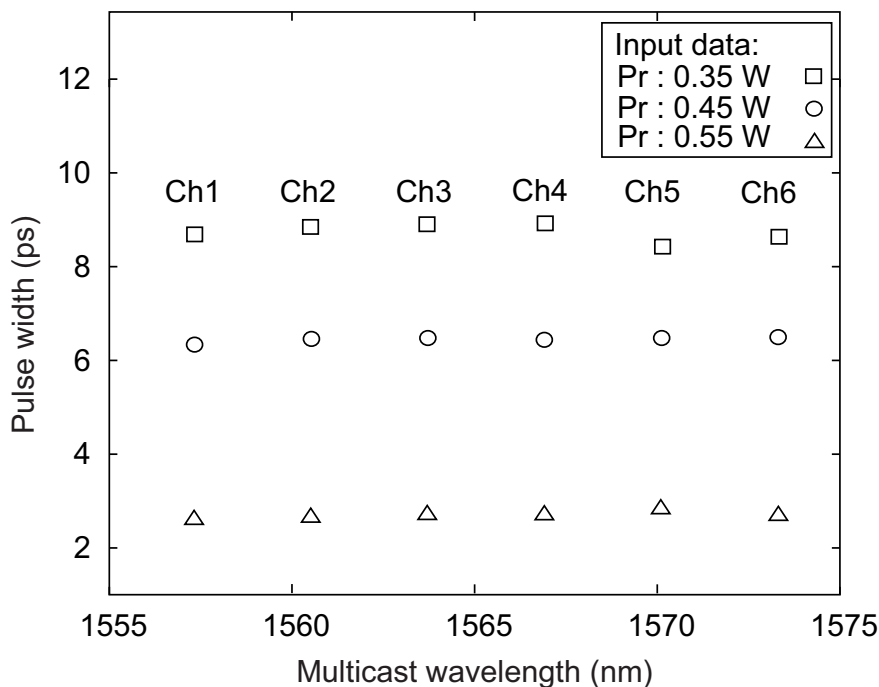
Figure 3.14: Variations of wavelength and pulse width multicast channels for the input data signals at different P_r values.

and six CWs input data signals were broadened at the same time while increment the P_r value over the adiabatic soliton compression. All-optical wavelength multicasting technique with wide wavelength operation is highly desirable in the optical networks. Wide wavelength conversion could be characterized in terms of the employed N number of input data signal and pumps to deliver the source information to a certain number of destination wavelengths. In order to to investigate the quality of the converted signals at different pulse widths, the wavelength spacing between input CW probes were set equally to 400 GHz (3.2 nm). At the fixed pump wavelength of 1553 nm, six input CWs probe channels at 1532.68 nm (Ch 6), 1535.88 nm (Ch 5), 1539.08 nm (Ch 4), 1542.28 nm (Ch 3), 1545.48 nm (Ch 2), and 1548.68 nm (Ch 1) interacted with the pump data to yield six up-converted multicast channels located at 1557.32 nm (Ch 1), 1560.52 nm (Ch 2), 1563.72 nm (Ch 3), 1566.92 nm (Ch 4), 1570.12 nm (Ch 5), and 1573.32 nm (Ch 6). Approximately, 20.3-nm up conversion from 1557.32 to 1573.32 nm were achieved within our proposed scheme. Similarly, the same operation can be done for multicast channels tends towards the C band shorter wavelength area if the

input probe signals were located towards the long wavelength area. Approximately, 10 multicast channels are possible to be converted (6 up-conversion and 4 down-conversion channels) at the pump-probe wavelength detuning of $2\lambda_p - (\lambda_{sN} + N \cdot 3.2nm)$ in the C-band wavelength ranges from 1530 to 1565 nm.
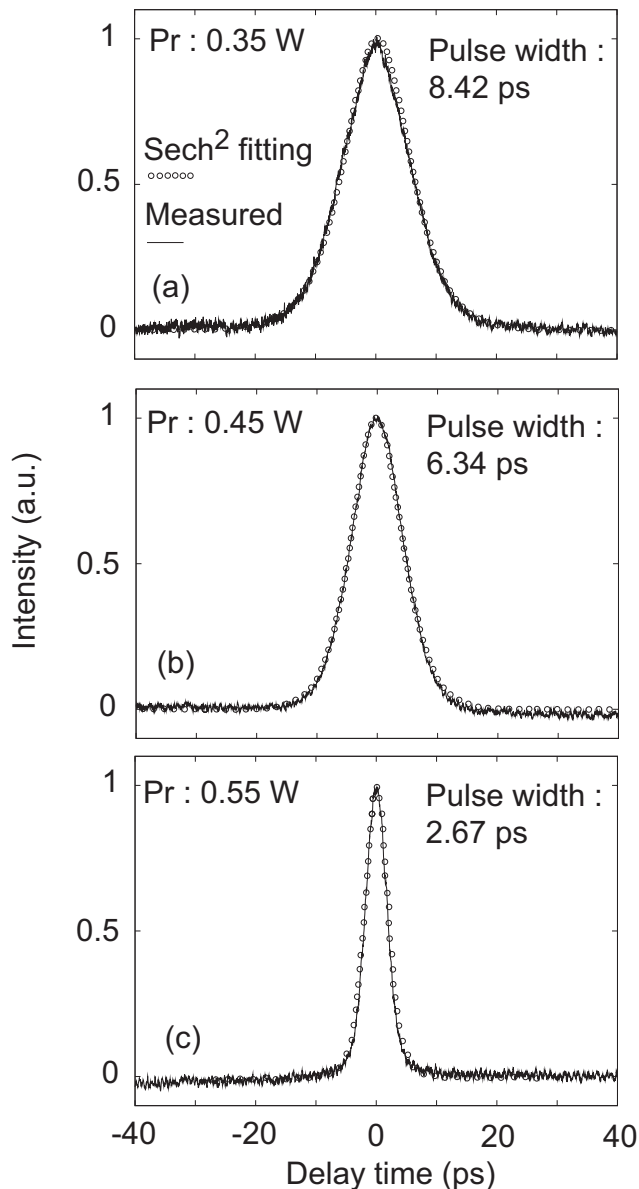
Figure 3.15: Variations of pulse width with the converted multicast wavelength in channel 3 (Ch 3) for the input data signal at P_r values of (a) 0.35 W, (b) 0.45 W and, (c) 0.55 W.

Figure 3.14 plots the variations of the converted pulse width for three P_r values.

The variations of the compressed pulse width were less than 0.1 ps for a constant P_r value. In addition, the multicast converted channel pulse widths were narrower than those of the input data signal. The multicast conversion channels were further quantified by autocorrelation trace measurement for channel 3 (Ch 3) at three P_r values of input RZ data, as shown in Fig. 3.15. For example, at the P_r values of 0.35, 0.45, and 0.55 W, the converted multicast pulse widths were 8.42, 6.34, and 2.67 ps, respectively. The generated copies underwent pulse pedestal suppression and further pulse compression during the parametric process because of the quadratic pump and idler amplitude relation [52, 56]. These traces were well fitted by sech^2 fitting and had free pedestal pulses. The time-bandwidth product of the pulses in all cases was found to be less than 0.41. For example, the calculated time-bandwidth-product was 0.32 for the input data and the multicasting signal at P_r value of 0.55 W. This value was closer to the transform-limited value of the sech^2 pulse profile. Approximately seven-fold pulse compression was obtained from the input data and a P_r value of 0.55 W. These results show that high-quality multicast pulses were obtained using our proposed scheme.

Although the transmission performance after multicast signal is not demonstrated in this paper, it is expected that the experiment can be done using our proposed scheme with different transmission link. It should be noted that in any installed transmission network, the effect of dispersion is cumulative. In a single channel transmission without any dispersion compensation scheme [28], a narrower pulse width such as 2.67 ps is expected to be more sensitive to dispersion at longer transmission distance. In order to optimize the transmission performance under the circumstances of large cumulative dispersion, a wider pulse width up to 8.42 ps is possible. We believe that, with the combination between our proposed scheme and dispersion compensation module in the transmission link, longer achievable transmission distance can be obtained [7], [30]. Furthermore, the advantage of the pedestal free multicast signal at the pulse width of 2.67 ps is capable of being multiplexed to high bit-rate up to 160 Gb/s.

Figure 3.16 shows three eye patterns, namely, Ch 1, Ch 3, and Ch 6, compared to the back-to-back input data signal at different P_r values. Clear, widely opened eye patterns of the multicasting signals were obtained for all channels at a high output quality. The system performance of the proposed wavelength and picosecond-width-tunable converted multicast scheme was further evaluated through BER measurements,
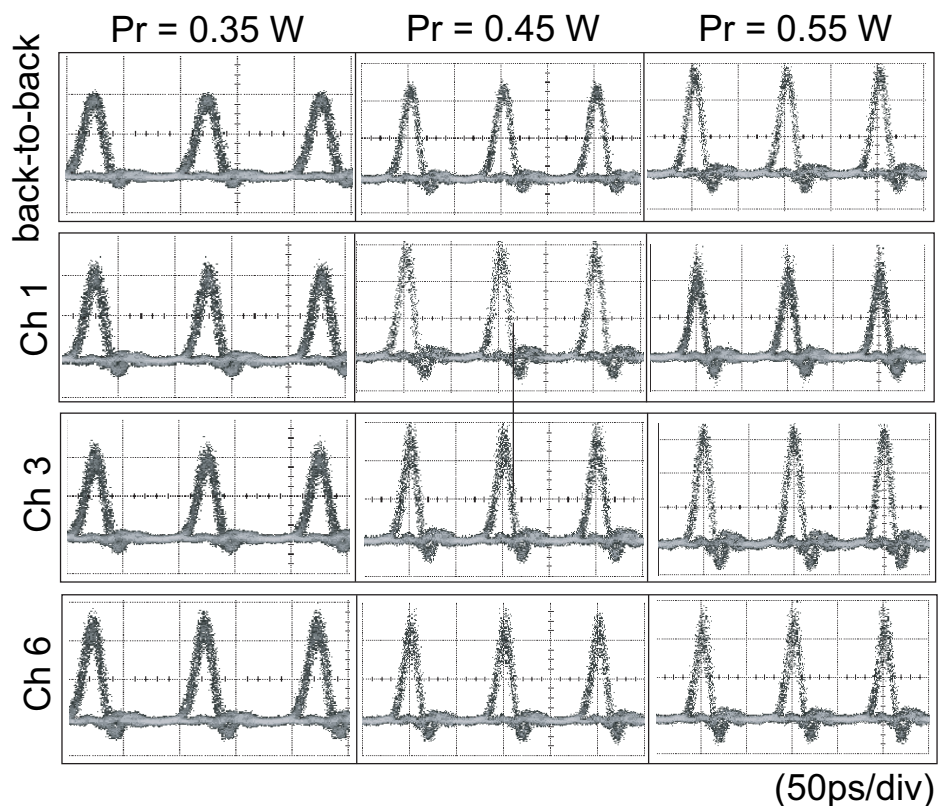
Figure 3.16: Multicast channel eye patterns for 10 Gb/s RZ-OOK data input at P_r values of 0.35, 0.45, and 0.55 W.

as shown in Fig. 3.17. The signal qualities of the copied multicast signals were investigated at P_r values of 0.35 W, 0.45 W, and 0.55 W. This measurement was performed for a probe wavelength that varied from 1532.68 to 1548.68 nm, which is located in the C-band tuning range. Compared to the back-to-back signals, the converted multicast channels for P_r values of 0.35, 0.45, and 0.55 W had maximum power penalties of 1.2, 0.8, 1.0 dB, respectively. It is apparent that with shorter pulse widths, the converted multicast channel had a slightly higher power penalty. Overall, the power penalties of the converted multicast channels in the different cases mentioned above were not significantly different. The results indicated relatively uniform output performance; they are consistent with the eye pattern measurements. Using our proposed scheme, compressed RZ data from a RASC can be used as a high-speed data stream for multicasting and different applications in future optical networks.
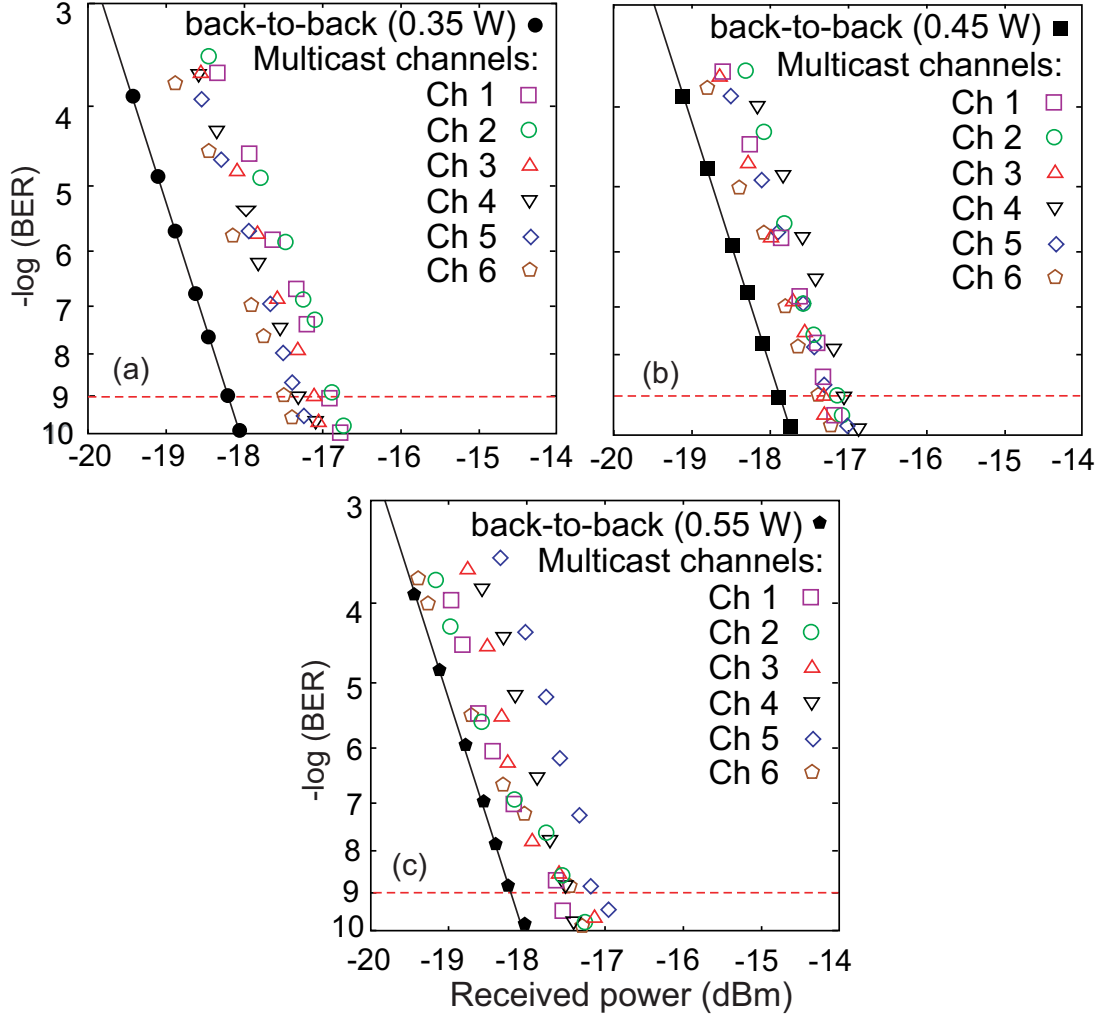
Figure 3.17: BER curves of the back-to-back signal and multicast channel at different RZ-OOK pulse source at P_r values of (a) 0.35 W (b) 0.45 W, and (c) 0.55 W.

3.4 Conclusions

In this chapter, we examined two concepts of an all-optical signal processing using single modulation format either OOK or DPSK. In the first section under this chapter, for the first time, we successfully demonstrated waveform-wavelength conversion of NRZ-DPSK-to-RZ-DPSK with simultaneous signal reshaping and flexible width-tunable operations in combination using RASC and a fiber-based FWM switch. In the first experiment, we demonstrated the concept of a broadband waveform-wavelength conversion for a 10-Gb/s RZ-DPSK signal at about 54-nm separation with the fixed

width of a compressed RZ clock. We then demonstrated waveform-wavelength conversion at different RZ clock pump widths by tuning the Raman pump power up to 0.90 W. The experimental results showed that, by tuning the Raman pump power of the compressed RZ clock from 0.20 to 0.90 W, a converted RZ-DPSK signal with pulse width compression down to 2.87 ps and pedestal-free pulse could be obtained. Furthermore, the phase information of the converted RZ-DPSK signal was identical to the input NRZ-DPSK signal. In addition, negative power penalties below 1.95 dB were achieved in comparison between degraded input NRZ-DPSK data signal and its regenerated converted RZ-DPSK signal. These findings confirmed that the proposed scheme is a promising method for achieving an impairment-free picosecond width-tunable regenerated converted RZ-DPSK signal.

Finally, in the last section of this chapter, simultaneous multicasting conversion from one to six channels for different cases of input data signals from the RASC was performed. Width-tunable pulse width and wavelength multicasting within the C-band with approximately 20.3 nm of separation for various compressed RZ data inputs have also been demonstrated. Penalties of less than 1.2 dB were obtained for all multicasting outputs from the RASC. Output pulse widths with a flexible tuning range down to 2.67 ps were also achieved.

References

[1] N. Sambo, F. Cugini, G. Bottari, and P. Iovanna, "Toward high-rate and flexible optical networks," *IEEE Commun. Mag.*, vol. 50, no. 5, pp. 66–72, May 2012.

[2] L. Yan, A. L. Willner, X. Wu, A. Yi, A. Bogoni, Z. Y. Chen, and H. Y. Jiang, J. Lightwave Technol., "All-optical signal processing for ultrahigh speed optical systems and networks," *J. Lightwave Technol.*, vol. 30, no. 24, pp. 3760–3770, Dec. 2012.

[3] D. Norte, and A. E. Willner, "All-optical data format conversions and reconversions between the wavelength and time domains for dynamically reconfigurable WDM networks," *J. Lightwave Technol.*, vol. 14, no. 6 pp. 1170– 1182, June 1996.

[4] D. Norte, and A. E. Willner, "Multistage all-optical WDM-to-TDM-to-WDM and TDM-to-WDM-to-TDM data-format conversion and reconversion through 80 km of fiber and three EDFA's," *IEEE Photon. Technol. Lett.*, vol. 7, no. 11, pp. 1354–1356, Nov. 1995.

[5] H. Satobayashi, W. Chujo, and T. Ozeki, "Hierarchical hybrid OTDM WDM network.pdf," in *Proceedings of IEEE/LEOS Summer Topics,* pp. WF3-47, 2002.

[6] F. Parmigiani, L. Provost, P. Petropoulos, D. J. Richardson, W. Freude, J. Leuthold, A. D. Ellis, and I. Tomkos, "Progress in multichannel all-optical regeneration based on fiber technology," *J. Sel. Top. Quantum Electron.*, vol. 18, no. 2, pp. 689–699, Mar/Apr 2012.

[7] L. -S. Yan, S. M. R. M. Nezam, A. B. Sahin, J. E. McGeehan, T. Luo, C. Reeves-Hall, and A. E. Willner, "Performance optimization of RZ data format in WDM

REFERENCES

systems using tunable pulse-width management at the transmitter," *J. Lightwave Technol.*, vol. 30, no. 3, pp. 1063–1067, March 2012.

[8] Z. Jiang, D. E. Leaird, and A. M. Weiner, "Width and wavelength-tunable optical RZ pulse generation and RZ-to-NRZ format conversion at 10 GHz Using spectral line-by-line control," *IEEE Photonics Technol. Lett.*, vol. 17, no. 12, pp. 2733–2735, Dec. 2005.

[9] H. -G. Weber and M. Nakazawa: *Ultrahigh-speed optical transmission technology* (Springer, New York, 2010) p. 399.

[10] M. Matsumoto, "Fiber-based all-optical signal regeneration, " *IEEE J. Sel. Top. Quantum Electron.*, vol. 18, no. 2, pp. 738–752, Mar/Apr 2012.

[11] C. Xu, X. Liu, and X. Wei, "Differential phase-shift keying for high spectral efficiency optical transmissions," *J. Sel. Top. Quantum Electron.*, vol. 10, no. 2, pp. 281–293, Mar/Apr 2004.

[12] P. Devgan, R. Tang, V. S. Grigoryan, and P. Kumar, "Highly efficient multichannel wavelength conversion of DPSK signals," *J. Lightwave Technol.*, vol. 24, no. 10, pp. 3677–3682, Oct. 2006.

[13] C. Xu, X. Liu, L. F. Molleanauer, and X. Wei, "Comparison of return-to-zero differential phase-shift keying and on-off keying in long-haul dispersion managed transmission," *IEEE Photon. Technol. Lett.*, vol. 15, no. 4, pp. 617–619, Apr. 2003.

[14] H. G. Weber, R. Ludwig, S. Ferber, C. S. Langhorst, M. Kroh, V. Marembert, C. Boerner, and C. Schubert, "Ultrahigh-speed OTDM-transmission technology," *J. Lightwave Technol.*, vol. 24, no. 12, pp. 4616–4627, Dec. 2006.

[15] J. Wang, J. Sun, X. Zhang, D. Huang, M. M. Fejer, "All-optical format conversions using periodically poled lithium niobate waveguides," *IEEE J. Quantum Electron.*, vol. 45, no. 2, pp. 195–205, Feb. 2009.

[16] G. K. P. Lei, Y. Dai, J. Du, and C. Shu, "Wavelength multicasting of DPSK signal with NRZ-to-RZ format conversion," *Electron. Lett.*, vol 47, no. 11,pp. 808–810, July 2011.

[17] Y. Yu, B. Zhou, W. Wu, and X. Zhang, "All-Optical Parallel NRZ-DPSK to RZ-DPSK format conversion at 40 Gb/s based on XPM effect in a single SOA," *Opt. Express.*, vol. 19, no.15, pp. 14720–14725, Jul 2011.

[18] G. M. Sharif, Q. Nguyen-The, M. Matsuura, and N. Kishi, "All-optical Wavelength-shift-free NRZ-DPSK to RZ-DPSK Format Conversion with pulsewidth tunability by an SOA-based switch," *IEICE Trans. Electron.*, vol. E97-C, no. 7, pp. 755-761, July 2014.

[19] M. Matsuura, B. P. Samarakoon, and N. Kishi, "Wavelength-shift-free adjustment of the pulsewidth in return-to-zero on-off keyed Signals by means of pulse compression in distributed Raman amplification," *IEEE Photon. Technol. Lett.*, vol. 21, no. 9, pp. 572–574, May 2009.

[20] Q. Nguyen-the, M. Matsuura, H. N. Tan, and N. Kishi, "All-Optical NRZ-to-RZ data format conversion with picosecond duration-tunable and pedestal suppressed operation," *IEICE Trans. Electron.*, vol. E94-C, no. 7, pp. 1160–1166, July 2011.

[21] A. A. M. Saleh, and J. M. Simmons, "Evolution toward the next-generation core optical network," *J. Lightwave Technol.*, vol. 24, no. 9, pp. 3303–3321, Sept. 2006.

[22] A. Ding, and G-S. Poo, "A survey of optical multicast over WDM networks," *Computer Communications*, vol. 26, pp. 193–200, 2003.

[23] L. Gong, C. Zhou, X. Liu, W. Zhao. W. Lu, and Z. Zhu, "Efficient resource allocation for all-optical multicasting over spectrum-sliced elastic optical networks," *Opt. Commun. Netw.*, vol. 5, no. 8, pp. 836–847, Aug. 2013.

[24] X. Yu, G. Xiao, and T-H. Cheng, "Dynamic multicast traffic grooming in optical WDM mesh networks: lightpath versus light-tree," *Opt. Commun. Netw.*, vol. 5, no. 8, pp. 870–880, Aug. 2013.

[25] I. Kaminow, and T. Li, *Optical Fiber Telecommuncations IV-B (Systems and Impairments)*, Academic Press, 2002.

[26] B. P-P Kuo, P. C. Chui, and K. K-Y. Wong, "A comprehensive study on crosstalk suppression techniques in fiber optical parametric amplifier by modulation format," *IEEE J. Sel. Top Quantum Electron.*, vol. 14, no. 3, pp. 659–665, May/June 2008.

REFERENCES

[27] L. S Sahasrabudehe, and B. Mukerjee,"Light-trees: Optical multicasting for improved performance in wavelength-routed networks," *IEEE Commun. Mag.*, vol. 37, pp. 67–73, Feb. 1999.

[28] M. Matsura, N. Kishi, and T. Miki,"Performances of a widely pulsewidth-tunable multiwavelength pulse generator by a single SOA-based delayed interferometric switch," *Opt. Express*, vol. 13, pp. 10010–10021, 2005.

[29] H. Nguyen-Tan, M. Matsuura, and N. Kishi,"Transmission performance of a wavelength and NRZ-to-RZ format conversion with pulsewidth tunability by combination of SOA- and fiber-based switches," *Opt. Express*, vol. 16, pp. 19063–19071, 2008.

[30] C. Yu, L. -S. Yan, T. Luo, Y. Wang, Z. Pan, and A. E. Willner,"Width-tunable optical RZ pulse train generation based on four-wave mixing in highly nonlinear fiber," *IEEE Photon. Technol. Lett.*, vol. 17, no. 3, pp. 636–638, March 2005.

[31] G. Contestabile, A. Maruta, S. Sekiguchi, K. Morito, M. Sugawara, and K. Kitayama, "All-Optical wavelength multicasting in a QD-SOA," *J. Quantum Electron.*, vol. 47, no. 4, pp. 541–547, Apr. 2011.

[32] D. Wang, T-H. Cheng, Y-K. Yeo, Z. Xu, Y. Wang, G. Xiao, and J. Liu,"Performance comparison of using SOA and HNLF as FWM medium in a wavelength multicasting scheme with reduced polarization sensitivity," *J. Lightwave Technol.*, vol. 28, no. 24, pp. 3497–3505, Dec. 2010.

[33] S. Gao, and X. Xiao, "All-optical wavelength multicasting based on cascaded four-wave mixing with a single pump in highly nonlinear fibers," *Opt. Commun.*, vol. 285, no. 5, pp. 784–789, March 2012.

[34] K. K. Chow, and C. Shu,"All-optical signal regeneration with wavelength multicasting at 6x10 Gb/s using a single electroabsorption modulator," *Opt. Express*, vol. 12, no. 13, pp. 3050–3054, June 2004.

[35] G. K. P. Lei, and C. Shu, "4 x 10 Gb/s wavelength multicasting with tunable NRZ-to-RZ pulse format conversion using time- and wavelength-interleaved pulses," *Opt. Commun.*, vol. 285, pp. 2525–2529, 2012.

[36] C.-S Bres, N. Alic, E. Myslivets, and S. Radic, "Scalable multicasting in one-pump parametric amplifier," *J. Lightwave Technol.*, vol. 27, no. 3, pp. 356–363, Feb. 2009.

[37] K. K. Chow, and L. Chinlon, "Applications of photonic crystal fibers (PCFs) in nonlinear signal processing," *Proc. 5th International Conference on Optical Internet (COIN)*, vol. MoA2-1, pp. 26–30, July 2006.

[38] M. Karasek, J. Kanka, P. Honzatko, J. Vojtech, and J. Radil, "10 Gb/s and 40 Gb/s multi-wavelength conversion based on nonlinear effects in HNLF," *Proc. Proc. 5th International Conference on Optical Internet (COIN)*, vol. Tu.D1.7, pp. 155–161, 2006.

[39] B. R. Koch, J. S. Barton, M. Masanovic, Z. Hu, J. E. Bowers, and D. J. Blumenthal, "Monolithic mode-locked laser and optical amplifier for regenerative pulsed optical clock recovery," *IEEE Photon. Technol. Lett.*, vol. 19, no. 9, pp. 641–643, 2007.

[40] O. Aso, A. Shin-Ichi, T. Yagi, M. Tadakuma, Y. Suzuki, and S. Namiki, "Broadband four-wave mixing generation in short optical fibres," *Electron Lett.*, vol. 36, no. 8, pp. 709–711, Apr 2000.

[41] I. Ismail, M. Matsuura, and N. Kishi, "NRZ-DPSK-to-RZ-DPSK format conversion with multiple-function using Raman adiabatic-soliton compressor," *Proc. Asia Communications and Photonics Conference (ACP 2014)*, AF3D.7, Shanghai, China, Nov. 2014.

[42] I. Ismail, Q. Nguyen-The, M. Matsuura, and N. Kishi, "6-fold wavelength multicasting using tunable-width picosecond pulse source from Raman adiabatic-soliton-compressor," *Proc. OptoElectronics and Communications Conference (OECC)*, vol. WE7F2, July 2014.

[43] S. V. Chernikov, D. J. Richardson, E. M. Dianov, and D. N. Payne, "Picosecond soliton pulse compression based on dispersion decreasing fiber," *Electron. Lett.*, vol. 28, no. 19, pp. 1842–1844, Sept. 1992.

[44] S. V. Chernikov, J. R. Taylor, and R. Kashyap, "Experimental demonstration of step-like dispersion profiling in optical fibre for soliton pulse generation and compression," *Electron. Lett.*, vol. 30, no. 8. pp. 433–435, Mar. 1994.

REFERENCES

[45] T. Inoue, H. Tobioka, K. Igarashi, and S. Namiki,"Optical pulse compression based on stationary rescaled pulse propagation in a comblike profiled fiber," *J. Lightwave Technol.*, vol. 24, no. 7, pp. 2510–2522 July 2006.

[46] G. P. Agrawal: *Nonlinear Fiber Optics* (Academic Press, New York, 1995) 2nd ed., Chap. 5, p. 145.

[47] G. Contestabile, R. Proietti, N. Calabretta, A. D'Errico, M. Presi, and E. Ciaramella: Proc. Optical Fiber Communications Conference/National Fiber Optic Engineers Conference (OFC/NFOEC), 2008, p. OMN2.

[48] Y. Yu, X. Zhang, J. Hu, and D. Huang: Proc. Conference on Lasers and Electro-Optics/Quantum Electronics and Laser Science Conference and Photonic Applications Systems Technologies (CLEO/QELS), 2008, p. JWA103.

[49] Y. Yu, X. Zhang, F. Wang, and D. Huang: Proc. Conference on Lasers and Electro-Optics/Quantum Electronics and Laser Science Conference and Photonic Applications Systems Technologies (CLEO/QELS), 2010, p. JThE61.

[50] C. Boerner, C. Schubert, C. Schmidt, E. Hilliger, V. Marembert, J. Berger, S. Ferber, E. Dietrich, R. Ludwig, B. Schmauss, and H. G. Weber: Electron. Lett. **39** (2003) 1071.

[51] A. Argyris, H. Simos, A. Ikiades, E. Roditi, and D. Syvridis,"Extinction ratio improvement by four-wave mixing in dispersion-shifted fibre," *Electron. Lett.*, vol. 39, no. 2, pp. 230–232, Jan. 2003.

[52] A. Bogris, and D. Syvridis,"Regenerative properties of a pump-modulated four-wave mixing scheme in dispersion-shifted fibers," *J. Lightwave Technol.*, vol. 21, no. 9, Sept. 2003.

[53] T. E. Stern, G. Ellinas, and K. Bala: *Multiwavelength optical networks: Architectures, design, and control* (Cambridge University Press, 2009), Chap. 4, p. 230.

[54] Z. Pan, C. Yu, and A. E. Willner,"Optical performance monitoring for the next generation optical communication networks," *Opt. Fiber Technol.*, vol. 16, no. 1, Jan. 2010.

[55] A. Nag, M. Tortatore, and B. Mukherjee,"Optical network design with mixed line rates and multiple modulation formats," *J. Lightwave Technol.*, vol. 28, no. 4, pp. 466–475, Feb. 2010.

[56] T. Tanemura, H. C. Lim, and K. Kikuchi,"Suppression of idler spectral broadening in highly efficient fiber four-wave mixing by binary-phase-shift-keying modulation of pump wave," *IEEE Photon. Technol. Lett.*, vol. 13, no. 12, pp. 1328–1330, Dec. 2001.

[57] J. Hansryd, P. A. Andrekson, M. Westlund, J. Lei, and P-O. Hedekvist,"Fiber optical parametric amplifiers and their applications," *J. Sel. Top Quantum Electron.*, vol. 18, no. 3, pp. 506–520, May/June 2002.

[58] T. Torounidis, M. Karlsson, and P. A. Andrekson,"Fiber optical parametric amplifier pulse source: Theory and experiments," *J. Lightwave Technol.*, vol. 23, no. 12, pp. 4067– 4073, Dec. 2005.

REFERENCES

Chapter 4

Mixed Modulation Formats All-Optical Signal Processings

This chapter is devoted a few demonstrations of an all-optical signal processings using mixed modulation format of OOK and DPSK either in WDM and OTDM schemes. In the first section, an all-optical demultiplexing of 40-Gb/s hybrid OTDM channels by using RASC-flexible control-window is demonstrated. In the second section, simultaneous four channels of mixed data formats waveform-wavelength conversion with tunable-width converted signals deploying the same devices as in Chapter 3. Four input NRZ mixed format probe channels at different wavelengths are interacted with compressed RZ clock pump to yield four converted RZ mixed data channels, where only one case of signal modulation format allocation is chosen. A full comparison for waveform-wavelength conversion in different format allocation is out of the research scope. Then, in the last section describes the experimental concept and results of the transmission performance between the midspan of TDCM and OPC with specialty using multichannel-mixed OOK and DPSK format.

4.1   Introduction

The increment of demand for higher capacity in optical networks, mixed modulation formats for signal transmission in WDM systems become essential. In future optical network applications, the modulation format may be upgraded from commonly used OOK to upgraded format DPSK or mixed together in backbone long-haul transmission

4. MIXED MODULATION FORMATS ALL-OPTICAL SIGNAL PROCESSINGS

lines. Thus, the influence of both formats in different applications must be considered and studied. The shift towards updated formats is necessary because one of the major problems that needs to be improved is the reduction of transmission impairments. Furthermore, in the future, mixed formats may co-exist in backbone long-haul transmission lines. Simultaneous multiple channel with mixed formats is beneficial because the reduction numbers of converter can be reduced. Due to this, studies relating to mixed modulation formats have been relatively few and so far there has not been any research focusing on all-optical signal processing of mixed modulation formats using the same optical signal converter. Thus, the consideration of this transition to facilitate the maintenance in optical networks is very important.

Different type of modulation formats and bit-rate have become an essential requirement to achieve future high speed operation in OTDM and optical networks [1]. In the future optical network, the combination between different format and bit-rate may co-exist in the same transmission lines or even in the same carrier wavelength [2-4]. In the past, various demultiplexing techniques have been proposed and demonstrated [5-10]. However, the demultiplexing schemes so far are limited in terms of bit-rate and modulation format flexibility. FWM in HNLF holds a great interest in demultiplexing due to its fast nonlinear response and can operate to various modulation format and bit-rate [12]. Furthermore, an important issue for OTDM is the ability of the converter for selecting one or multiple tributary channel regardless of different line rates and format for further signal processing [13]. Reference in [9] has been successfully demonstrated a hybrid OTDM demultiplexing using EAM. However, the demultiplexer has a wider switching window which may degrade the quality performance of the target channel as part of an adjacent data may still include in the switching window. The intention of the present study under section 4.2 is to provide the converter with abilities to demultiplexing an ultra-short pulses with various signal durations and format.

Over the past few years, all-optical waveform-wavelength conversion has become an essential building block to provide flexible network management and interface between the WDM and the OTDM networks [14-18]. An important requirement during the waveform-wavelength conversion is the ability of the format converter in processing a signal regardless of different line rates and format [19]. For decades, the OOK modulation format, either non-NRZ or RZ has been used as the format of choice in various conversion schemes [20–23]. In comparison with other formats, OOK has the

94

advantage of relatively easy feasibility and small transceiver bandwidth [24]. On the other hand, advanced modulation format such as DPSK has attracted a remarkable interest in response to high demand for power efficiency increment in data transmission and bandwidth. In addition, DPSK format has the advantageous qualities such as less susceptibility to impairments and relatively tolerant to narrow-band optical filtering [25-29]. In the past, various schemes for NRZ-to-RZ format conversion for single and multiple-channels have been proposed and demonstrated. Although these investigations reported many interesting results, to the best of our knowledge, no research has focused on multiple channels format conversion with simultaneous mixed modulation formats in a single optical device. In the future optical network, the combination between the traditional OOK modulation format with an alternative DPSK format may co-exist in the same transmission lines or even in the same carrier wavelength [30]. This is supported by Ref. [3] study which reveals that by employing transmission system with different modulation formats can relaxes the feasibility constraints on high-bit-rate light-paths which can lead to a lower cost network design compared to a single modulation format system. Therefore, multichannel mixed modulation format conversion within the same module has a promising merit in increasing network flexibility and enable simultaneous optical processing in a cost effective for future optical network.

WD is a technology used to combine or to retrieve many optical signals of different optical carrier wavelengths in a fiber. In the past, the NRZ-OOK modulation format has traditionally been used as the format choice in optical transmission systems. However, in the next generation of WDM optical network, the transmission of mixed modulation formats over a single optical fiber is increasingly being studied to compensate chromatic dispersion in high bit-rate transmission systems [2, 3, 24]. Up to date, two common approaches that mostly utilized impairment of chromatic dispersion and nonlinear effects in high bit-rate transmission systems involve dispersion management and optical phase conjugation [31–34]. Dispersion management by using DCF is the traditional technique used in optical communication systems [35]. However, DCF does not offer any possibility for dispersion tuning range and limitation use in high speed due to high PMD [36, 37]. For most applications, a dispersion tuning range that covers negative and positive values is required. TDCM is an alternative approach to DCF with the advantages that can replace various lengths of DCF and compensate residual dispersion in high-speed optical transmission systems above 10 Gb/s. This is not only

cost saving but also can eliminate the midspan amplifier usage in some networks, an attractive strategy to pursue. However, to the best of our knowledge, no experimental demonstration of in-line TDCM using multichannel mixed modulation formats has been reported.

OPC is an attractive method to compensate both chromatic dispersion and nonlinearity of long haul transmission [38–40]. This technique used the generated of optical phase conjugated signals in FWM in the midspan of a transmission links. A number of transmission experiments based on OPC have been already demonstrated by using various schemes such as optical fibers [41], periodically poled lithium noibate (PPLN) [42], chalcogenide glass waveguides [43], silicon waveguides [44], SOA [45] and quantum-dot SOA [30]. So far, OPC operations for signals with OOK, and DPSK formats have been presented. However, OPC operation for WDM mixed formats of OOK and DPSK have not been addressed. In the section 4.4, we present the first report of comparison using the multichannel-mixed format over transmission performance between an optimized in-line TDCM transmission scheme and OPC in a highly nonlinear fiber (HNLF). In both cases, bit-error-rate (BER) results as well as detected signals eye patterns were compared one to another.

4.2 Demultiplexing of Mixed OTDM Modulation Formats

In this section, all-optical demultiplexing of 40-Gb/s hybrid OTDM channels by using RASC flexible control-window is demonstrated. Error-free operations with less than 1.3-dB power penalties were obtained and this scheme is expected to be scalable toward higher bit-rates.

This section is organized as follows: First, the background and state of the art techniques which is introduced in subsection 4.2.1. The concept of the research is discussed in subsection 4.2.2. Finally, subsections 4.2.3 and 4.2.4 present the experimental setup, results and discussion for mixed format all-optical demultiplexing.

4.2.1 State of the Art Techniques

Optical short pulse generation with high repetition rate has attracted a lot of interest for various applications in today's dynamic networks [46–49]. A demonstration of such signal with different applications in OTDM and RZ signal regeneration at high bit rate

have been reported in [5, 8]. This scheme is a gainful technique that can produce a pulsed idler with identical repetition rate as the pump and potentiality can demultiplex the OTDM signals while offering power amplification in the FWM process. It is also found that the generated gating window pulse requires a spectral broadening of the higher pump power in order to increase the threshold for SBS and the temporal gating window duration is always fixed. The adiabatic soliton compression techniques have attracted much attention to generate high-quality short-duration pulse trains in the order picoseconds [50]. This useful approach can be extended by using a high quality tunable ultra-short duration of the RZ clock pulse introduced in our experiment, which has benefited over CW due to flexible spectral width. It can also provide energy in the fiber parametric gate without the use of extra EDFA compared to other schemes. Previously, we have demonstrated the compression for multiwavelength pulse trains at bit rate 10 Gb/s by using a multiwavelength pulse compression and its application to OTDM-to-WDM operation by using only OOK format [51]. However, signal processing for OTDM hybrid format is difficult to be implemented, and there has been no report using the adiabatic soliton compression in distributed Raman amplification for mixed signals demultiplexing. It would be more attractive to offer some more advantages, such as simultaneous dual-format demultiplexing with high quality picosecond input-output pulse width signal.

In this section, for the first time, we demonstrate a proof concept for demultiplexing of arbitrary lower rate 10 Gb/s tributary channels from a 40 Gb/s mixed amplitude and phase format data signals with the advantageous use of RASC as a higher power output of the fiber-based FWM gate. It would also be useful to be able to demultiplex a single OTDM channel with different formats to reduce complexity and cost at the system level. Thus, the scalability for flexible higher bit-rate demultiplexing and different granulaties for tributary channels by using our proposed system is evident and further discussed.

4.2.2   Concept

Insets a to b in Fig. 4.1 described the formation of the single ultra-short pulse compression of the RZ clock pulse train. Formation of the hybrid OTDM OOK-DPSK is shown in inset c to d. The RZ pulse train with repetition 10 Gb/s and with pulse duration τ are separately encoded in creation different tributaries pulses of RZ-OOK and
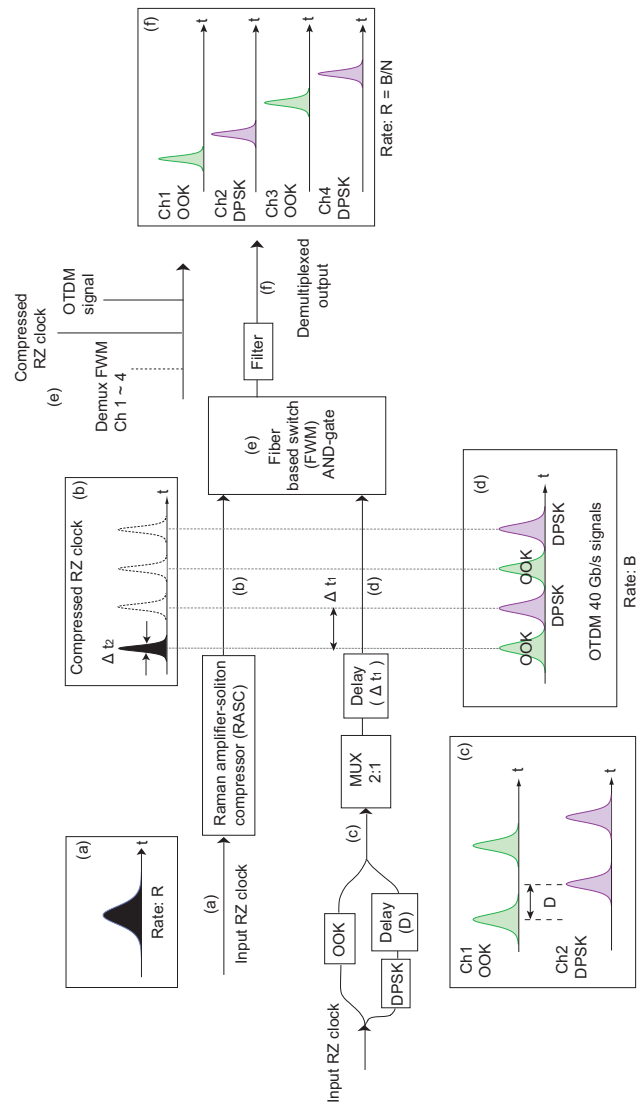
Figure 4.1: Operational principle for optical demultiplexing for OTDM 40 Gb/s hybrid mixed modulation format.

RZ-DPSK. The pulses are temporally offset from one another by delays D. 2 x 10 Gb/s tributary channels in inset c, which one is separately modulated in RZ-OOK format and the other one in RZ-DPSK format are optically multiplexed in the 2:1 multiplexer to form a 40 Gb/s OTDM hybrid modulation format signal.

In the demultiplexing process, an input RZ clock pulse train acts as the pump signal, while hybrid OTDM mixed data stream signal acts as the gated probe signal. Both OTDM signal and RZ clock pulse are synchronously time interact and launched into a HNLF to generate a FWM demultiplexed channel. The demultiplexing is based on parametric degenerate FWM in HNLF, that converts RZ clock pulse power into a new demultiplex signals with a wavelength of λ_{demux} ($\lambda_{demux} = 2\lambda_{pump}$ - λ_{probe}). By controlling the time shifting between OTDM stream and RZ clock pulse train, FWM demultiplexed channel is chosen either RZ-OOK or RZ-DPSK carried by the data signal will appear. FWM channel is chosen and pass through a broader optical band pass filter for signal demodulation and analyses. Here, we present a proof concept of the demultiplexing demonstration at 40 Gb/s simultaneous data modulation of the amplitude and phase of the optical carrier with the advantages use of RASC as a higher power output in the fiber parametric gate and flexibility to tune to picosecond pulse width by controlling Raman-pump power.

4.2.3 Experimental Setup

The experimental setup is depicted in Fig. 4.2. A 10 Gb/s RZ clock at the wavelength of 1552.5 nm was generated with an ECL and an EDFA. An EDFA and OBPF were used to compensate the EAM insertion loss. A TDCM was employed to suppress the frequency chirping induced by the EAM. The detailed operation of RASC can be referred from Ref. [4], respectively. Tuning the Raman-pump power (P_r) could provide the pulse width tuning function for the RZ clock signal. Therefore, the application to bit-rate flexible dual-format OTDM demultiplexing can be realized. The generated pulse at wavelength 1558 nm from optical comb generator (OCG) was filtered by two OBPFs to obtain the pulse width around 4.0 ps. The pulse train was modulated simultaneously in a LNMs by a 10 Gb/s data from a PPG. A PC and a VOA were used to adjust both signals having the same peak power and polarization. The 20 Gb/s data signal was multiplexed to generate a 40 Gb/s OTDM data signal using the bit-rate multiplexer. Both signals were then sent to a 500 m HNLF with a zero dispersion wavelength of

Figure 4.2: Experimental setup for optical demultiplexing for OTDM 40 Gb/s hybrid mixed modulation format.

1552 nm for parametric interaction in which OTDM signals were set as probe signal. The HNLF had a dispersion slope of 0.032 ps/nm ^{2}/km and nonlinear coefficient of 12.6 W^{-1}km^{-1}. FWM channel at a new wavelength of 1547 nm was passed through a broader OBPF after amplification by an EDFA for signal demodulation and analyses.

4.2.4   Experimental Results and Discussions
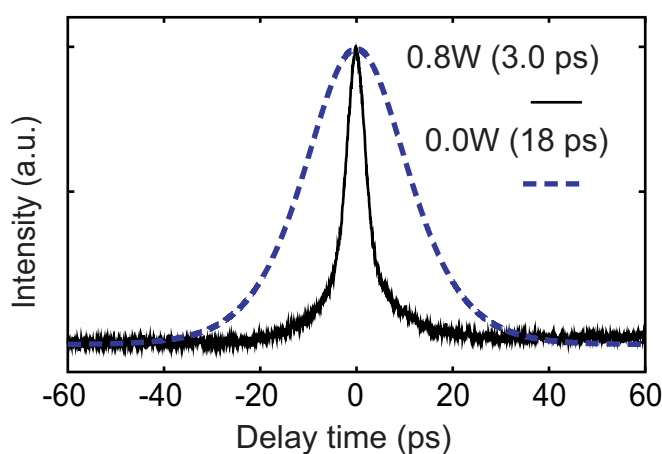
Figure 4.3: Autocorrelation traces sampling gate of compressed RZ clock at the Raman pump power of 0.0 and 0.80 W.

OTDM data streams may consist of different format that depends on the network size. It is very important that flexibility in extracting optical demultiplexing pulses regardless the input modulation format of OTDM signals, time slot and bit-rate. An FWM signal can be generated when the pump and input OTDM data signals are injected simultaneously in HNLF. Here, the RZ clock pump and OTDM signal act as a gating and gated pulses, respectively. The characteristics of the control pump signal play an essential role of the smooth, short pulse width with pedestal-free channels after FWM process. An input RZ clock pump introduced in our scheme has several advantages compared with a CW pump. Eventhough CW pump is fully bit-rate and need no synchronization, the limitation are higher average pump power and need phase modulation to decrease SBS effect. In this experiment, the Raman pump power (P_r) from RASC was set at 0.80 W since the converted pulse width after FWM will be more compressed.

4. MIXED MODULATION FORMATS ALL-OPTICAL SIGNAL PROCESSINGS
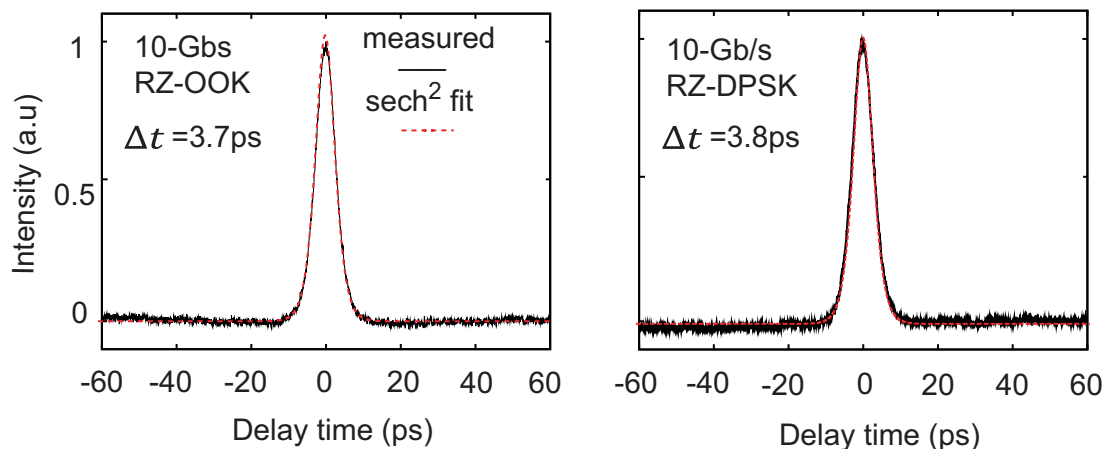
Figure 4.4: Autocorrelation traces of the RZ clock from 10 Gb/s RZ-OOK and RZ-DPSK base data.

Figure 4.3 provides the autocorrelation trace function of the compressed RZ pulse. The initial input of RZ clock pulse with 18 ps long was considerably compressed down to 3.0 ps as the Raman pump power was controlled up to 0.80 W. The RZ compressed clock was narrower than the input OTDM signals. If the width of the RZ clock pump is smaller than 3.0 ps, it becomes difficult to extract the FWM signal using the OBPF due to the spectral overlap at small pump width. The output compressed pulse were well fitted to $sech^2$ functions and the time-bandwidth product of 0.37 estimated at 0.80 W showed that transform-limited pulses were attained. It should be noted that the use of soliton pulse with an ideal $sech^2$ profile will be expected to obtain better demultiplexing performance. With the RZ control gating window around 3.0 ps, it is possible to demultiplex 40 Gb/s hybrid OTDM signal to 10 Gb/s tributaries channels. The key limitations in higher bit-rate of OTDM signals are caused by pulse spreading due to dispersion and crosstalk in the demultiplexer. Therefore, to optimize the pulse spreading it is desirable that the input pulse signals is located close to ZDW of HNLF. Furthermore, to avoid possible crosstalk between adjacent channels, it is necessary to ensure that the pulses width was smaller compared to the one bit period of the multiplexed stream. Thus, as shown in Fig. 4.4, the measured pulse widths of 10 Gb/s RZ-OOK and RZ-DPSK were around 3.7 and 3.8 ps, respectively. Both pulses were well fitted with $sech^2$ function, showing the good quality data after OCG filtering. Figs. 4.4 (a) and (b) show eye patterns of the OOK-DPSK tributaries. Fig. 4.5 (c) indicates the

(a)

(b)

OOK   DPSK   (50-ps/div.)
tributary tributary

(c)
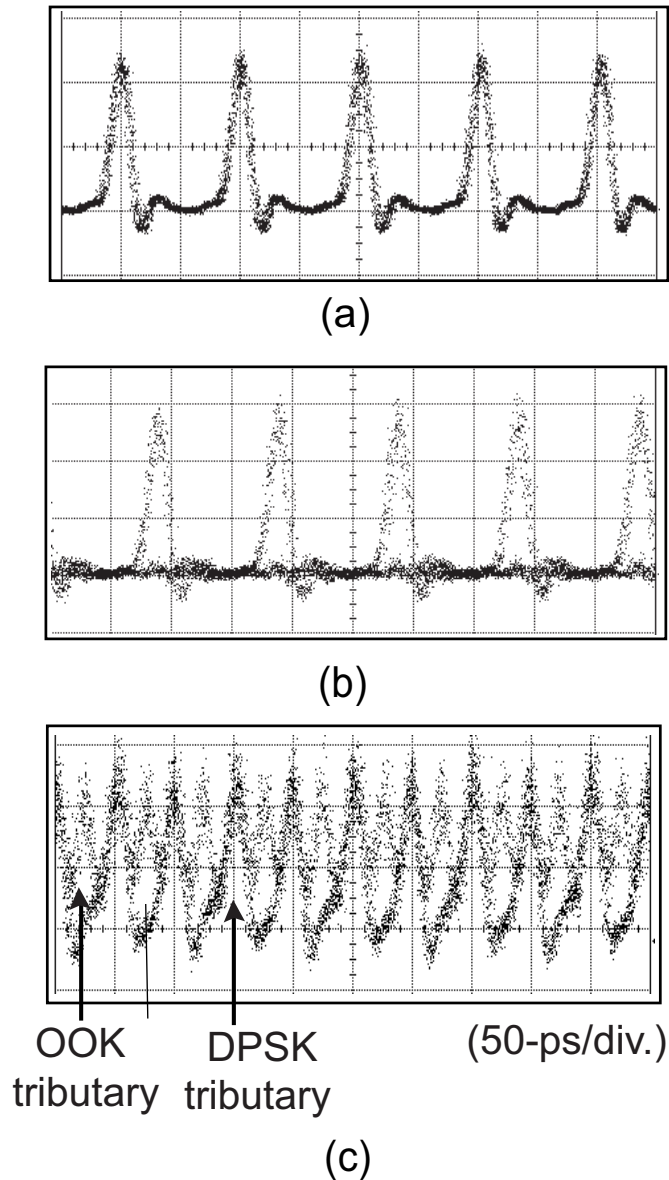
Figure 4.5: Eye patterns of the 10 Gb/s base data of (a) RZ-DPSK (b) RZ-OOK (c) 40 Gb/s hybrid data signal captured by 30 GHz sampling oscilloscope, (50 ps/div).

eye patterns of 40 Gb/s OTDM hybrid data stream consisted of every even channel of RZ-DPSK signals and every odd channel of RZ-OOK signals. All neighboring channels were temporally offset from one another by the delays 25 ps.

Fig. 4.6 (a) and (b) show the spectra at the output of the HNLF with the OTDM signal located at 1558 nm and RZ clock pump at 1552.5 nm. The synchronization
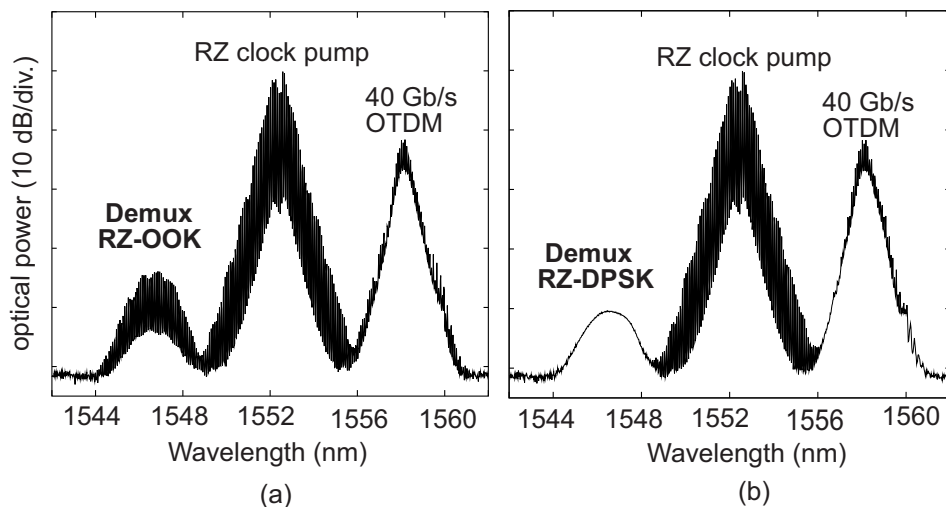
Figure 4.6: FWM spectra after demultiplexing for (a) RZ-OOK channel and (b) RZ-
DPSK channel.

between RZ clock pump pulse and OTDM signal was accomplished by manual mapping
the time interaction every 25 ps using an ODL. Thus, this provides the time selective
function for the demultiplexing, either RZ-OOK or RZ-DPSK tributary channels. The
RZ pulse clock was fed into the HNLF experiences pulse compression or broadening,
depending on whether its amplitude was larger or smaller than that of the fundamental
soliton. If Raman-pump power was high, the pulse width was adiabatically compressed
and at the same time, the spectral width of the pulse was broadened, accordingly.
Furthermore, the spectra of the data signal after demultiplexing were also broaden
due to the reshaping effect in the parametric process. Another important scheme for
high-speed OTDM systems is the clock recovery function. Eventough the clock recovery
scheme is not performed in this work, at higher bit-rate 160 Gb/s, the potential scheme
as in refs. [52, 53] can be considered.

The demultiplexing performance was further investigated by measuring the BER
of the output signals at the Raman pump power of 0.80 W. The demodulated eye
patterns of 4 × 10 Gb/s demultiplexed hybrid tributary channels are shown in Fig.
4.8 (a). It can be seen that the eye patterns are well preserved with less deterioration.
In Fig. 4.8 (a) shows that all demultiplexed channels can be achieved with power
penalties smaller than 1.3 dB. The superior performance of RZ-DPSK tributary channel
was observed in comparison with demultiplexed RZ-OOK channel due to its constant
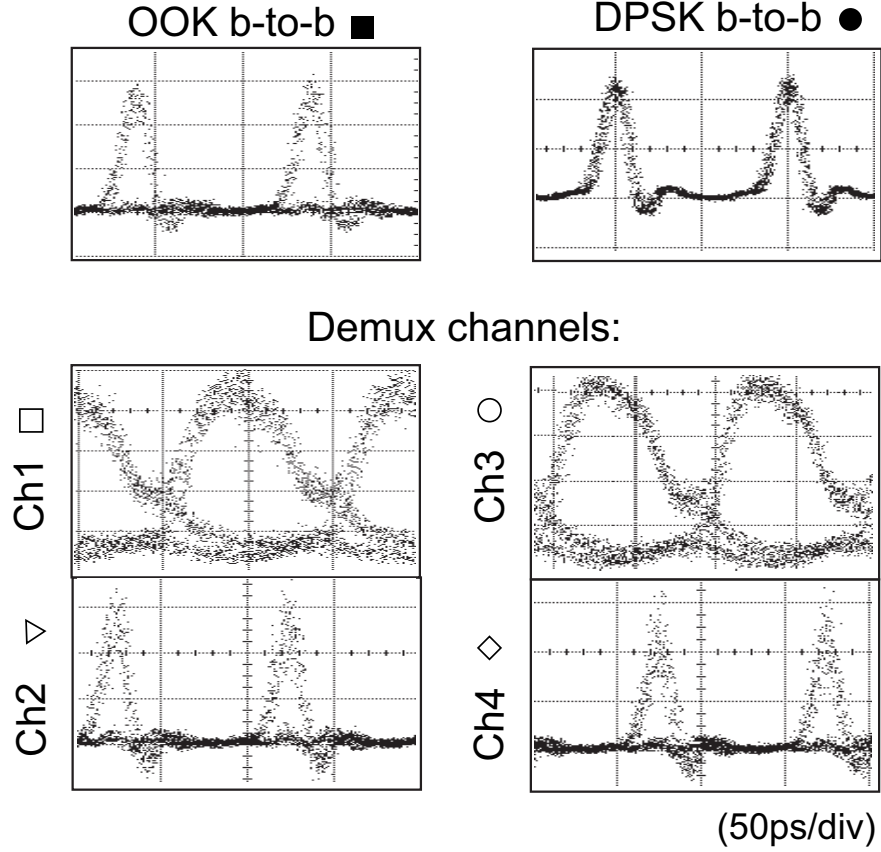
Figure 4.7: All demultiplexing channel during Raman pump power 0.80 W for demodulated eye patterns (50 ps/div.)

intensity profile characteristic [5, 54]. FWM process in HNLF can provide all-optical reshaping together with demultiplexing conversion when proper adjustment of the RZ pump and OTDM signal relative to the zero dispersion wavelength of the HNLF. The achievement of the extinction ratio enhancement of the converted FWM channel relative to the input signal. The results in Fig. 4.8 (b) as the measured demultiplexed pulse widths for Ch1, Ch2, Ch3 and Ch4 were 2.60, 2.62, 2.65 and 2.68 ps, respectively. This compression and pedestal removal of the pulse was predicted since the intensity of the demultiplexed signal was proportional to the intensity of the compressed RZ clock [55]. The calculated time-bandwidth-product was 0.37 at the worst channel. Potential flexible higher bit-rate can be achieved by optimization for shorter pulse operations of the RASC compression process, and increment time slot of dual-format channels.
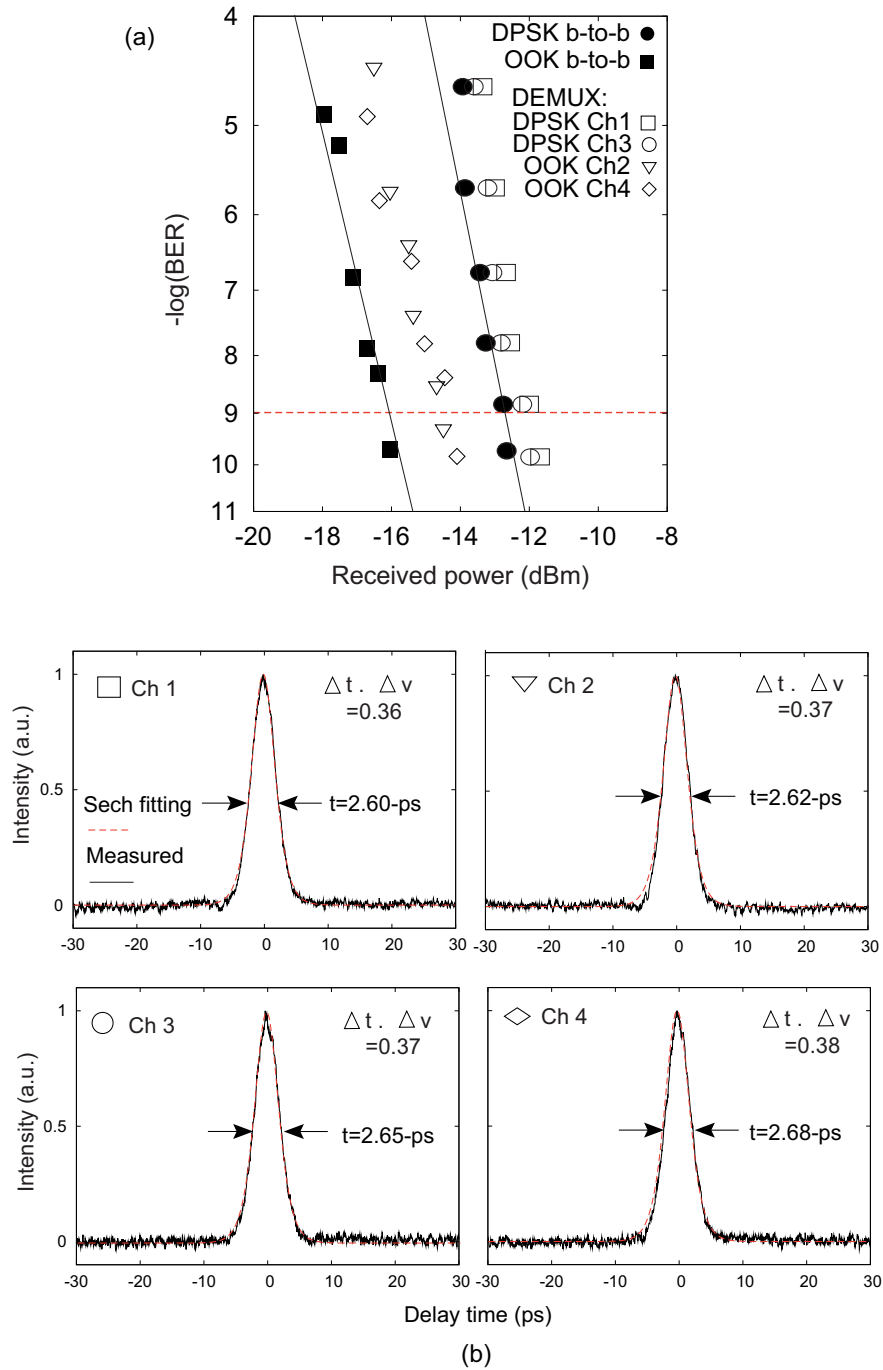
Figure 4.8: (a) BER measurements and (b) autocorrelation traces for all demultiplexing channel at Raman pump power of 0.80 W.

4.3 Multichannel Mixed Modulation Format Waveform-Wavelength Conversion

In this section, we demonstrate a simultaneous NRZ-to-RZ format conversion for 4 x 10-Gb/s multichannel mixed data formats of OOK and DPSK, deploying a single fiber-based FWM and a RASC. The fiber-based switch in HNLF performs as an AND logic function based on parametric process between mixed data signals and the compressed RZ clock from RASC. By flexibly tuning the Raman pump power from RASC, good quality converted RZ mixed data signals with different pulse width can be achieved. Bit-error-rate measurements show negative power penalties with pedestal-free pulses.

This section is organized as follows: Firstly, the state of the art techniques and purpose of this work is introduced in subsection 4.3.1. The concept of the work is discussed in subsection 4.3.2. Then, section 4.3.3 and 4.3.4 present the experimental setup, results and discussion for mixed formats OOK-DPSK NRZ-to-RZ conversions. Finally, subsection 4.3.5 summarizes the main results from this chapter.

4.3.1 State of the Art Techniques

To date, several methods have been proposed to realize an all-optical format conversion based on various devices and nonlinear properties. Among these, FWM in HNLF holds a great interest and most promising approach to all-optical format conversion due to the fast nonlinear response, capable to operate in various modulation formats and bit-rate. In addition, the characteristics of the converted signal after format conversion play an important role in optimizing system performance. Besides, the advantages of the converted signal are capable to be adopted in long-haul transmission systems and the formation of higher bit-rate OTDM [13, 31]. The creation of high-bit-rate OTDM systems require both a narrow width and pedestal-free signal. In order to become preferable, the best outcome is to provide a practical function such as tunable pulse width to flexibly control the conversion performances with various signal parameters over the changes in the existing system. The advantage to flexibly shorten and manipulate width-tunable converted signals to change the transmission distance is useful and can support wider bandwidth requirements. An adiabatic soliton pulse compression is a gainful technique that potentially produces a highly compressed pulse with minimal pedestal while offering power amplification. The technique consists of anomalous

dispersion fiber with constant dispersion and apply a distributed optical gain through
the fiber to increase the soliton power and at the same time reduce the pulse duration.
However, multichannel NRZ-to-RZ mixed format conversion with tunable duration has
not been examined so far.

For the first time, we extended our research based on previous work in section 3
with capability for an all-optical multichannel NRZ-to-RZ mixed format conversion
with picosecond width pulses. Our method is based on combination between fiber
based FWM AND-gate and compressed RZ pulse pump from RASC. By changing a
Raman pump power in RASC, a picosecond width-tunable converted data with a good
conversion performance throughout the operating range can be achieved. Furthermore,
FWM operation is effective not only preservation of the information of the optical signal,
but also the pedestal component suppression after waveform conversion. Besides, the
mixed modulation format conversion can be realized without significant BER penalty.
Overall, our approach shows the importance of the pulse width flexibility in a picosecond
range for the converted multichannel dual format RZ data, which is beneficial in linking
and interfacing OTDM system and WDM networks.

4.3.2   Concept and Setup

A conceptual diagram of our proposed scheme is shown in Fig. 4.9 (a). The first stage is
the used of RASC. The operation is based on adiabatic pulse compression in distributed
Raman amplification. It generated picosecond width-tunable RZ clock and worked as
a pump in the fiber-based switch to perform the data format conversion. The RZ clock
pulse duration can be reduced as its fundamental soliton peak power (N=1) increases
with the increment of the Raman-pump power (P_r). In the second stage, fiber-based
switch in a HNLF performed as an AND logic function between mixed input of two
format channels NRZ-OOK and NRZ-DPSK and the RZ clock signal. FWM operation
in HNLF is effective for not only preservation of the information of the optical signal
but also the pedestal component suppression in the output pulse.

The experimental setup is illustrated in Fig. 4.9 (b). A 10-Gb/s input RZ clock
at a 1553-nm wavelength was generated with an ECL and an EAM. An EDFA and an
OBPF were used to amplify the signal loss from EAM and also to set the conditions for
fundamental soliton power in the RASC. A TDCM was used to suppress the frequency
chirping induced by the EAM. Based on adiabatic soliton compression operation, the
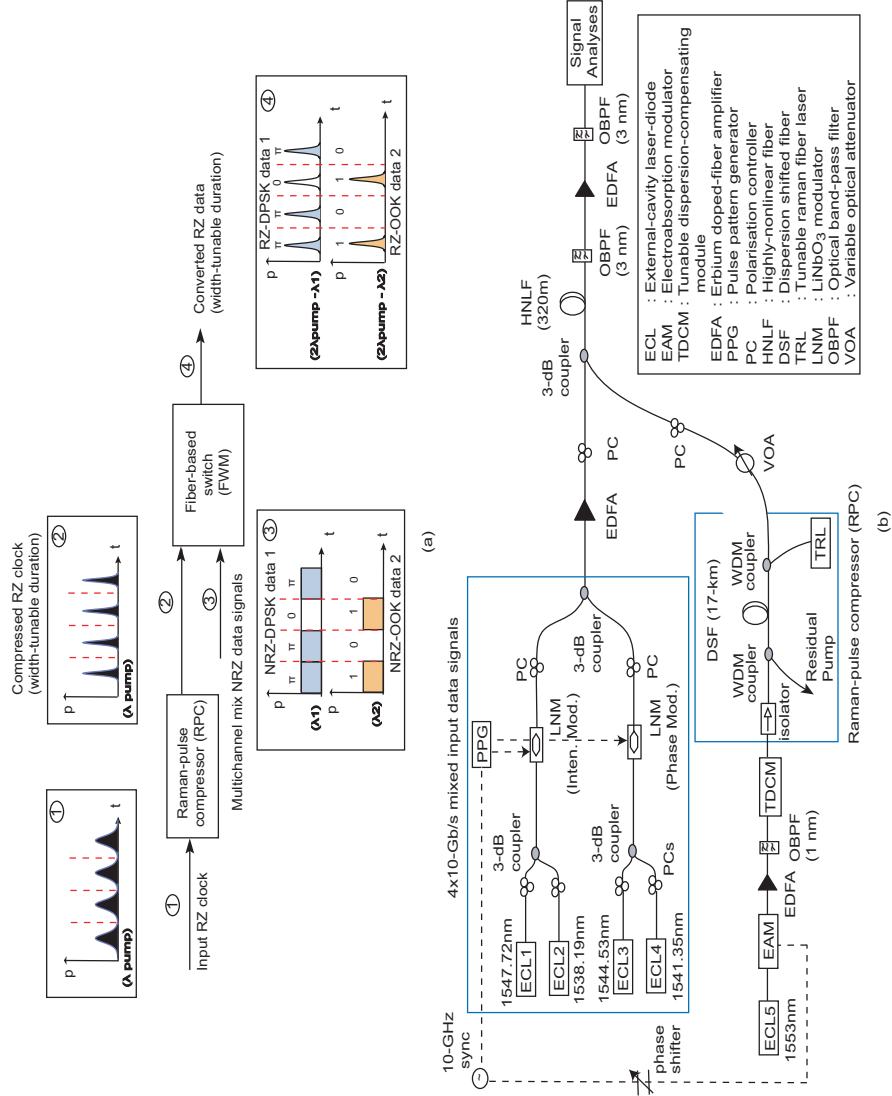
Figure 4.9: (a) Operational principle and (b) experimental setup for multichannel NRZ-to-RZ mixed OOK and DPSK waveform-wavelength conversion with picosecond output.

RASC component characteristics is the same as in previous chapter 3. A VOA was employed to control power after the signal had passed through the RASC and before the signal was sent to the HNLF. The compressed RZ clock pulse was set as a pump signal. The phase shifter was used to control the time delay of the compressed RZ clock with respect to its overlap with the input multichannel mixed format data signals.

Conversely, the input data signals of NRZ mixed channels at the wavelength from 1547.72 nm to 1538.19 nm were generated by modulating a CWs light in LNMs with

10 Gb/s PRBS of length 2^{31}-1 from PPG. Both mixed format data input signals were synchronized with the compressed RZ clock using direct synchronization instead of clock recovery. The data signals were amplified using an EDFA with an OBPF before it passed through a 3-dB coupler. PCs were used to maximize the interaction between the two input signals. Both the RZ clock and the multichannel mixed format data signals were passed through a HNLF to generate the FWM products. The detail characteristic of the HNLF is the same as in the chapter 3. Two OBPFs were used after the HNLF to isolate the FWM product and to remove ASE produced by the EDFA. The bandwidth of the OBPFs was 3 nm. The quality of the converted pulse was measured using an autocorrelator and BERT with a preamplified receiver.

4.3.3   Experimental Results and Discussions
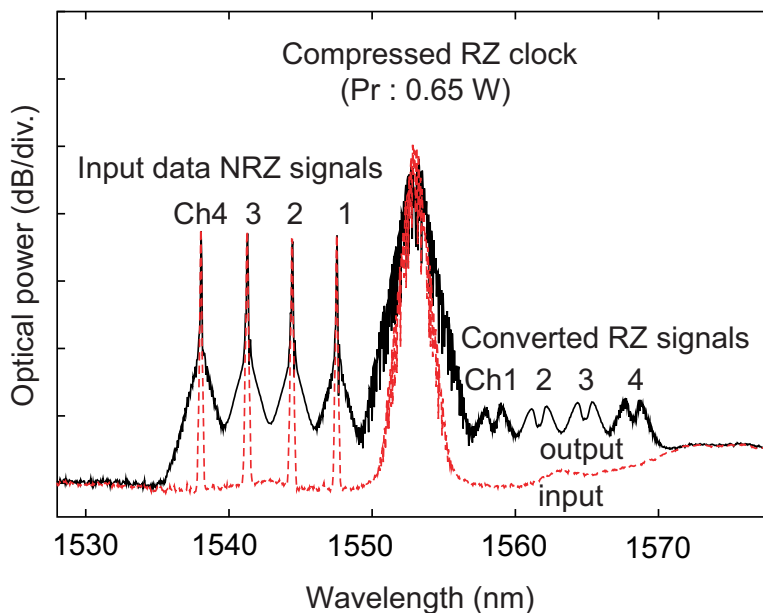
Figure 4.10: Optical spectra input and output of the HNLF for the proposed format conversion.

Figure 4.10 shows the FWM spectra at the input (dashed line) and output (solid line) of the HNLF of 4×10 Gb/s mixed format conversion using compressed RZ clock at a P_r setting of 0.65 W. Four input NRZ mixed format probe channels at the wavelength range from 1547.72 and 1538.19 nm interacted with compressed RZ clock at 1553 nm to yield four converted RZ mixed data channels. Each channel of NRZ-DPSK signals (Ch 2

and 3) were located at the middle of NRZ-OOK signals (Ch 1 and 4). A full comparison for format conversion in different format allocation is out of the research scope. The format allocation in our experiment was chosen based on the basis for the lowest possible average BER values. The main aim of the present study is to investigate the ability of the proposed scheme to format converted the mixed data signals with picosecond range. After FWM interaction, the NRZ signals in both formats were successfully converted to an RZ data signal with preservation in both phase and amplitude information. Four converted mixed format RZ data signals with 400 GHz spacing were individually located at the wavelength of 1558.28, 1561.47, 1564.65 and 1567.81 for channel 1 (Ch 1), Ch 2, Ch 3, and Ch 4, respectively. In addition, the converted spectral outputs of were also broadened at the same time with the increment of P_r value over the adiabatic soliton compression. Fig. 4.10, also shows that the spectral of each converted channels have a small dip at the area of the pulse peaks. This probably originating from the negative frequency chirps caused by nonlinearity effect during FWM process [56].

Figure 4.11 provide the autocorrelation traces of the compressed RZ clock, and converted RZ mixed data signal at odd channels (Ch 1 and Ch 3) as a function of three P_r values. As shown in Fig. 4.12 (a), the initial input of the RZ clock pulse with 18 ps long was considerably compressed to 12.73, 10.54 ps, and 4.00 ps when the P_r value were set at 0.35, 0.45, and 0.65 W, respectively. The pulse duration was narrowed at the same time with the increment of the Raman-pump power during over the adiabatic soliton compression. In addition, the compressed RZ pulse was well fitted to $sech^2$ function. The time bandwidth product of the RZ clock pulses at all P_r settings was measured to be less than 0.41. At the P_r value of 0.65 W, a small pedestals were observed which resulted from small deviation from the precise adiabatic conditions in the experiment, such as gain variation and initial pulse soliton condition. On the other hand, as shown in the fig. 4.11 (b) and (c), the autocorrelation traces of the converted RZ mixed data signals at Ch 1 and Ch 3 were narrowed after FWM process. A significant improvement of the pulse pedestal at Ch3 is achieved together with a pulse duration as short as 2.73 ps with $sech^2$-shaped at the P_r value of 0.65 W, for total pulse compression of 7-fold. This findings resulted from the optimum compression after FWM process, that converted almost pedestal-free signal because the FWM signal power varied quadratically with respect to the output of the compressed RZ clock power as mentioned in Eq. (2.27) under Chapter 2 [55]. From the Eq. (2.27), the unit of dBm for the slope between
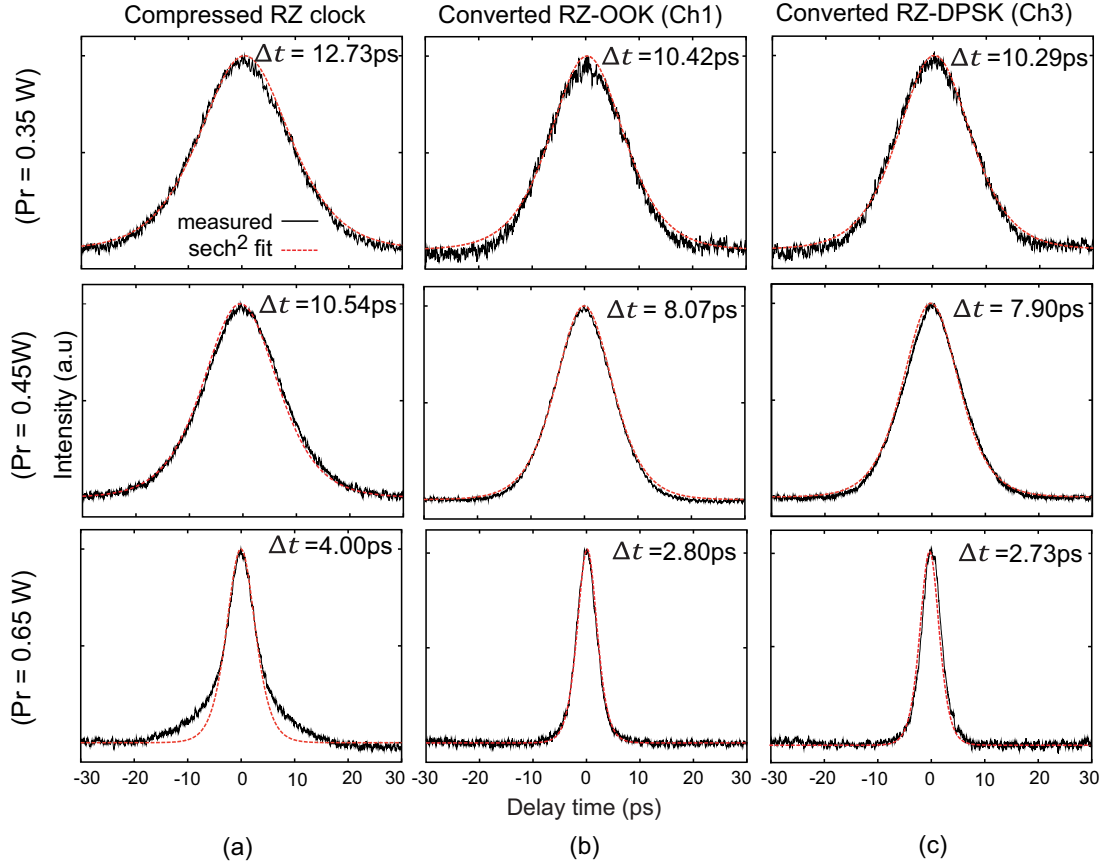
Figure 4.11: The autocorrelation traces of the compressed RZ clock, converted RZ mixed data signal at odd channels (Ch 1 and Ch 3) as a function of three different P_r values.

pump and converted FWM signal was 2. Thus, the converted signal extinction ratio will be two times larger than the suppressing noise at level "0". With the increment of RZ clock pump power, the level 1 of the amplitude noise will be reduced. Furthermore, the converted signals should be transform limited and have $sech^2$ form and a pedestal should be small. Otherwise, the nonlinear interaction between signals will occur during the transmission through the fiber and the information will be lost. In order to attain smaller width, the value of P_r need to be increased, however, the pulse waveform is significantly distorted if P_r exceed 0.65 W. In order to increase to higher bit-rate, the use of shorter pulse width that occupy a wider spectral per channel is compulsory. The converted pulse duration around 2.73 ps was sufficiently small to serve as the 160 Gb/s OTDM data signals' source.

The results of the BER measurement are shown in Fig. 4.12, while Fig. 4.13 (a) is
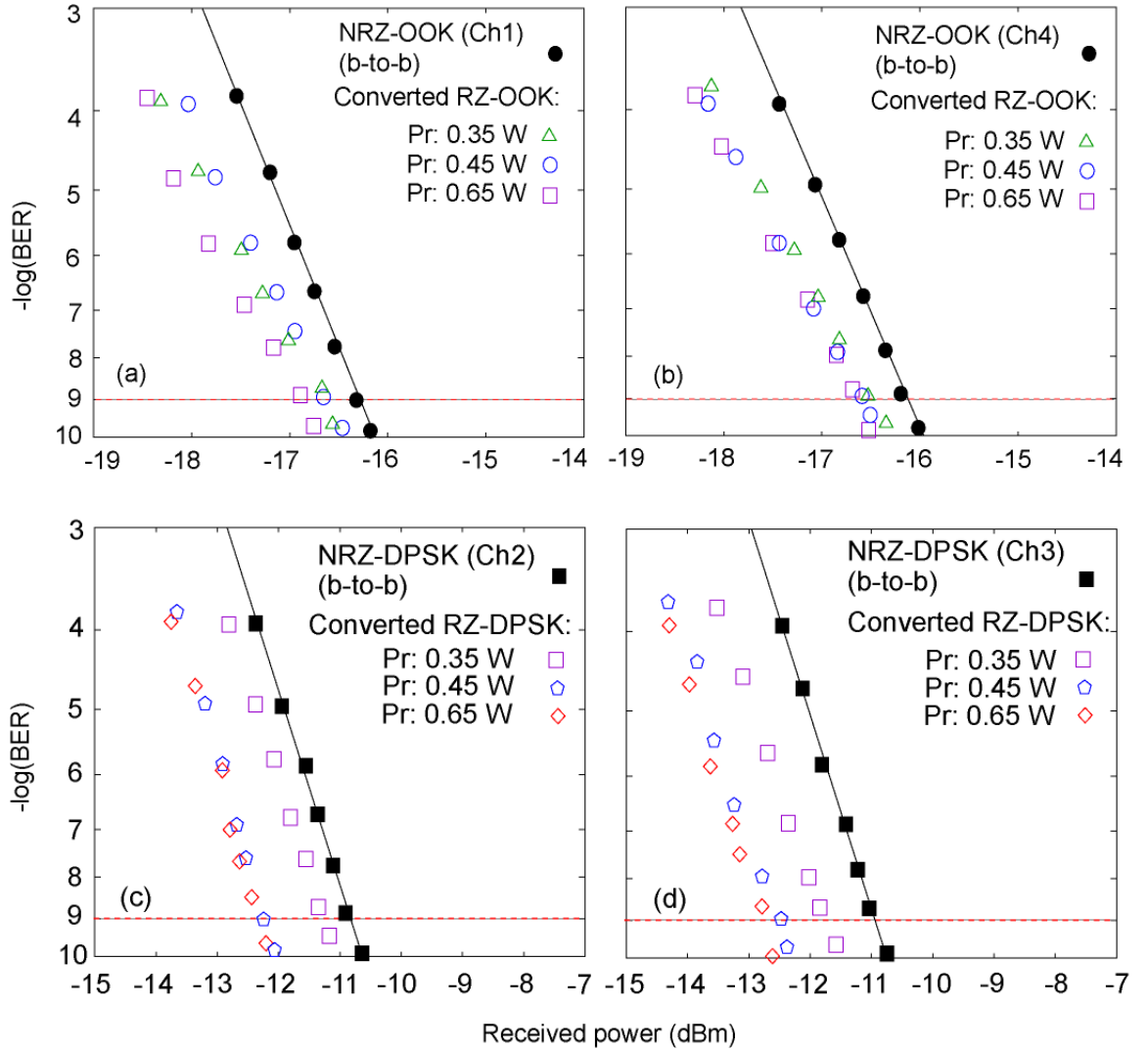
Figure 4.12: BER measurements of converted RZ-OOK and RZ-DPSK signals from Ch1 to Ch4 at P_r values of 0.35, 0.45, and 0.65 W, respectively.

the summarized data where the power penalties of the converted channels at a BER of 10^{-9} are shown. The power penalties were varied based on different format and channel to channel. The pulse durations of the converted RZ output signals depends mainly on the input compressed RZ clock pulse width. As mentioned above, analysis also showed that power penalty was reduced with the decreased of the RZ clock input pulse duration, which should attributed to the increased tuning of the P_r value and higher extinction ratio improvement. In addition, the RZ-DPSK converted signal clearly outperforms
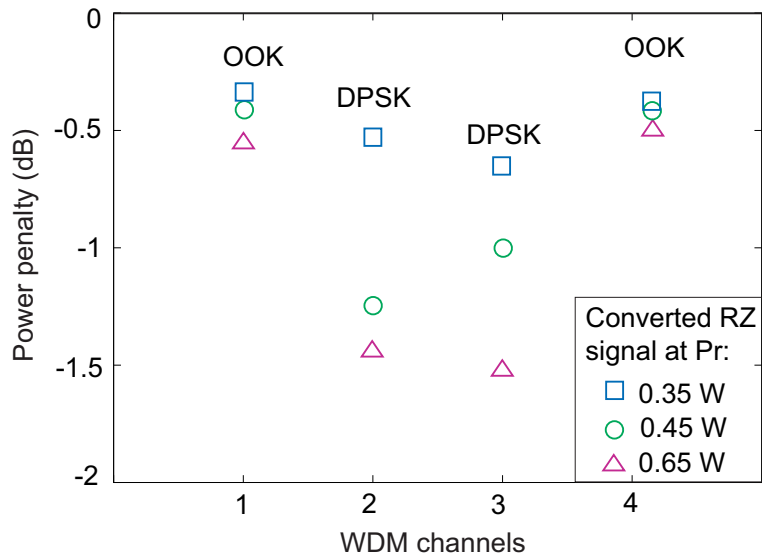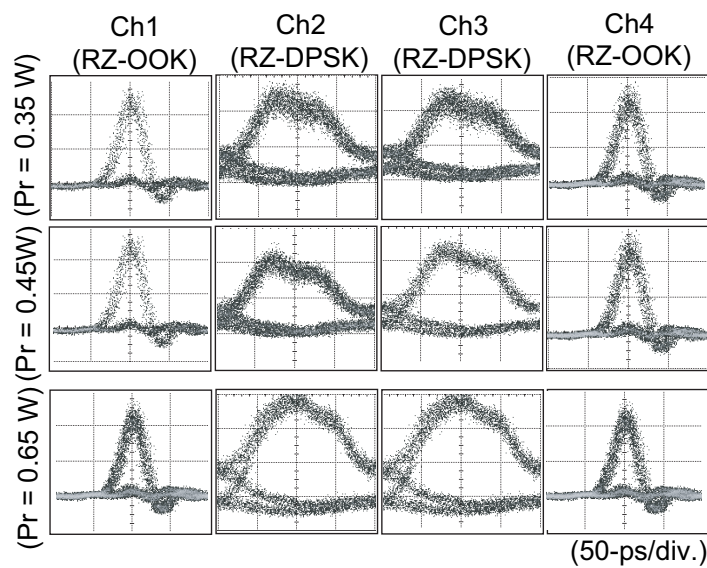
Figure 4.13: (a) Power penalty and (b) demodulated eye patterns for the converted RZ-OOK and RZ-DPSK signals from Ch1 to Ch4 at P_r values of 0.35, 0.45, and 0.65 W, respectively.

RZ-OOK converted signal. For example, the improvements in power penalties of the converted RZ-DPSK signals at Ch 3 were observed, with negative penalties values -1.64, -1.32, and -0.81 dB at three P_r setting, respectively. In contrast, compared

with the RZ-OOK converted signal at Ch 1, the power penalty was slightly higher and had negative values of -0.34, -0.41, and -0.55 dB at the same settings as mentioned above. The respective demodulated eye patterns of both converted RZ-DPSK and RZ-OOK channels remained clean and open after format conversion with different P_r values as shown in Fig. 4.13 (b). Clearer eye pattern was enhanced when input RZ clock was set at the P_r value of 0.65 W. In 10 Gb/s WDM design the important issue is the crosstalk. The degradation of the performance occurred whenever crosstalk leads to transfer of power from one channel to another due to the nonlinear effects in optical fiber. Furthermore, work in ref. [57] have highlighted that interchannel crosstalk severely degrades the quality of the converted signals when single type of modulation format such as OOK are passed simultaneously through the same processors. Some crosstalk also can occurred even in a perfectly linear channel due to the imperfect nature of various WDM components such as optical filters, and switches. From above results, RZ-DPSK converted signals were found to outperform RZ-OOK signals in both power penalties and pulse width compression. DPSK signals have advantages over OOK signals when used in multichannel conversion due to its high tolerance to fiber nonlinearities. Part of this higher tolerance is thought come from the intrinsic structure of the DPSK format constant-intensity profile in each pulse bit with no missing pulses [58]. These results clearly demonstrate that $4\times$ 10 Gb/s NRZ mixed data signals have been successfully converted to a RZ mixed data signals with a picosecond duration.

4.4 Multichannel Mixed Format Transmission Performance between OPC and In-Line TDCM Schemes

Chromatic dispersion accumulates along an optical fiber that causes ISI and limits the transmission reach. In this chapter, we demonstrated the transmission performance between the midspan of TDCM and OPC using multichannel mixed OOK and DPSK formats. The OPC scheme has the advantage over the penalties performance compared to TDCM scheme.

This section is being organized as follows: First, the subsections 4.4.1 and subsection 4.4.2 present the experimental setup, results and discussion for generation of 4×10 Gb/s WDM picosecond pulse source and its application to all channel OTDM demultiplexing.

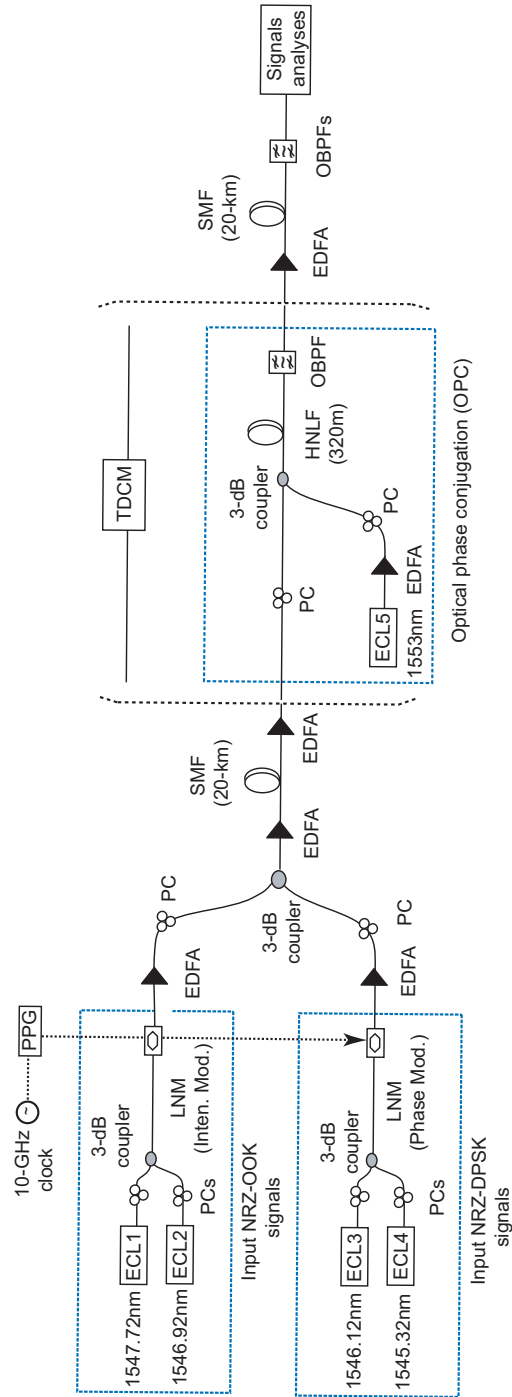# 4. MIXED MODULATION FORMATS ALL-OPTICAL SIGNAL PROCESSINGS

4.4.1   Experimental Setup

The experimental setup shown in Fig. 4.14, employs 10 Gb/s four-channel mixed format signal systems were chosen. The first two channels were NRZ-OOK and the third and fourth were NRZ-DPSK signals. The channel spacing was 0.8 nm. The NRZ-OOK data signal having the wavelengths of 1547.72 (Ch1), 1546.92 (Ch2) and NRZ-DPSK at the wavelengths 1546.12 (Ch3), 1545.32 nm (Ch4) were generated by modulating a continuous wave (CW) light in a LiNbO3 with intensity and a phase modulator LNM with 10 Gb/s) PRBS of length 2^{31}-1 from PPG. To compensate the insertion loss of the modulator and adjust the injected signals powers into the transmission line, the signal was amplified using EDFA. PCs at the input of the coupler were employed to adjust polarization states for all the signals. All signals were transmitted into 20 km SSMF with a dispersion value of 17 ps/nm/km. After 20 km signal transmission, all channels were amplified by an EDFA and then injected into a TDCM or an OPC for the compensation of chromatic dispersion. The TDCM (Teraxion, RS-232) used in our scheme was a fully integrated module with a wide bandwidth and a large dispersion range from $\pm$ 900 ps/nm. Alternatively, OPC scheme was based on FWM in a HNLF consists of an ECL at a wavelength of 1553 nm for a pump source. The HNLF had a dispersion slope of 0.032 ps/nm^2/km and nonlinear coefficient of 12.6 W^{-1} km $^{-1}$. In the OPC, the transmitted input data signals were converted into the phase-conjugated FWM signals. OBPF was used after HNLF to isolate the conjugate product and to remove ASE produced by an EDFA. After the amplification by the EDFA located at the output of the midspan TDCM or OPC, the signal was transmitted into a 20 km SSMF link. The total transmission distance was 40 km in this scheme. Finally, the transmitted signals were selected by an OBPF, then converted into the electrical signals by a balanced photo-diode after OOK and DPSK-demodulation for NRZ-OOK and NRZ-DPSK signals, and measured BER characteristics by an error analyzer to evaluate the performance of the signals.

4.4.2   Experimental Result and Discussion

To investigate the transmission performance of mixed channels of NRZ-OOK and NRZ-DPSK signals, we compared the performance of the two schemes, midspan TDCM and OPC-based systems. Two channels of NRZ-OOK and NRZ-DPSK format were located

Figure 4.14: Experimental setup of the proposed transmission performance between mid-span TDCM and OPC schemes.
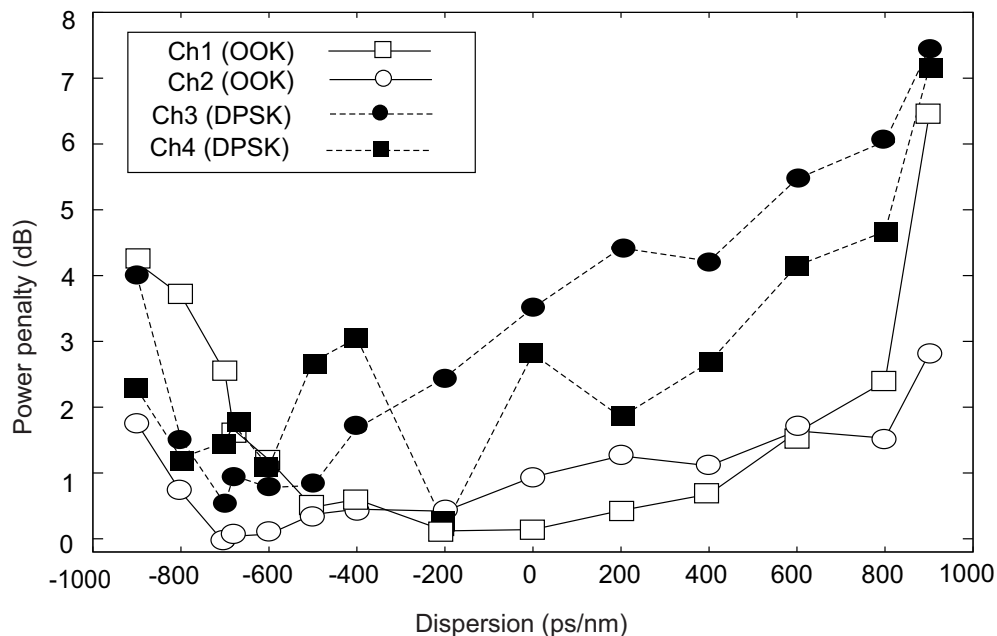
Figure 4.15: TDCM transmission aided system results for all channels power penalty
against dispersion settings.

at the Ch1, 2 3, and 4 respectively. A full comparison in different format allocation is
out of the research scope. The channel spacing between four channels is 100 GHz. The
loss of the SSMF is compensated using EDFA for signal amplification. Fig. 4.15 shows
the employed modulator response of a different dispersion settings by using TDCM.
The total accumulated dispersion of the transmission line was equal to 680 ps/nm.
At the first stage the compensated dispersion was adjusted from -900 to 900 ps/nm
with every 200-ps/nm step to investigate the optimal compensation level between each
channel. The optimal compensation value, providing lower power penalties is equal to
-600 ps/nm.

The BER is displayed in Fig. 4.16. In multiple channel system for different formats
were used, each BER values in each channel not only dependent on the individual
modulation format capability to resist from interchannel distortion, but also form that,
which modulation format is used in the channel, which is the source of this disorders.
Eventough dispersion effects can be reduced by using TDCM schemes, it was found
that the first channel of NRZ-OOK and last channel of NRZ-DPSK had the biggest
penalties in comparison with the middle channels with the value of 1.0 and 1.1 dB,
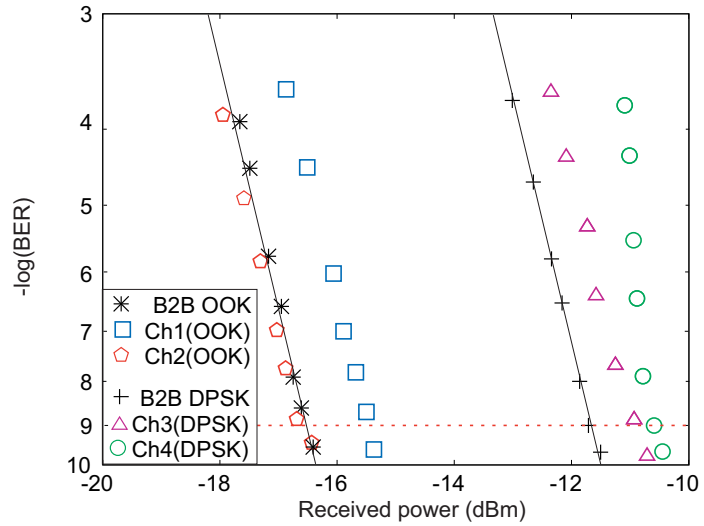
Figure 4.16: BER measurements for TDCM transmission aided system results.
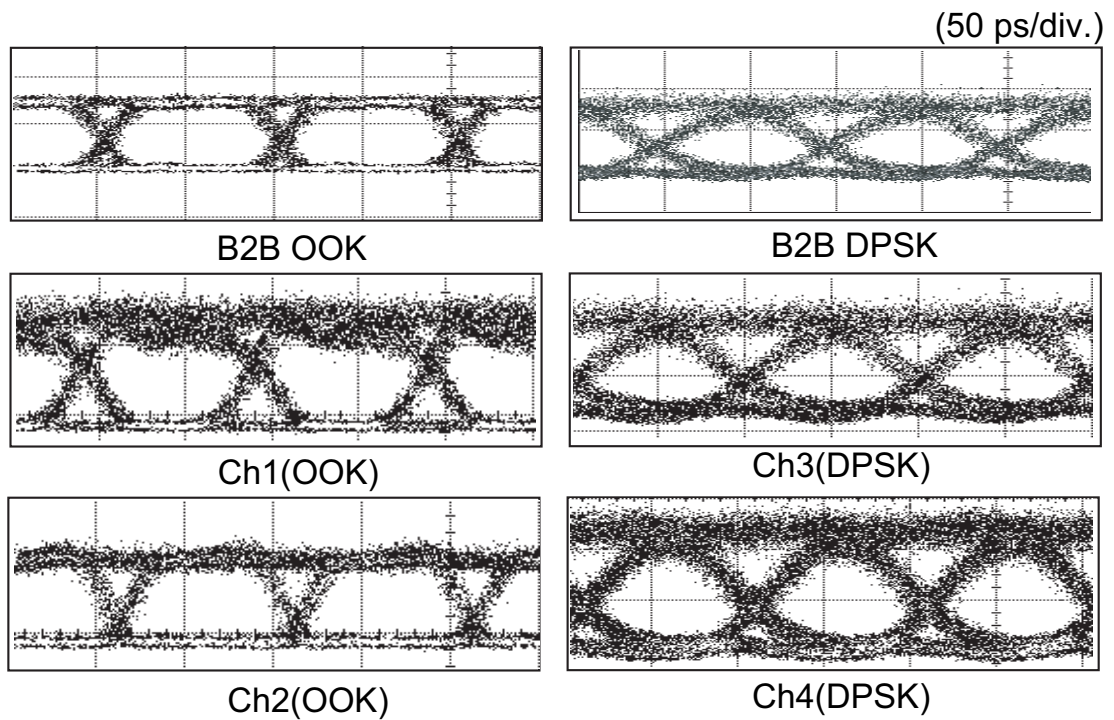
Figure 4.17: Demodulated eye patterns for TDCM transmission aided system results (50 ps/div).

respectively. When two signals with the same formats were located near to each other, the performance degradation induced by crosstalk was much higher than middle two channels. As displayed in the same figure, the power penalties for the center channel (Ch3 and Ch4) with different type of formats were less than 0.5 dB. This result partly due to different formats abilities allocated near to each other was less exposed to noise as mentioned above. Furthermore, Fig. 4.17 shows the demodulated channel eye patterns, clear eye opening were obtained in all channels with relatively small noise level.
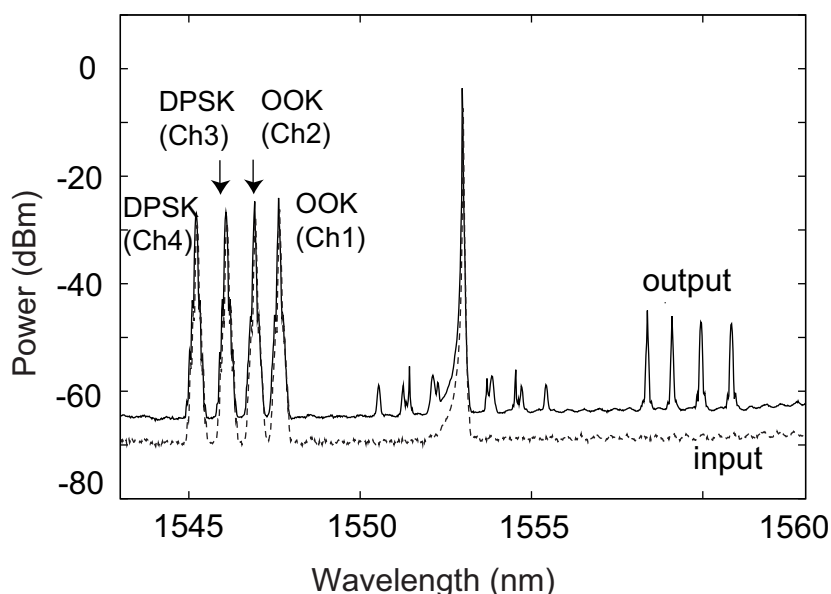
Figure 4.18: OPC transmission aided system results for signal spectra at the input (dashed line) and output (solid line) after HNLF.

Fig. 4.18 to 4.20 show the obtained results from OPC transmission based scheme. The optical spectrum observed at the output of the HNLF is shown in Fig. 4.18. The spectra show the input Ch1 to Ch4 (dashed line) and the desired output conjugates channels (solid line). To fulfill the FWM phase-matching requirement, the pump and probe signals is located in the spectral region around zero dispersion wavelength. To prevent unwanted non-degenerate FWM overlapping with OPC signals, the pump was placed 6 nm away from the first channel. Thus, the channel crosstalk among signals can be reduced and converted signals can be filtered out efficiently using filters. Fig. 4.19 shows that the penalties occurred in OPC were acceptably small with values of 0.39, 0.2, 0.24 and 0.34 dB for Ch1 to Ch4, at 10^{-9} BER. These indicated that the
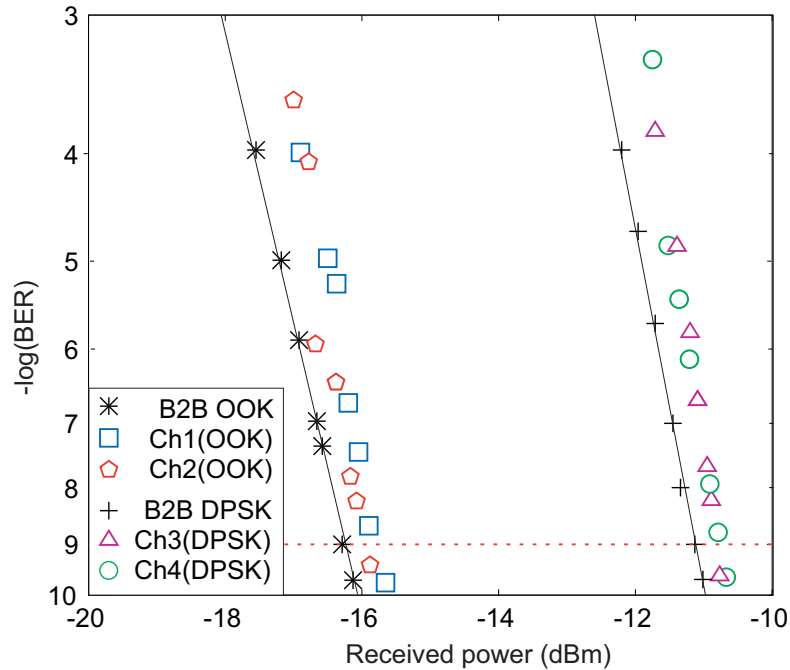
Figure 4.19: BER measurements for OPC transmission aided system results.

accumulated dispersion in the first half on the transmission link was canceled out in the second half of the transmission link. The demodulated eye patterns after OPC as depicted in Fig. 4.20 were widely opened. In this work, the sensitivity towards polarization was not considered.

Compared to the deployed dispersion compensation schemes based on TDCM, the OPC scheme performed slightly better BER results. The performance degradation may comes from nonlinear phase noise, whereas in the OPC scheme the noise was reduced through midspan link. Phase shift format transmission performance such as DPSK format can severely impaired by the nonlinear phase noise [59, 60]. Using OPC system, the nonlinear phase noise can slightly be reduced [61]. However, unlike OPC scheme, TDCM method can compensate both even and odd dispersion as result is shown previously under Fig. 4.15. Note that, OPC scheme does not change the third-order odd dispersion [62]. Thus, the odd-order dispersion compensation can be solved in the future investigation using an alternative method that proposed in the refs. [63, 64].
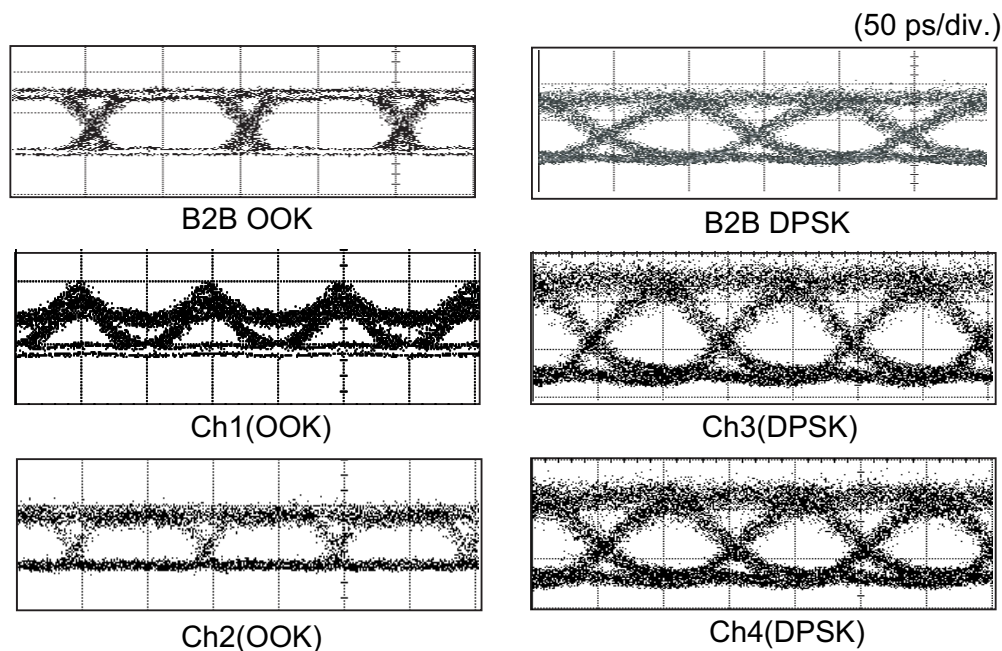
(50 ps/div.)

Figure 4.20: Demodulated eye patterns for OPC transmission aided system results (50-ps/div.)

4.5 Conclusions

In conclusions, this chapter is represented a few demonstrations of an all-optical signal processing using mixed modulation format of OOK and DPSK either in WDM and OTDM schemes. For the first time under first section, we have analyzed all-optical DEMUX based on 40-Gb/s hybrid OTDM channels by using RASC flexible gating-window. Nearly transform-limited value and error free operations have been achieved for all demultiplexed outputs with a maximum power penalty of 1.3 dB. In the second section of this chapter, we also successfully demonstrated mixed formats multichannel conversion after fiber-based switch for the first time. The experimental results show that, a high quality picosecond ultra-short converted pulses were achieved with negative power penalties at reference pulses compared with the input back-to-back signals. Lastly, in the last section, we believe for the first time, relevant impairment for SSMF in the fiber optic transmission performance of WDM $4\times$ 10 Gb/s multichannel mixed formats was compared between TDCM and OPC based system. The overall performance of OPC method was slightly better than TDCM scheme. The obtained results

will provide a guideline for an optimum design of TDCM and OPC that can be used in optical designs where signals with different formats coexist.

References

[1] R. S. Tucker, G. Einsenstein, and S. K. Korotky, "Optical time-division multiplexing for very high bit-rate transmission," *J. Lightwave Technol.*, vol. 6, no. 11, pp. 1737–1749, Nov 1988.

[2] N. Sambo, P. Castoldi, F. Cugini, G. Bottari, "Toward high-rate and flexible optical networks," *IEEE Comms. Mag.*, vol. 50, no. 5, pp. 66–72, May 2012.

[3] A. Nag, M. Tornatore, B. Mukherjee, "Optical network design with mixed line rates and multiple modulation formats," *J. Lightwave Technol.*, vol. 28, no. 4, pp. 466–475, Feb. 2010.

[4] M. Matsumoto, "Simultaneous reshaping of OOK and DPSK signal by a fiber-based all-optical regenerator," *Opt. Express*, vol. 14, no. 4, pp. 1430–1438, Feb. 2006.

[5] G.-W. Lu, K. Abedin, T. Miyazaki, and M. Marchic, "RZ-DPSK OTDM demultiplexing using fibre optical parametric amplifier with clock-modulated pump," *IEEE Electron. Lett.*, vol. 45, no. 4, pp. 221–222, Feb. 2009.

[6] C. Bres, A. O. J. Wiberg, B. P. -P. Kuo, J. M. Chavez-Boggio, C. F. Marki, N. Alic, and S. Radic, "Optical demultiplexing of 320 Gb/s to 8 x 40 Gb/s in single parametric gate," *J. Lightwave Technol.*, vol. 28, no. 4, pp. 434–440, Feb. 2010.

[7] P. Samadi, L. R. Chen, I. A. Kostko, P. Dumais, C. L. Callender, Sarkis Jacob, and Brian Shia, "Reconfigurable OTDM demultiplexing using FWM in highly nonlinear fiber and a tunable planar lightwave circuit," *IEEE Photon. Technol. Lett.*, vol. 24, no. 1, pp. 13–15, Jan. 2012.

REFERENCES

[8] J. Hansryd, and P. A. Andrekson, "O-TDM demultiplexer with 40-dB gain based on a fiber optical parametric amplifier," *IEEE Photon. Technol. Lett.*, vol. 13, no. 7, pp. 732–734, Jul. 2001.

[9] N. Deng, C-Kit Chan, and L-Kuan Chen, "A hybrid OTDM scheme with enhanced demultiplexing performance," *IEEE Photon. Technol. Lett.*, vol. 19, no. 19, pp. 1454–1456, Oct. 2007.

[10] H. Hu, H. C. Mulvad, M. Galili, E. Palushani, J. Xu, A. T. Clausen, L. K. Oxenlowe, and P. Jeppesen, "Polarization-insensitive 640 Gb/s demultiplexing based on four wave mixing in a polarization-maintaning loop," *J. Lightwave Technol.*, vol. 28, no. 12, pp. 1789–1795, March 2010.

[11] R. Ramaswami, and K. N. Sivarajan, *Optical Networks: A practical perspective*, London, United Kingdom: Academic Press, 2nd ed., pp. 223, 2002.

[12] S. Kawashini and O. Kamatani, "All-optical time division multiplexing using four-wave mixing," *Electron. Lett.*, vol. 30, no. 20, pp. 1697, Sept. 1994.

[13] H-Georg. Weber, R. Ludwig, S. Ferber, C. Schmidt-Langhorst, M. Kroh, V. Marembert, C. Boerner, and C. Schubert, "Ultrahigh-speed OTDM-transmission technology," *J. Lightwave Technol.*, vol. 24, no. 12, pp. 4616–4627, Dec. 2006.

[14] H. Nguyen. Tan, M. Matsuura, T. Katafuchi, and N. Kishi, "Multiple-channel optical signal processing with wavelength-waveform conversion, pulsewidth tunability, and signal regeneration," *Opt. Express*, vol. 17, no. 25, pp. 22960-22973, 2009.

[15] L. -S. Yan, A. -L. Yi, W. Pan, B. Luo, and J. Ye, "Simultaneous NRZ-to-RZ format conversion and one-to-six error-free channel multicasting using a single pump in a highly nonlinear fiber," *Opt. Express*, vol. 18, no. 20, pp. 21404–21409, Sept. 2010.

[16] W. Astar, Jeffrey B. Driscoll, X. Liu, J. I. Dadap, W. M. J. Green, Y. A. Vlasov, G. M. Carter, and R. M. Osgood ,"All-optical format conversion of NRZ-OOK to RZ-OOK in a silicon nanowire utilizing either XPM or FWM and resutling in a receiver sensitivity gain of $\sim$2.5 dB," *IEEE J. Sel. Top Quant.*, vol. 16, no. 1, pp. 234–249, Jan/Feb. 2010.

[17] Y. Yu, B. Zou, W. Wu, and X. Zhang, "All-optical parallel NRZ-DPSK to RZ-DPSK format conversion at 40 Gb/s based on XPM effect in a single SOA," *Opt. Express*, vol. 19, no. 15, pp. 14720–14725, Jul. 2011.

[18] W. Yu, L. Huo, D. Lu, and C. Lou, "A novel optical picosecond-duration NRZ-to-RZ format converter with simultaneous wavelength multicasting using a single-stage Mach-Zehnder modulator," *Opt. Commun.*, vol. 285, pp. 4302–4306, Jul. 2012.

[19] A. Reale, P. Lugli, and S. Betti, "Format conversion of optical data using four-wave mixing in semiconductor optical amplifiers," *IEEE J. Sel. Top Quant.*, vol. 7, pp. 703–709, 2001.

[20] H. K. Lee, K. H. Kim, J. T. Ahn, M. -Y. Jeon, and E. H. Lee, "All-optical format conversion from NRZ to RZ signals using a walk-off balanced nonlinear fibre loop mirror," *Electron Lett.*, vol. 32, no. 25, pp. 2335–2336, Dec. 1996.

[21] G. G. Lee, Y. J. Kim, C. S. Park, H. J. Lee, and C-Soo. Park, "Experimental demonstration of 10-Gb/s data format conversions between NRZ and RZ using SOA-loop-mirror," *J. Lightwave Technol.*, vol. 23, no. 2, pp. 834–841, 2005.

[22] J. Dong, X. Zhang, F. Wang, Y. Yu, and D. Huang, "Single-to-dual channel NRZ-to-RZ format conversion by four wave mixing in single semiconductor amplifier," *Electron Lett.*, vol. 44, no. 12, pp. 763–764, June 2008.

[23] K. Mishina, S. Kitagawa, and A. Maruta, "All-optical modulation format conversion from on-off-keying to multiple-level phase-shift-keying based on nonlinearity in optical fiber," *Opt. Express*, vol. 15, no. 13, pp. 8444–8453, 2007.

[24] P. J. Wizer and R. -J. Essiambre, "Advanced modulation formats for high-capacity optical transport networks," *J. Lightwave Technol.*, vol. 24, no. 12, pp. 4711–4728, 2006.

[25] P. Groumas, V. Katopodis, C. Kouloumentas, M. Bougioukos, and H. Avramopoulos, "All-optical RZ-to-NRZ conversion of advanced modulated signals," *IEEE Photon. Technol. Lett.*, vol. 24, no. 3, pp. 179–181, Feb. 2012.

REFERENCES

[26] S. L. Jansen, D. van den Borne, B. Spinnler, S, Calabro, H. Suche, P. M. Krumm-rich, W. Sohler, G. D. Khoe, H. de Waardt, "Optical phase conjugation for ultra long-haul phase-shift-keyed transmission," *J. Lightwave Technol.*, vol. 24, no. 1, pp. 54–64, Feb. 2006.

[27] J. Wang and J. M. Kahn, "Impact of chromatic and polarization-mode dispersions on DPSK systems using interferometric demodulation and direct detection," *J. Lightwave Technol.*, vol. 22, no. 2, pp. 362–371, Feb. 2004.

[28] C. Xu and X. Wei, "Differential phase-shift keying for high spectral efficiency optical transmissions," *IEEE J. Sel. Top Quant.*, vol. 10, no. 2, pp. 281–293, March/Apr. 2004.

[29] C. Xu and X. Wei, "A comparative study of DPSK and OOK WDM transmission over transoceanic distances and their performance degradations due to nonlinear noise," *J. Lightwave Technol.*, vol. 21, no. 9, pp. 1933–1943, Sept. 2003.

[30] M. Matsuura and N. Kishi,"Multichannel transmission of intensity- and phase-modulated signals by optical phase conjugation using a quantum-dot semiconductor amplifier," *Opt. Lett.*, vol. 38, no. 10, pp. 1700–1702, May 2013.

[31] S. A. Hamilton, B. S. Robinson, T. E. Murphy, S. J. Savage, and E. P. Ippen,"100 Gb/s Optical time-division multiplexed networks," *J. Lightwave Technol.*, vol. 20, no. 12, pp. 2086–2100, Dec. 2002.

[32] D. M. Pepper, and A. Yariv,"Compensation for phase distortions in nonlinear media by phase conjugation," *Opt. Lett.*, vol. 5, no. 2, pp. 59–60, Feb. 1980.

[33] S. Watanabe and M. Shirasaki,"Exact compensation for both chromatic dispersion and Kerr effect in a transmission fiber using optical phase conjugation," *J. Lightwave Technol.*, vol. 14, pp. 243–248, Mar. 1996.

[34] T. Kato, M. Hirano, A. Tada, K. Fukuada, T. Fujii, T. Ooishi, Y. Yokoyama, M. Yoshida, and M. Onishi,"Dispersion flattened transmission line consisting of wide-band non-zero dispersion shifted fiber and dispersion compensating fiber module," *Opt. Fiber Tech.*, vol. 8, no. 3, pp. 231–239, 2002.

[35] X. Chen, X. Xu, M. Zhou, D. Jiang, X. Li, J. Feng, and S. Xie, "Tunable dispersion compensation in a 10-Gb/s optical transmission system by employing a novel tunable dispersion compensator," *IEEE Photon. Technol. Lett.*, vol. 16, no. 1, pp. 188–190, Jan. 2004.

[36] R. Jones, J. Doylend, P. Ebrahimi, S. Ayotte, O. Raday, and). Cohen, "Silicon photonic tunable optical dispersion compensator," *Opt. Express*, vol. 15, no. 24, pp. 15836–15841, Nov. 2007.

[37] L. G. Nielsen, M. Wandel, P. Kristensen, C. Jorgensen, L. V. Jorgensen, B. Edvold, B. Palsdottir, and D. Jakobsen, "Dispersion-compensating fibers," *J. Lightwave Technol.*, vol. 23, no. 11, pp. 3566–3579, 2005.

[38] C. R. Doerr, R. Blum, L. L. Buhl, M. A. Cappuzzo, E. Y. Chen, A. Wong-Foy, L. T. Gomez, and H. Bulthuis, "Colorless tunable optical dispersion compensator based on a silicon arrayed-waveguide grating and a polymer thermooptic lens," *IEEE Photon. Technol. Lett.*, vol. 18, no. 11, pp. 1222–1224, June 2006.

[39] S. L. Jansen, S. Spalter, G.-D. Khoe, H.de Waardt, H. E. Escobar, L. Marshall, and M. Sher, "16 × 40 Gb/s over 800 km of SSMF using mid-link spectral inversion," *IEEE Photon. Technol. Lett.*, vol. 16, no. 7, pp. 1763–1765, Jul. 2004.

[40] S. L. Jansen, D. van den Borne, P. M. Krummrich, S. Spalter, G. -D. Khoe, and H. de Waaardt, "Long-haul DWDM transmission systems employing optical phase conjugation," *IEEE J. Sel. Top Quant.*, vol. 12, no. 4, pp. 505–520, Jul/Aug. 2006.

[41] P. Minzioni, V. Pusino, I. Cristiani, L. Marazzi, M. Martinelli, C. Langrock, M. M. Fejer, and V. Degiorgio, "Optical phase conjugation in phase-modulated transmission systems:experimental comparison of different nonlinearity-compensation methods," *Opt. Express*, vol. 18, no. 17, pp. 18119–18124, Aug. 2010.

[42] S. Watanabe, T. Naito, and T. Chikama, "Compensation of chromatic dispersion in a single-mode fiber by optical phase conjugation," *IEEE Photon. Technol. Lett.*, vol. 5, no. 1, pp. 92–95, Jan. 1993.

[43] I. Brener, "160 Gbit/s wavelength shifting and phase conjugation using periodically poled LiNbO$_3$ waveguide parametric converter," *Electron. Lett.*, vol. 36, no. 21, pp. 1788–1790, Aug. 2002.

REFERENCES

[44] M.D. Pelusi, F. Luan, D.-Y. Choi, S.J. Madden, D.A.P. Bulla, B. Luther-Davies, and B.J. Eggleton, "Optical phase conjugation by an As2S3 glass planar waveguide for dispersion-free transmission of WDM-DPSK signals over fiber," *Opt. Express.*, vol. 18, no. 25, pp. 26686–26694, Dec. 2010.

[45] S. Ayotte, H. Rong, S. Xu, O. Cohen, and M. J. Panicciae, "Multichannel dispersion compensation using a silicon waveguide-based optical phase conjugator," *Opt. Lett.*, vol. 32, no. 16, pp. 2393–2395, 2007.

[46] J.P.R. Lacey, S. J. Madden, M. A. Summerfield, R. S. Tucker, and A. I. Faris, "Four-channel WDM optical phase conjugator using four-wave mixing in a single semiconductor optical amplifier," *Electron Lett.*, vol. 31, no. 9, pp. 743–744, Apr. 1995.

[47] H. Hu, H. C. Mulvad, C. Peucheret, M. Galili, A. Clausen, P. Jeppensen, and L. K. Oxenlowe, "10 GHz pulse source for 640 Gbit/s OTDM based on phase modulator and self-phase modulation," *Opt. Express*, vol. 19, no. 26, pp. 343–349, Dec. 2011.

[48] Y. Zhou, B. P. P. Kuo, K. K. Y. Cheung, S. Yang, P. C. Chui, and K. K. Y. Wong, "Wide-band generation of picosecond pulse using fiber optical parametric amplifier and oscillator," *IEEE J. Quantum Elect.*, vol. 45, no. 11, pp. 1350–1356, Nov. 2009.

[49] T. Sakamoto, T. Kawanishi, and M. Tsuchiya, "10 GHz, 2.4 ps pulse generation using a single-stage dual-drive Mach-Zender modulator," *Opt. Lett.*, vol. 33, no. 8, pp. 890–892, Nov. 2008.

[50] K. Igarashi, K. Katoh, K. Kikuchi, K. Imai, and M. Kourogi, "Generation of 10-GHz 2-ps optical pulse train over the C band based on an optical comb generator and its application to 160-Gbit/s OTDM systems," in 34th *European Conference on Optical Communication (ECOC)*, pp. Tu.3.D.1 (2008).

[51] M. Matsuura, B. P. Samarakoon, and N. Kishi, " Wavelength shift-free adjustment of the pulsewidth in return-to-zero on-off keyed signals by means of pulse compression in distributed Raman amplification," *IEEE Photon. Technol. Lett.*, vol. 21, no. 9, pp. 572–574, May 2009.

[52] H. N. Tan, Q. Nguyen-The, M. Matsuura, and N. Kishi, "Reconfigurable All-Optical OTDM-to-WDM Conversion Using a Multiwavelength Ultrashort Pulse Source Based on Raman Compression," *J. Lightwave Technol.*, vol. 30, no. 6, pp. 853–863, Mar. 2012.

[53] G. Contestabile, R. Presi, M. Calabretta, E. Ciaramella, "All-optical clock recovery for NRZ-DPSK signals," *IEEE Photon. Technol. Lett.*, vol. 18, no. 23, pp. 2544–2546, 2006.

[54] Y. Yu, X. Zhang, J. Hu and D. Huang, "All-optical clock recovery from NRZ-DPSK signals at flexible bit rates," *Conference on lasers and electro-optics/quantum electronics and laser science conference and photonic applications systems technologies (CLEO)*, pp. JWA103 (2008).,

[55] N. Alic, R. M. Jopson, J. Ren, E. Myslivets, R. Jiang, A.H. Gnauck, and S. Radic,"Impairments in deeply-saturated optical parametric amplifiers for amplitude- and phase-modulated signals," *Opt. Express*, vol. 15, no. 14, pp. 8997-9008, 2007.

[56] N. K. Das, Y. Yamayoshi, and H. Kawaguchi,"Analysis of basic four-wave mixing characteristics in a semiconductor optical amplifier by beam propagation method," *IEEE J. Quantum Electron.*, vol. 36, no. 10, pp. 1184–1192, Oct. 2000.

[57] P. Devgan, R. Tang, V. S. Grigoryan, and P. Kumar,"Highly efficient multichannel wavelength conversion of DPSK signals," *J. Lightwave Technol.*, vol. 24, no. 10, pp.3677–3681, Oct. 2006.

[58] Pak. S. Cho and Jacob B. Khurgin, "Suppression of Cross Gain modulation in SOA using RZ-DPSK modulation format," *IEEE Photonics Technol. Lett.*, vol. 15, no. 1, pp. 162–164, Jan. 2003.

[59] H. Kim and A. H. Gnauck, "Experimental investigation of the performance limitation of DPSK systems due to nonlinear phase noise," *IEEE Photon. Technol. Lett.*, vol. 15, no. 2, pp. 320–322, Feb. 2003.

[60] T. Mizuochi, K. Ishida, T. Kobayashi, J. Abe, K. Kinjo, K. Motoshima, and K. Kasahara, "Comparative study of DPSK and OOK WDM transmission over

REFERENCES

transoceanic distances and their performance degradations due to nonlinear phase noise," *J. Lightwave Technol.*, vol. 21, no. 9, pp. 1933–1943, 1996.

[61] S.L. Jansen, D. van den Borne, P. M. Krummrich, S. Spalter, and H. de Waardt, " Long-haul DWDM transmission systems employing optical phase conjugation," *IEEE J. Sel. Top Quant.*, vol. 12, no. 4, pp. 505–520, July/Aug. 2006.

[62] B. P. -P. Kuo, E. Myslivets, A. O. J. Wiberg, S. Zlatanovic, C-S. Bres, S. Moro, F. Gholami, A. Peric, N. Alic and S. Radic, "Transmission of 640-Gb/s RZ-OOK channel over 100-km SSMF by Wavelength-Transparent Conjugation," *J. Lightwave Technol.*, vol. 29, no. 4, pp. 516–523, Feb. 2011.

[63] M. Tsang and D. Psaltis, "Dispersion and nonlinearity compensation by spectral phase conjugation," *Opt. Lett.*, vol. 28, no. 17, pp. 1558–1560, Sept. 2003.

[64] J. Pina, B. Abueva, and C. G. Goedde "Periodically conjugated solitons in dispersion-managed optical fiber," *Opt. Commun.*, vol. 176, pp. 397–400, Apr. 2000.

Chapter 5

Summary and Outlook

Nowadays, the transition era of optical technologies is striving by the introduction of more advanced modulation formats, exploiting new transmission schemes and multiplexing systems to provide better services or to meet the sub networks specifications. Although many nonlinear photonic devices have been studied and their usefulness has been demonstrated, there are still many challenges in order to realize commercial ultrafast communication networks. In future, it is likely that mixed transmission lines may exist where different modulation formats and different bit-rates will be transmitted in the same fiber. Therefore, the independent format and bit-rate all-optical signal processing is desirable. Furthermore, as we move towards higher bit-rates and combination between WDM and OTDM, smaller pulse width as picosecond pulses are required to be multiplexed and form higher tributaries. Moreover, for high capacity optical transmission systems, high quality characteristics of the input and converted output pulses are also mandatory. In this thesis, we propose a simple technique to convert a single and multiple channels conversions using a single pump in fiber-based all-optical AND-gates FWM scheme using either single 10 Gb/s or mixed modulation formats in $4 \times$ 10-Gb/s based WDM and 40-Gb/s OTDM systems. All experimental considerations presented in this thesis are based on CW and tunable-width compressed RZ pulse from RASC as input pump signals. As for compressed RZ pulses from RASC as input pump signal, picosecond tunable-width pulses in various operating regimes can be successfully converted. For instance, if the pump signal is located around ZDW of the fiber-based medium, the phase matching condition is satisfied and the converted signal is proportional to the square of the signal field. Furthermore, it is possible to achieve reshaping

properties of FWM process, as the input signal has more larger duration that RZ clock pump, the converted signal inherits qualities of the compressed clock from the shape and improved extinction-ratio.

In chapter 3, several optical signal processing schemes using single modulation formats were performed. In the first section, we have successfully demonstrated waveform-wavelength conversion of NRZ-DPSK-to-RZ-DPSK with simultaneous signal reshaping and flexible width-tunable operations in combination between RASC and also a fiber-based AND-gate FWM switch. In the first experiment, we demonstrated the concept of a broadband waveform-wavelength conversion for a 10-Gb/s RZ-DPSK signal at about 54-nm separation with the fixed width of a compressed RZ clock. Secondly, the demonstration of waveform-wavelength conversion showed that, by tuning the Raman pump power of the compressed RZ clock from 0.20 to 0.90 W, a converted RZ-DPSK signal with pulse width compression down to 2.87 ps and pedestal-free pulse could be obtained. Furthermore, the phase information of the converted signal was similar to the input data signal. In addition, negative power penalties below 1.95 dB were achieved in comparison between degraded input NRZ-DPSK data signal and its regenerated converted RZ-DPSK signal. These findings confirmed that the proposed scheme is a promising method for achieving an impairment-free picosecond width-tunable regenerated converted RZ-DPSK signal. Other than that, the result also suggested a possibility of a higher bit rate operation at 80 Gb/s or more.

We also experimentally demonstrated a multicasting conversion method, utilizing pulse data from a RASC and a fiber-based FWM switch in an HNLF. Simultaneous multicasting conversion from one to six channels for different cases of input data signals from the RASC was performed. Width-tunable pulse width and wavelength multicasting within the C-band with approximately 40.6 nm of separation for various compressed RZ data inputs also have been demonstrated. Penalties of less than 1.2 dB were obtained for all multicasting outputs from the RASC. Meanwhile, output pulse widths with a flexible tuning range down to 2.67 ps were achieved. Our proposed scheme could be used as applications in gateway node connecting optical network segments using different kinds of modulation formats and multiplexing techniques.

In the chapter 4, various concepts to realize mixed formats optical signal processing has been proposed and demonstrated. Apart from that, optical networks use a combination of OTDM and WDM to increase and optimize the transmission capacity

or bit-rate. So, far OTDM demultiplexing is focused on processing single data format instead of mixed modulation formats. Furthermore, the demultiplexing required an optical gate with a fast switching time that is shorter than the bit period, for example, 6.25 ps for 160 Gb/s. Thus, an appropriate optical pulse source is needed. Moreover, a method for improving the performance of single pump demultiplexer at 40 Gb/s can be realized by using RZ pulsed pumps with flexible short pulsewidths. All-channel OTDM demultiplexing using gating window compressed RZ clock from RASC is proposed and experimentally demonstrated in section 4.1. When the flexible compressed RZ clock is synchronized with the time slot by 25 ps corresponding to the tributary channel either RZ-DPSK or RZ-OOK, the desired channel can be selected and forwarded to the receiver. Meanwhile, BER measurement showed an error-free operation and the superior performance of RZ-DPSK tributary channel was observed in comparison with RZ-OOK channel. This was due to its constant intensity profile characteristic. Thus, our experiment shows the potential using OTDM hybrid data stream that can be upgraded to higher bit rates 160 Gb/s due to benefit gained from flexible gating window from RASC component as a pump employed in our system.

Recently, several researches proposed and demonstrated format conversion for multichannel operation based on a single device, mainly with single format. Waveform-wavelength converters operation in single channel with single modulation format is cumbersome for flexible network management. Furthermore, it would be much more attractive to convert multichannel with mixed formats in a single converter, for it can lead to a simple network topology infrastructure. In addition, the ability to offer some more advantages on top of the basic waveform-wavelength conversions, such as tunable output pulse-width as well as data conversion with mixed formats is more beneficial. The demonstration of multichannel conversion of NRZ-to-RZ mixed format OOK and DPSK signals with picosecond width-tunable and pedestal-free operations after fiber-based AND-gate FWM are continued and explained in section 4.2. The experimental results show that, by changing the pump power of a compressed RZ clock, an RZ mixed format converted signal with picosecond pulsewidth of 2.73 ps could be obtained. Additionally, high quality picosecond ultra-short converted pulses were achieved with negative power penalties at reference pulses, compared with the input back-to-back signals.

5. SUMMARY AND OUTLOOK

The first commercial all-optical signal dispersion compensation is likely to be compatible only with single type modulation formats such as OOK or DPSK. In the section 4.3, we studied two chromatic dispersion compensation methods that can be implemented between each transmission link. The schemes are TDCM and OPC. In the last chapter, relevant impairment for SSMF in the fiber optic transmission performance of WDM 4×10 Gb/s multichannel mixed formats was compared between TDCM and OPC based system. The overall performance of the TDCM was impairment produced by dispersion noise and crosstalk where as the performance of the OPC was less affected. Moreover, different modulation formats have its advantages and disadvantages. Generally, there is no single format that is better than others.

Under section 4.2 and 4.3, our start model of multichannel mixed formats conversion is only based on 10 Gb/s four-channel system with one type of combined formats. Future research should therefore concentrate on a full comparison in different format allocation for various applications. One possible solution is the use of input mixed WDM scheme contains three input channels with total nine different combinations formats. For example, DPSK-OOK-DPSK, OOK-DPSK-OOK and etc. The next step for mixed formts multiple channel system performance evaluation is to increase the channel bit-rate and also transmission length.

———————————————————————————————

Publications

List of Publications related to this thesis

Refereed Journal Papers

1. **I. Ismail**, Q. N. The, M. Matsuura, G. M. Sharif, and N. Kishi, "Wide range operation of an all-optical NRZ-DPSK-to-RZ-DPSK regenerative waveform-wavelength conversion with flexible width-tunability," *OSJ Optical Review*, vol. 22, no. 3, pp. 489-495, June 2015.

2. **I. Ismail**, Q. N. The, M. Matsuura, and N. Kishi, "One to six wavelength multicasting of RZ-OOK based on picosecond-width-tunable pulse source with distributed Raman amplification," *IEICE Transactions on Electronics*, vol. E98-C, no. 8, pp. 816-823, Aug. 2015.

Refereed International Conference Papers

1. **I. Ismail**, Q. N. The, M. Matsuura, and N. Kishi, "Multichannel tunable pulsewidth NRZ-to-RZ conversion of intensity- and phase-modulated signals using Raman adiabatic-soliton compressor," *19th OptoElectronics and Communications Conference (OECC)*, 2014, WE7B4, Melbourne, Australia, July 2014.

2. **I. Ismail**, Q. N. The, M. Matsuura, and N. Kishi, "6-fold wavelength multicasting using tunable-width picosecond pulse source from Raman adiabatic-soliton-compressor," *19th OptoElectronics and Communications Conference (OECC)*, 2014, WE7F2, Melbourne, Australia, July 2014.

3. **I. Ismail**, Q. N. The, M. Matsuura, and N. Kishi, "Simultaneous multichannel mix format OOK and DPSK NRZ-to-RZ waveform conversion with picosecond width-tunability, " *Triangle Symposium on Advanced ICT 2014 (TriSAI)*, 2014, Session 16-3, Beijing, China, Sep. 2014.

4. **I. Ismail**, M. Matsuura, and N. Kishi, "NRZ-DPSK-to-RZ-DPSK format conversion with multiple-function using Raman adiabatic-soliton compressor," *Asia Communications and Photonics Conference (ACP)*, 2014, AF3D.7, Shanghai, China, Nov. 2014.

5. **I. Ismail**, Q. N. The, M. Matsuura, and N. Kishi, "Multichannel-mixed OOK and DPSK format transmission performance between midspan TDCM and OPC system," *Asia Communications and Photonics Conference (ACP)*, 2014, ATh3A.137, Shanghai, China, Nov. 2014.

6. **I. Ismail**, M. Matsuura, N. Kishi, and Q. N. The, "Raman amplifier-soliton compressor and its application to all-channel hybrid OTDM demultiplexing," *20th Opto-Electronics and Communications Conference (OECC)*, 2015, PWe.35, Shanghai, China, June 2015.

Refereed National Conference Papers

1. **I. Ismail**, Q. N. The, M. Matsuura, G. M. Sharif, and N. Kishi, "Novel picosecond width-tuning NRZ-DPSK-to-RZ-DPSK conversion using a Raman amplification compressor and HNLF-based switch," *IEICE General Conference*, 2014, B-10-65, Niigata, Mar. 2014.

Curriculum Vitae

Irneza received B.E. Degree from The Ryukyus University, Okinawa, Japan in 2002 and M.E. degree from University of Technology Malaysia (UTM), Johor, Malaysia in 2010. She received a Fellowship Scheme awarded by the Ministry of Higher Education Malaysia and University of Science Islamic, Malaysia (USIM) in year 2012 for her outstanding matrix result during her M.E studies. She came to Japan to pursue her graduate studies at the University of Electro-Communications (UEC) from October 2012. Her research interest is in all-optical signal processing using nonlinear fiber optics and Raman amplifier for WDM and OTDM systems. She is currently a Ph.D student in Department of Communication Engineering and Informatics, The University of Electro-Communications, Tokyo, Japan. She also a Student Member of IEEE and IEICE Communications Society.